NUCLEAR MAGNETIC RESONANCE STUDY OF Co IMPURITY IN DILUTE ALLOYS

Masahiro Matsumura

(I) NUCLEAR MAGNETIC RESONANCE STUDY IN CrVCo AND MoReCo ALLOYS

(II) NUCLEAR MAGNETIC RELAXATION IN ANTIFERROMAGNETIC CrVCo AND CrMoCo ALLOYS

February 1977

PART I

NUCLEAR MAGNETIC RESONANCE STUDY IN CrVCo AND MoReCo ALLOYS

Contents

Abstract

Magnetic states of Co impurity in dilute $Cr_{1-x}V_x$Co and $Mo_{1-x}Re_x$Co alloys were investigated systematically by nuclear magnetic resonance technique and partly magnetic susceptibility measurements.

In CrVCo alloys, the magnitude of effective moment, 3 μ_B in CrCo alloy decreases monotonically with the increase of V concentration X, and the localized moment disappears in X≥0.3 alloys. The internal field at ^{59}Co in antiferromagnetic state decreases with the increase of X, which is consistent with the decrease of the effective moment. On the other hand, ^{59}Co signals associated with nonmagnetic Co atoms were observed at liq.^{4}He temperature in X ≥ 0.2 alloys. The Knight shift of ^{59}Co, K ~ +1.7% in large X alloys decreases rapidly down to +0.11% in X=0.2 alloy, and the nuclear spin-lattice relaxation rate T_1^{-1} of ^{59}Co increases oppositely to the change of the density of states of conduction electrons, when X decreases over X=0.4. The Korringa relation for nonmagnetic impurity d-state in Anderson model with five-fold degenerate d-orbitals explains qualitatively the behavior of K and T_1 against X. In X=0.25 and 0.2 alloys, the results of NMR and magnetic susceptibilities indicate the coexistence of magnetic Co atoms(with localized moment) and nonmagnetic Co atoms(with no localized moment) as that in MoNbFe alloys. The integrated intensity of ^{59}Co resonance associated with nonmagnetic Co atoms and the decrease of

the internal field of ^{59}Co in antiferromagnetic state suggest that the magnitude of the localized moment decreases from 3 μ_B to about 2 μ_B. This behavior is different from that of MoNbFe alloys.

In normal phases in MoReCo alloys, fairly large negative Knight shift of ^{59}Co in MoCo alloy decreases its absolute value with the increase of Re concentration X. T_1^{-1} of ^{59}Co decreases also oppositely to the change of the density of state of conduction electrons. These behaviors of K and T_1 can also be qualitatively interpreted by the Korringa relation. T_1 of ^{59}Co in superconducting mixed state in X=0.3 alloy deviates from T_1T=const. , and increases nearly exponentially. However the effective energy gap $2\Delta' = 1.8\ k_BT_C(0)$ is appreciably small compared with that of host site $2\Delta = 3.5\ k_BT_C(0)$, which may suggest the existence of the localized excited state.

§ 1. Introduction

It is well known that 3-d impurities in nonmagnetic host metal widely change their magnetic states from the case where impurity has localized moment to that where impurity has no localized moment, typically as in CuMn and AlMn. These impurity d-states had been grasped by Friedel,[1] Anderson,[2] and Wolff[3] with the concept of a virtual bound state as that this state is placed in the conduction band of the host metal and mixes with states of conduction electrons, however, still remains the local correlation as an intra atomic Coulomb interaction U and exchange interaction J for degenerate d-states between electrons in this state which are responsible for a formation of a localized moment. In the limit $U/\Gamma \ll 1$, impurities have no localized moments, while in the limit $U/\Gamma \gg 1$, the Anderson model is effectively identified with the s-d exchange interaction model.[4] Here Γ is the width of the impurity state due to interaction with the conduction electrons. In this limit, anomalies in the low temperature magnetic, thermal, and transport properties have been observed in many alloys (so-called "Kondo effect")[5]. It has been considered to be the essence of the Kondo effect that the magnetic state of the impurity itself changes with temperature in the coupling with conduction electrons and the localized moment disappears in the ground state in the case of antiferromagnetic s-d exchange interaction.[5] Then it is believed that the ground state of the Anderson model is a nonmagnetic singlet for any finite value of U. Recently,

Yamada, Yosida, and Yoshimori have developed a theory of the ground state for any finite U by the perturbation expansion of Anderson model for U=0, and studied in detail the low temperature properties of the impurity d-state.[6)]

We have investigated the magnetic state of Co impurities in the dilute $\underline{Cr}_{1-x}V_x$Co and $\underline{Mo}_{1-x}Re_x$Co alloys by nuclear magnetic resonance technique and partly by the magnetic susceptibility measurement. The magnetic susceptibility measurement in the dilute $\underline{Cr}$Co alloy above the Néel temperature has shown that Co atom has a localized magnetic moment of about 2.9 μ_B.[7)] Below the Néel temperature, the localized Co moments are strongly coupled with the spin density wave of the matrix. In the alloys with Co more than about 1 at%, the sinusoidal spin density wave state transforms to a simple antiferromagnetic state.[8)] ^{59}Co resonance in the antiferromagnetic state was obtained at about 67 MHz in zero external field.[9)] In the dilute $\underline{V}$Co alloys, on the other hand, Co atoms have no magnetic moment. Recent NMR study in this system[10)] has indicated that the virtual bound state of Co atom spreads out into the conduction electron states of the host metal, and Co atom is completely nonmagnetic in Friedel-Anderson sence. Then it would be expected that the magnetic state of Co atom widely changes from the magnetic limit to the nonmagnetic limit by changing the composition of the matrix $Cr_{1-x}V_x$, so it will be interesting to investigate the intermediate region between $\underline{Cr}$Co and $\underline{V}$Co alloys.

In $\underline{MoNb}$Fe alloys, whose matrix is just below the $Cr_{1-x}V_x$ alloy in the periodic table, the local moment formation of Fe impurity

is a little complicated. The results of the magnetic susceptibility measurement[11] and Mössbauer effect study[12] have indicated that the Fe atoms surrounded by more than seven Mo atoms in their nearest neighbor sites have a magnetic moment of 2.2 μ_B, and the others are nonmagnetic, as are first pointed out by Jaccarino and Walker.[13] The similar "environment effect" is also observed in RhPdCo[13] and TiMoCo[14] alloys. It is also interesting to investigate whether this "environment effect" is observed also in $Cr_{1-x}V_xCo$ alloys.

Mo is the 4-d transition element placed just below Cr in periodic table. The spin density wave in Cr metal does not exist in Mo metal. It has been known from NMR[15], magnetic susceptibility[16] and electric resistance measurements,[17] that the dilute MoCo system is typical Kondo alloy and the Kondo temperature is about 45 K. It is also well known that Cr and Mo are just placed in a valley of the density of states of conduction electrons on bcc phase of transition metals. Then, in order to investigate the change of the magnetic states of Co atom against the density of states of conduction electrons, Re metal which is placed in 5-d transition series in right neighbor of Mo, is introduced into host metal. Moreover, the superconducting transition temperature increases rapidly from 0.92 K to about 12 K when Re metal is introduced to Mo metal.[18] Then, MoReCo alloy is the favorable system to investigate the impurity effect not only at host sites but impurity sites in the superconducting state. Recent theories have

predicted that the localized excited state is formed in the superconducting energy gap. In this MoReCo system, we will study at first place the magnetic state of Co atom in normal state, and then supply the experimental informations in superconducting state.

These stand points in these systems are illustrated in Fig.1.

§ 2. Experimental

(1). Sample Preparation.

(A). $Cr_{1-x}V_xCo$ Alloys.

The purities of the starting materials used in this work were following : V and Cr were 99.99 % pure and Co were 99.9 % pure. The samples were prepared by fusion of the elements in an argon arc furnace using a tungsten electrode and a water cooled hearth of copper. The ingots were remelted most usually at least eight times for homogeneity. In order to insure homogeneity all alloys thus obtained were annealed at 1200 °C for one week under an argon gas. Several alloys are cut into two parts. One was used in NMR measurements, and the other was used in magnetic susceptibility measurements. The compositions of V and Co in the alloys used in magnetic susceptibility measurements were determined by chemical analysis. The relative accuracy of the nominal concentration was estimated better than 1 % and 0.1 % for V and Co, respectively. The ingots were crushed and powdered in an agate mortar for NMR measurement. The particle size is smaller than 74 μ. The crystal structure of these powdered samples was confirmed to be bcc phase by X ray diffraction.

(B) $Mo_{1-x}Re_x$(V)Co Alloys

The purities of Mo, Re, V and Co metals used in this work were 99.98, 99.99, 99.99 and 99.99 % ,respectively. In order

to investigate the electronic structure of the matrix, a few percent V metal was introduced as a probe. The appropriate quantity of these powdered starting metals were mixed and hydrostatically pressed into a small briket. The obtained briket was melted in an argon arc furnace. The ingots were remelted at least ten times for homogeneity. On the sample annealed at 1500 °C for 24 hours in vacuo, the transverse decay curve in NMR measurement did not indicate a single exponential one, however, on the sample with no heat treatments, a single exponential decay curve was observed. Then measurements were performed on the samples with no heat treatment. The ingots were crushed into powder for NMR measurements. The crystal structure of these samples was confirmed to be bcc phase by X ray diffraction.

(2). NMR Method.

The measurements in paramagnetic phase were accomplished with the phase coherent crossed-coil spin echo spectrometer at the frequencies of 3, 4.7, and 10 MHz. In the cases of need, a high speed multichannel signal averager and a boxcar integrator were employed to improve the signal-to-noise ratio. The former was most convenient to measure spin-lattice relaxation time T_1 and transverse relaxation time T_2, while the latter was especially useful to obtain resonance profiles and resonance shifts. Temperature measurements below 4.2 K were based on the appropriate vapor pressure scale. Temperatures from 4.3 to 77 K were achieved by passing cold He gas over the

sample near which a AuCo 2.1 % thermo couple junction was placed.

Resonance shifts of ^{59}Co were obtained at constant frequency by comparing the measured field strength at maximum resonance intensity against the following frequency/field ratio.

$$^{59}Co : \quad \nu^{(59)}/H = 1.0054 \text{ KHz/Oe}^{19)}$$

The field strength was determined by measuring the ^{27}Al NMR frequency in liq.$AlCl_3$ placed near by the sample using the frequency/field ratio.

$$^{27}Al : \quad \nu^{(27)}/H = 1.1094 \text{ KHz/Oe}$$

The NMR measurements of ^{27}Al were performed with CW spectrometer.

The nuclear spin-lattice relaxation times T_1 were measured from a recovery of the spin echo amplitude after the sequence of rf pulses which saturate the nuclear magnetization.
When the direct measurement of T_1 was difficult , T_1 was estimated from the temperature dependence of the transeverse relaxation time T_2 as will be described later. T_2 was determined from a reduction of the spin echo amplitude against the interval between two pulses. Spin echo amplitude depends on this interval τ , as

$$M = M_0 \exp(-2\tau/T_2)$$

here, M is the observed echo amplitude. The true echo intensity M_0 is obtained by extrapolating to $\tau=0$ in intensity measurements.

The NMR measurements in antiferromagnetic phase were performed with the phase incoherent frequency valiable spin echo spectrometer in zero external field. The line shape was determined by plotting the amplitude of the spin echo signal against frequency. In order to obtain true line shape, the corrections for the transverse relaxation described above and for the different Boltzmann factor at respective frequencies were considered. The rf field strength in the sample coil was kept as constant as possible over the frequency range from 15 MHz to 80 MHz.

(3). Measurements of The Superconducting Transition Temperatures.

The superconducting transition temperature $T_c(0)$ in zero field was measured by a.c. susceptibility, while the transition temperature $T_c(H)$ in a field was determined as follows. The upper critical fields Hc_2 were measured by a.c. susceptibility at respective temperatures to obtain Hc_2 vs. T curve, and then $T_c(H)$ was estimated in respective fields. The temperatures below 4.2 K were determined by the vapor pressure of liq. ^{4}He and above 4.2 K were determined by the temperature dependence on the resistance of a carbon resistor. The measurements were performed on powdered samples after etching the surface of ingots.

(4). Magnetic Susceptibility Measurements.

Magnetic susceptibility measurements were performed with usual magnetic balance method.

§ 3. Experimental Results

(A). $\underline{Cr_{1-x}V_xCo}$ Alloys.

(1). Magnetic Susceptibility Measurements.

In first place, we describe results of the magnetic susceptibility measurements which supply macroscopic information for the magnetic state of Co impurities. In order to investigate the contribution of Co atoms to the magnetic susceptibilities, we have measured the temperature dependences of susceptibilities in $\underline{CrV_{99}Co_1}$ and in CrV alloys. The measurements were made in a number of fields up to 10.1 KOe over the temperature range 4.2 K to 660 K. Magnetization did not change linearly with the magnetic field and bended slightly in higher magnetic field. This field dependence of the magnetic susceptibility was stronger at low temperature and was observed even in the matrix, so cannot be accepted all as being due to impurity-impurity interactions. Then all magnetic susceptibilities of these alloys were measured in low magnetic field, 4.8 KOe for initial susceptibilities. As a typical example, the temperature dependences of the susceptibilities in $(Cr_{0.95}V_{0.05})_{99}Co_1$ and $Cr_{0.95}V_{0.05}$ alloys were shown in Fig.2. The susceptibility in $(Cr_{0.95}V_{0.05})_{99}Co_1$ alloys has a maximum value at about 25 K which we assign to the ordering temperature T_N of this system. We assume in this figure that the susceptibility of a magnetically dilute alloy χ_a is the sum

of an impurity susceptibility χ_i and a background matrix susceptibility χ_m, as

$$\chi_a = f\chi_i(T) + (1-f)\chi_m(T)$$

where f represents a fraction of the impurity. Then the value of χ_i is obtained by subtraction of the appropriate curve over the entire temperature range. Thus obtained χ_i could be written experimentally as follows,

$$\chi_i(T) = \chi_0 + C/T + \theta$$

where χ_0 is the temperature independent term, C and θ are regarded as Curie-constsnt and Curie-Weiss temperature, respectively. Since any kind of local moment behavior of the susceptibility should disappear as T^{-1} when $T\to\infty$, χ_0 can be determined directly from very high temperature measurements. The large χ_0 value has previously been reported for RhMn and MoCo alloys,[16] but has not clearly been attributed to a certain origin and only used as a parameter in a least-square-fit analysis to an above formura. The very large χ_0 value in X=0.25 alloy may be specially attributed to a contribution from the nonmagnetic Co atoms in this alloy as will be described later. Fig.3 shows the temperature dependences of $\Delta\chi^{-1} = (\chi_i - \chi_0)^{-1}$ in $CrV_{99}Co_1$ alloys for the concentration X from 0 to 0.25. The strong temperature dependences of $\Delta\chi$ reflect the local moment behavior of Co atom. As can be seen in this figure, the slope of this curve increases with the increase of V concentration. In X=0.3 alloys, the susceptibility of the alloy was in agreement with that of the matrix within

experimental errors, that is , $\chi_i - \chi_0 \approx 0$. The impurity moment can then be estimated from the slope of $\Delta\bar{\chi}^1$ vs. T curve in Fig.3. In Fig.4 the magnitude of the localized moment of Co impurity, μ_{eff} is plotted vs. the concentration X. The value of the magnetic moment on $Cr_{99}Co_1$ alloy is in good agreement with the value reported previously by Suzuki and Booth.[7] As can be seen in this figure, the magnetic moment is reduced slowly with increasing X. For $X \leq 0.04$ alloys, the spin density wave state is formed at $T \leq T_N$, but the magnetic moment at $T > T_N$ decreases monotonically over this region. Near the concentration with X=0.3, the moment disappears fastly. The values χ_0 , θ, μ_{eff}, and T_N are listed in Table I.

(2). Results of the Nuclear Magnetic Resonance.

(2-1). Antiferromagnetic State.

According to the previous report in CrCo alloys[9], ^{59}Co resonance in the antiferromagnetic state was obtained at about 67 MHz in zero external field. When Co concentration increased, two sub-peaks, which were attributed to Co having one and two Co atoms in its nearest neighbor sites, were found. The resonance line shape in CrVCo alloys is shown in Fig.5. The main peak corresponding to isolated Co sites shifts to lower frequency with the increase of V concentration. The first sub-peak observed in 3 at% Co alloys also shifts to lower frequency. These shifts indicate the reduction of the internal field of ^{59}Co. If one assumes that the localized moments

above T_N as described above are not changed below T_N and the internal field is related mostly with a hyperfine interaction between the localized moment and the associated nucleus, this reduction of the internal field is consistent with the X dependence of localized moments of Co atoms in the susceptibility measurements. The observed signals in antiferromagnetic states were obtained until X=0.05 and X=0.07 for Co 1 at% and 3 at% alloys, respectively. An addition of V metal to Cr reduces the ordering temperature T_N. The spin density wave state of the matrix persists to the alloy of V 4 at%[20]. CrVCo alloys are considered to be the system where the randomly distributed localized moments are ordered through conduction electron spin polarizations. In this system, as will be described minutely in PART Ⅱ, a reduction of T_N leads to a rapid decrease of the nuclear spin-lattice relaxation time which makes the observation of ^{59}Co resonance in larger X alloys hard by the pulsed NMR method. In $X \geq 0.1$ alloys, the magnetic ordering was not observed at least down to 4.2 K in the magnetic susceptibility measurements. We believe that T_N in $X \geq 0.1$ alloys are lower than the liq.^{4}He temperature because NMR results did not indicate a character of an ordering state.

(2-2). Paramagnetic State.

(a). Knight Shift K of ^{59}Co.

According to the previous report, the Knight shift of ^{59}Co in dilute VCo alloys is K=+1.57 % and independent of the

concentration of Co.[10] When Cr metal is introduced to V, ^{59}Co signals from nonmagnetic Co atoms were observed at 10 MHz in external field in $X \geq 0.2$ alloys. The X dependence of Knight shift in the alloys containing 1 at% Co measured at 1.2 K is shown in Fig.6. The value K=+1.7 % for X=0.9 alloy in our measurement, which is slightly large compared with that of VCo alloy, at first gradually and then rapidly reduces to K=+0.25% in X=0.2 alloy. As will be described later it is considered that the states of Co atom in X=0.25 and 0.2 alloys are rather magnetic compared with those in large X alloys and impurity-impurity interaction may affect resonance results. So, the concentration dependences of K were measured and results were indicated in Fig.7. The value K dose not so change with concentrations of Co in X=0.25 alloys, while the slight concentration dependence is observed in X=0.2 alloys. One would expect that the ^{59}Co resonance results on X=0.2 alloys with the concentrations less than 0.5 at% Co represent characters of the isolated impurity.

Although ^{59}Co resonance is not observed in the alloys for $0.15 \geq X > 0.07$ and K in X=0.2 alloys is very small but still positive, it is considered that the X dependence of K may suggest that the sign of the internal field of ^{59}Co in an antiferromagnetic state is negative.

(b). Linewidth of ^{59}Co.

The linewidth which is full value between half-amplitude points of spin echo amplitude is shown in Fig.8. The width is

fairly narrow in large X alloys but rapidly increases with decreasing X over X=0.4. This X dependence of width corresponds to that of the resonance shift. In X=0.2 and 0.25 alloys, the linewidth depends on the concentration of Co. The severe line broadening of ^{51}V in AuV[21], ^{59}Co in MoCo[15] and in CuCo[22] alloys at low temperatures were attributed to an inhomogeneous magnetic polarization of the impurities due to the s-d coupling between the local d-spin magnetization and RKKY conduction electron spin polarization(so-called "d-d double resonance mechanism")[23]. This indirect mechanism leads to a linewidth which is proportional to the square of the local d-spin susceptibility and to the impurity concentration. It may be considered that in X=0.3 alloys, the local d-spin susceptibility gradually appears and broadens the linewidth. However all of the linewidth cannot be attributed to the above mechanism since the concentration dependence is not very large. The residual linewidth in a limit of zero concentration may be attributed to the electric quadrupole broadening. Moreover the fluctuations of microscopic compositions in a host binary alloy may change the magnetic state of Co atoms and produce the broadening.

(c) Integrated Intensity for ^{59}Co Resonance.

The integrated intensities measured at 1.2 K are shown in Fig.9. The integrated intensity is generally proportional to the numbers of Co atoms associated with NMR signals. Fig.9 indicates that the numbers of Co atoms contributing to NMR

signals are about 78 % and 34 % in X=0.25 and 0.2 with Co 1 at% alloys ,respectively, of the values in $X \geq 0.3$ alloys. One would expect that ^{59}Co resonances from Co atoms with localized moments can not be observed by a pulsed NMR method because of excessively large shifts and of very fast nuclear spin relaxations through local moment fluctuations. Then the results of NMR and magnetic susceptibility indicate the coexistence of the nonmagnetic(no localized moment) and magnetic(localized moment) Co atoms in X=0.2 and 0.25 alloys. Fig.10 and 11 show the Co concentration dependences of the integrated intensity in X=0.2 and 0.25 alloys, respectively. The integrated intensities are almost proportional to Co concentrations which suggests the coexistence is a intrinsic nature in these systems.

(d) Nuclear Spin-Lattice Relaxation Time of ^{51}V.

The results of T_1 of ^{51}V are shown in Fig.12. The measurements in respective X alloys were achieved at 77 K because we wanted to eliminate contributions to T_1 from Co impurities as described later. The density of states of conduction electrons at the Fermi level on host V sites reflect on $(T_1T)^{-1}$ of ^{51}V measured at 77 K. As can be seen in Fig.12, T_1T of ^{51}V increases with decreasing X in qualitatively consistent with the X dependence of the density of states of conduction electrons illustrated in Fig.1. These results are in good agreement with the previous results in $Cr_{1-x}V_x$ alloys.[24)]

The temperature dependence of T_1 in X=0.2 and 0.3 alloys is shown in Fig.13. Measurements were performed on samples

with Co concentration 0, 0.1, 1 at% in X=0.2 alloys. The relaxation times in X=0.2 with Co 0.1 and 1 at% alloys do not follow a relation of T_1T=const., while T_1 in X=0.2 with Co 0 at% and X=0.3 with Co 1 at% alloys follow this relation. As described above, X=0.2 with Co 0.1 and 1 at% alloys, Co atoms with localized moment exist, then it will be considered that fluctuations of this moment make an additional relaxation path in matrix V sites. Various mechanisms have been considered for this relaxation processes, thus so-called BGS, GH mechanisms including the interaction between host nuclear spins and localized moments via RKKY interaction, and LD mechanism including direct dipole interactions between these spins.[5] These mechanisms make the relaxation time deviate from T_1T=const. that is the value in a system with no impuruties, and the deviation on T_1^{-1} is proportional to impurity concentration in all mechanisms. It is not our main purpose to obtain any convincing conclusions for these mechanisms on CrVCo alloys, however, it is considered qualitatively that the observed deviations from T_1T=const. indirectly indicate the existence of Co atoms with localized moments even in Co 0.1 at% alloy.

(e) Nuclear Spin-Lattice Relaxation Time of ^{59}Co.

The results of T_1 of ^{59}Co in respective X alloys containing 1 at% Co are shown in Fig.12 with the results of ^{51}V. In X=0.2 with Co 0.5 at% alloy, T_1 could not be measured directly for a poor spin echo intensity, then we have estimated T_1 from the temperature dependence of T_2. The temperature dependence of T_2 for Co 0.5 at % and 1 at% alloys is shown in Fig.14.

The experimental decay rate has the form $T_2^{-1} = T_2^{*-1} + AT$. The intercept T_2^{*-1} represents an intrinsic nuclear spin-spin interaction rate. The temperature dependent term A can be attributed to the life time effects resulting from spin-lattice relaxation process. According to Walstedt,[25] the rate AT can be represented $AT = \alpha T_1^{-1}$ assuming isotropic fluctuations of a hyperfine interaction. α is the enhancement factor to be equal to $(I+1/2)^2$ when first-order electric quadrupole broadening is so strong that only the central $(1/2 \leftrightarrow -1/2)$ transition is excited by the pulsed rf field. We have used this value $(I+1/2)^2 = 16$ for ^{59}Co. For the uncertainty of α, we have measured T_1 using both this indirect method and direct comb pulse method in Co 1 at% alloy. T_1T measured from the direct and indirect technique are 60 msecK and 59 msecK, respectively. The agreement is satisfactory within experimental errors.

It is cosidered that T_1 of ^{59}Co reflects the dynamical properties in the magnetic state of Co atoms. As can be seen in Fig.12, T_1T of ^{59}Co in X=0.9 alloy has almost the same value as that of ^{51}V and increases with the decrease of X down to X=0.5 whose behavior is consistent with T_1T of ^{51}V, however, abruptly decreases in contrast to the results of ^{51}V when the V concentration is reduced below X=0.4. This abrupt change of T_1 is consistent with the results of Knight shift and linewidth, and suggests that Co atoms become more and more magnetic when the density of states of conduction electrons decrease with the decrease of V concentration.

(B). $Mo_{1-x}Re_x(V)Co$ Alloys.

(1). Superconducting Transition Temperature $T_c(0)$, $T_c(H)$.

Co concentration dependences of superconducting transition temperatures $T_c(0)$ in zero external field in X=0.2 and 0.3 alloys are shown in Fig.15. $T_c(0)$ is slightly reduced by introducing V metal to host alloy. The reduction rate is 0.2~0.4 K/%. On the other hand Co impurities drop $T_c(0)$ more drastically than V. As can be seen in this figure, $T_c(0)$ changes almost linearly with Co concentrations and the reduction rate in X=0.2 alloys is slightly larger than that in X=0.3 alloys, which may suggest Co atoms in X=0.2 alloy are more magnetic than those in X=0.3 alloy. The reduction rates are about 4.2 K/% and 6.7 K/% on X=0.3 with V 3 at%, and X=0.2 with V 1 at% alloys, respectively. In X=0.2 alloy , the sample is all in normal state in a temperature region and at respective magnetic fields used in NMR measurements. The NMR measurements in superconducting state were performed in $(Mo_{0.7}Re_{0.3})_{96}V_3Co_1$ alloy. The superconducting transition temperatures in respective fields for ^{51}V and ^{59}Co in this alloy are listed in Table Ⅱ.

(2). Results of NMR in Normal Phase.

(a). Knight Shift of ^{59}Co.

The Knight shifts K measured at 10 MHz are plotted against the concentration of X in Fig.16. The values at X=0 refer to reference 15. In X=0 alloys, ^{59}Co spectra indicate

the existences of two resonances.[15] One has small shift ($K \approx +0.5\%$) and the other has large negative value which depends on the concentration of Co. The resonance with small shift has recently been attributed to the intermetalic compound Mo_6Co_7.[15] It has been considered that the dependence on Co concentration of the resonance with large negative shift, which is associated with the true Co impurities in Mo metal, is almost due to this Mo_6Co_7. The strong concentration dependence in X=0 alloys becomes weak with the increase of X, and in X=0.3 alloys concentration dependence was not observed within experimental errors. In our measurement at 40 MHz, 1.4 K, the two resonances as in X=0 alloys were observed in $(Mo_{0.9}Re_{0.1})_{99}Co_1$ alloy, however, the echo intensity corresponding to Mo_6Co_7 was fairly suppressed compared with that in $Mo_{99}Co_1$ alloy. The same behavior was observed on ^{59}Co resonance line shape in $(Mo_{0.95}Cr_{0.05})_{99}Co_1$ alloy, in which the echo intensity corresponding to Mo_6Co_7 is largely suppressed and Knight shift of ^{59}Co is $K=-6.4\%$ which is relatively large compared with that in $Mo_{99}Co_1$. It may be considered that a creation of Mo_6Co_7 is prevented when Re or Cr are supplied into MoCo alloy. As ^{187}Re and ^{185}Re resonances with severe second-order quadrupole broadenings overlap ^{59}Co resonance at 40 MHz, we have performed NMR measurements at 10 MHz where ^{187}Re and ^{185}Re resonance lines are further broadened and the intensities are negligibly small compared with that of ^{59}Co. The absolute value of the Knight shift decreases with increasing X. The decrease of the negative shift indicates the reduction of the impurity d-spin susceptibility.

(b). Nuclear Spin-Lattice Relaxation Time of ^{51}V and ^{59}Co.

The relaxation measurements were performed in 1 at% Co alloys. T_1 of ^{51}V was measured by comb pulse sequence method, while T_1 of ^{59}Co was measured directly by comb pulse method and indirectly from the temperature dependence of T_2. As a typical example, the temperature dependence of T_2 of ^{59}Co in X=0.2 alloy is shown in Fig.17. T_1T estimated by the same way as that described in CrVCo alloys is 20.5 msecK in just agreement with the value by the direct measurement at 1.2 K, 20.5 msecK. The intrinsic spin-spin relaxation rates T_2^{*-1} are obtained as 0.80 $(msec)^{-1}$ and 0.92 $(msec)^{-1}$ at 10 MHz and 4.7 MHz, respectively. This difference may be attributed to the field dependence of the linewidth. T_1 of ^{51}V and the estimated T_1 from T_2 of ^{59}Co in this alloy are plotted against T^{-1} in Fig.18. T_1 of ^{51}V obeys the relation T_1T=2.7 secK. It is noted that T_1 of ^{59}Co is in two orders of magnitude shorter than that of ^{51}V.

T_1 of ^{51}V in X=0.3 alloy is shown in Fig.20. The sample is in normal state in a magnetic field of 8.93 KOe down to 3.4 K. T_1 obeys the relation T_1T=2.1 secK in this normal region. The temperature dependence of T_2 of ^{59}Co in this sample is indicated in Fig.21. As can be seen in Table Ⅱ, this sample is in superconducting mixed state below 2.8 K in resonance field of 10 MHz, however, the temperature dependence of T_2 at 10 MHz indicates that T_1 of ^{59}Co persists to obey T_1T=const. The estimated value T_1T=24.2 msecK is also in good agreement

with the value by the direct measurement at 1.2 K, T_1T=26 msecK. The obtained T_2^{*-1}=0.90 $(msec)^{-1}$ is reasonable value compared with that of X=0.2 alloy.

The X dependences of T_1 of ^{51}V and ^{59}Co in normal state are shown in Fig.19. The dependence of ^{59}Co on X is opposite to that of ^{51}V. It is considered that the variation of the density of states of conduction electrons against X reflects on the result for ^{51}V, while the result for ^{59}Co indicates that the state of Co atom becomes further nonmagnetic with the increase of X, and is consistent with that of the Knight shift.

(3). Nuclear Spin-Lattice Relaxation in Superconducting Mixed State.

(a). T_1 of ^{51}V : Host Site.

T_1 of ^{51}V in each resonance field is indicated in Fig.20. In the superconducting mixed state, T_1 changes as $\exp(\Delta/k_BT)$ below the temperature corresponding to about $T_C(0)/T$=1.6, here 2Δ=3.5 $k_BT_C(0)$, except the results of 10 MHz where the resonance field is very close to the upper critical field Hc_2. Hc_2 at T=0 is about 15 KOe in this system. This low temperature behavior is consistent with the previous reports on the T_1 measurements in type Ⅱ superconductors[26], where it has been indicated that the order parameter in the region near the vortex center of about the coherence length is appreciably reduced from its zero field value, while the order parameter in the region far from the vortex core is equal to the value Δ_0

in zero external field at 0 K, under the condition $Hc_2 \gg H_{ext} \gg Hc_1$, then the order parameter in most part of the sample is equal to its zero field value and T_1 changes as $\exp(\Delta_0/k_BT)$.

In low temperature of about $T_c(0)/T \gtrsim 3$, T_1 deviates from this BCS like behavior. This suppression of the relaxation time can be interpreted from their field dependences that a relaxation to the vortex cores through spin diffusions becomes important rather than the direct relaxation to thermally excited conduction electrons.

According to previous reports for the usual type II superconductors, the dip of the relaxation time has been observed just below the transition temperature $T_c(H)$[26], however, this dip was not observed in this sample. The behavior of T_1 of ^{51}V at low temperature is as in usual type II superconductor and no appreciable impurity effect could be observed except near the transition temperature $T_c(H)$.

(b). T_1 of ^{59}Co : Impurity Site.

As is described in the section of normal phase, the temperature dependence of T_2 indicates that T_1T=const. down to 1.2 K at 10 MHz where the resonance field is very close to Hc_2. As is shown in Fig.21, the temperature dependence of T_2 at lower frequency 4.7 MHz does not clearly indicate T_1T=const. T_2^{-1} decreases more rapidly with decreasing temperature and tends to a constant value. From the measurement at liq.^{3}He temperature, 0.6 K, T_2^{*-1} is estimated as $1.05 \sim 1.10$ (msec)$^{-1}$.

As described above, $T_1^{-1} = (T_2^{-1} - T_2^{*-1})$, then obtained T_1 at respective temperatures are plotted against $T_C(0)/T$ in Fig.22. The agreement between the estimated T_1=105 msec (T_2^{*-1}=1.10 $(\text{msec})^{-1}$), 80 msec (T_2^{*-1}=1.05 $(\text{msec})^{-1}$) and the directly measured T_1=74 msec at 1.2 K is satisfactory. T_1 is nearly proportional to $\exp(\Delta'/k_BT)$, and the "effective energy gap" at Co sites, Δ' is obtained as $2\Delta' \sim 1.8\ k_BT_C(0)$ which is relatively smaller than the value $2\Delta = 3.5\ k_BT_C(0)$ for the host V sites in spite of large experimental errors.

§ 4. Discussions

(A). Localized Moment of Co Impurity in CrVCo Alloys.

The magnetic susceptibility measurements and the NMR measurements indicate the coexistence of the magnetic (with localized moment) and the nonmagnetic (with no localized moment) Co impurities in at least X=0.2 and 0.25 alloys. One can not generally separate these two kinds of Co atoms in susceptibility measurement in which the effective moment is obtained assuming that all Co atoms have the same contribution to the susceptibility. If the moment of the each magnetic Co atom has a same value, μ_0 and nonmagnetic Co atoms do not contribute to the susceptibility with Curie-Weiss behavior, μ_0 is obtained from the measured μ_{eff} as

$$\mu_0 = \mu_{eff}\sqrt{N/N_{mag.}} = \mu_{eff}\sqrt{N/N-N_{nonmag.}}$$

here N, $N_{mag.}$ and $N_{nonmag.}$ are the numbers of total, magnetic and nonmagnetic Co atoms in the alloy, respectively. In X=0.2 and 0.25 alloys, $N_{nonmag.}/N$ were estimated in previous section. Then the values of $\mu_0 = 2.0(\pm 0.2)\,\mu_B$ and $1.7(\pm 0.8)\,\mu_B$ are obtained in X=0.2 and 0.25 alloys, respectively, and plotted in Fig.4. The magnitude of the localized moment, $3\mu_B$ in CrCo alloy reduces to about $2\,\mu_B$. This reduction of the magnitude is more directly shown in the X dependence of the internal field of ^{59}Co in antiferromagnetic phase. The values of $H_{int.}$ and μ_{Co} normalized at CrCo alloy are indicated in Fig.23, where $\mu_{Co} = g\,\mu_B S$ is

obtained from $\mu_{eff}=g\,\mu_B\sqrt{S(S+1)}$ assuming that g=2 and all Co atoms have localized moment in this region. The X dependences of these normalized μ_{Co} and $H_{int.}$ are fairly consistent with each other. Therfore, it would be concluded that the magnitude of the moment of Co atoms with localized moments decreases with the increase of X from 3 μ_B to about 2 μ_B.

In $\underline{Mo_{1-x}Nb_x}Fe$ alloys, μ_0 is not dependent on Nb concentration X. The X dependence of μ_{eff} follows a relation

$$(\mu_{eff}/\mu_0)^2 = P_Z^z(X) \qquad P_Z^z(X) = \sum_{r=z}^{Z} \frac{Z!}{r!(Z-r)!}(1-x)^r x^{Z-r}$$

Here $P_Z^z(X)$ is the probability that one Fe atom has more than z Mo atoms in its nearest neighbor sites ; z=7 for MoNbFe alloys. In Fig.24, $(\mu_{eff}/\mu_0)^2$ is plotted against X in CrVCo alloys when μ_0 is taken as that of CrCo alloy. $(\mu_{eff}/\mu_0)^2$ does not fit $P_Z^z(X)$ line for any z value, and takes values between z=7 and z=8. In $X \geq 0.25$ alloys, $(\mu_{eff}/\mu_0)^2$ decreases more rapidly against X than $P_Z^z(X)$. N_{mag}/N obtained from the integrated intensity changes more rapidly with X than $P_Z^z(X)$, and crosses the line of z=7. Then it will be considered that z=7 is important condition for the coexistence, however, the coexistence is controlled not only by the configuration of nearest neighbors but also additively by long range effect.

(B). Nonmagnetic Co Impurity in CrVCo Alloys.

In general, the Knight shift of ^{59}Co supplies the information for the static feature of the magnetic state of Co

impurity, while the relaxation time supplies the information for the dynamical one. It will be considered that the Knight shift and the relaxation time for ^{59}Co in this system are owing to the impurity d-spin (core-polarization) and d-orbital hyperfine interactions. The observed K and T_1 for Co impurity are written when significant spin-orbit interaction is absent and d-spin and d-orbital interaction contribute separately,

$$K = K_d + K_{orb} \qquad T_1^{-1} = T_{1d}^{-1} + T_{1orb}^{-1}$$

We have ignored the direct s-contact interaction because its contribution is expected to be relatively unimportant for most 3-d impurities. It is generally known that K_d is negative and K_{orb} is positive. The shift and relaxation rate may be expressed in terms of the local d-spin and d-orbital susceptibility as

$$K_{(i)} = \mu_B^{-1} H_{hfs}^{(i)} \chi_{(i)}^{zz}(0)$$

$$T_{1(i)}^{-1} = k_B T \mu_B^{-2} \gamma_n^2 (H_{hfs}^{(i)})^2 \lim_{\omega \to 0} \chi_{(i)}^{+-}(\omega)/\omega$$

where $H_{hfs}^{(i)}$ is the appropriate hyperfine field per Bohr magneton, γ_n is the nuclear gyromagnetic ratio, and the other symbols have usual meaning. Dworin and Narath [27] have calculated the susceptibilities within Random Phase Approximation starting from the nonmagnetic Hartree-Fock ground state for the five-fold degenerate Anderson model, and obtained the local d-spin and d-orbital Korringa relation as

$$K_d^2 T_{1d} T = 5\mathcal{S} \qquad K_{orb}^2 T_{1orb} T = 10\mathcal{S}$$

$$\mathcal{S} = (\gamma_e/\gamma_n)^2 (\hbar/4\pi k_B)$$

here, γ_e is the gyromagnetic ratio of a conduction electron. Although the HF approximation is not suitable for dilute alloy systems, Shiba[28] has recently proved on the basis of the Yamada and Yosida theory for the ground state of the Anderson model that the Korringa relation is still valid at low temperature $T \ll T_K$ and low field $H \ll H_K$ ($H_K \approx k_B T_K / \mu_B$) in any order of U and J. In following, we want to discuss the magnetic state of Co impurities on this Korringa relation. The Korringa relation indicates that measurements of only K and T_1 are sufficient to investigate the magnetic state of an impurity. If the observed Knight shift and relaxation time obey this relation, one obtains the experimental Korringa product

$$K^2 T_1 T/\mathcal{S} = 10\ (1+\xi)^2/(2+\xi^2)$$

as pointed out by Narath et. al[29], here $\xi = K_{orb}/K_d < 0$ Then $K^2T_1T/\mathcal{S}$ must be in the range from 0 to 10, depending on the relative magnitude of K_d and K_{orb}. Experimental values of $K^2T_1T/\mathcal{S}$ are shown in Table Ⅲ. It is apparent that the model is appricable to the $X \leq 0.3$ alloys. In $X \geq 0.4$ alloys, the relaxation rate is rather small for large Knight shift. In V Co alloy, it has been considered that the large positive Knight shift of ^{59}Co is due to field induced Van Vleck orbital paramagnetism[10] which does not so much contribute to nuclear relaxation and the Van Vleck orbital susceptibility is not related to the Korringa relation[30]. One would expect that the first order orbital angular momentum vanish and any orbital contribution is then one of the Van Vleck type when the width of the

virtual bound state is strongly broadened and one can not distinguish the impurity d-state and conduction electron states of host transition metal. As can be seen in Fig.12, the increase of T_1T of ^{59}Co as well as ^{51}V in $X \geq 0.5$ alloys directly indicates that the impurity d-state spreads out into the band of conduction electrons and the local density of states at Co site varies in the same way as that of matrix V site. In X=0.25 and 0.2 alloys, the coexistence is observed as described above. It is not clear how the environment effect affects the magnetic state of Co impurity. However the results of K and T_1 in X=0.3 alloy where no localized moment exists suggest that the Korringa relation is useful in X=0.2 and 0.25 alloys. The estimated K_d and K_{orb} for $X \leq 0.3$ alloys are listed in Table Ⅲ. K_{orb} does not so change, but K_d changes more rapidly with the decrease of X. The X dependence of K in Fig.6 would be attributed to this negative contribution of K_d, and the abrupt increase of the relaxation rate in Fig.12 would be attributed to these enhanced local d-spin fluctuations.

In HF-RPA approximations, the static d-spin and d-orbital susceptibilities can be written as[27)]

$$\chi_d(0) = \lim_{\omega \to 0} \mathrm{Re}\, \chi_d(\omega) = 2 \rho_d \mu_B^2 (1-\alpha_d)^{-1}$$

$$\chi_{orb}(0) = \lim_{\omega \to 0} \mathrm{Re}\, \chi_{orb}(\omega) = 4 \rho_d \mu_B^2 (1-\alpha_{orb})^{-1}$$

where ρ_d is the total density of states of the impurity d-state at the Fermi level. then $\rho_d = 5 \frac{\Gamma}{\pi} (E_d^2 + \Gamma^2)^{-1}$. E_d is the d-state energy measured from the Fermi level, so $\rho_d \sim \frac{5}{3\pi} \Gamma^{-1}$.

α_d and α_{orb} is the spin and orbital enhancement factors as

$$\alpha_d = \frac{1}{5}(U+5J)\rho_d \quad , \qquad \alpha_{orb} = \frac{1}{5}(U-J)\rho_d$$

The conditions $\alpha_d=1$ and $\alpha_{orb}=1$ mean the spin and orbital instability in HF approximation. $\alpha_d \gg \alpha_{orb}$, then the spin enhancement always precedes the orbital enhancement. In recent theoretical studies, these instability can not happen in dilute alloys, however, the HF-RPA results may represent the qualitative feature of the impurity d-state. Γ is written as $\Gamma = \pi \rho(\varepsilon_F)\cdot|V|^2$, here $|V|$ is the s-d mixing rate in Anderson Hamiltonian and $\rho(\varepsilon_F)$ is the density of states of conduction electrons at the Fermi level. Then one may interpret the change of K and the opposite behavior of T_1T of ^{59}Co to that of ^{51}V as that Γ becomes smaller and smaller with decreasing X and consequently χ_d and χ_{orb} are gradually enhanced assuming that $|V|$ is not dependent on the change of X.

(C). Magnetic State of Co Impurity in MoRe(V)Co Alloys in Normal Phase.

The experimental Korringa products $K^2T_1T/\mathcal{S}$ for respective X alloys are listed in Table Ⅳ. The condition $0 \leq K^2T_1T/\mathcal{S} \leq 10$

is satisfied in these alloys. The separated K_d, K_{orb} are also listed in Table Ⅳ. The absolute values of K_d decrease with the increase of X, while the values of K_{orb} does not so much change. As can be seen in Fig.16, the dependences of K on Co concentration are observed in $X \leq 0.2$ alloys. The relatively small values of K_{orb} or K_d in X=0.1 alloy compared with the others are owing to the concentration dependence of K. If one uses the observed values K=-4.2% and T_1T=6.9 msecK for $Mo_{99}Co_1$ alloy,[15] one can obtain the value of K_d= -5.5% and K_{orb}=+1.3%. These values are smaller than that for $Mo_{99.9}Co_{0.1}$ alloy listed in Table Ⅳ. As no dependence on Co concentration is observed in X = 0.3 alloy, K_{orb} does not change so much or rather slightly decreases with the increase of X for an isolated impurity limit. The reduction of observed absolute value of K may be attributed to that of K_d. When the same discussion as that for CrVCo alloys is applied, this behavior of K_d will be explained as that the width of the impurity d-state becomes large because of the increase of the density of states of conduction electrons as is illustrated in Fig.1, and as a result the enhancement of static and, at the same time, dynamical d-spin susceptibility is suppressed when Re concentration increases. It will be considered that the opposite behavior of T_1T of ^{51}V and ^{59}Co directly represent this qualitative view point.

On the other hand, one may consider the Kondo temperature of the system is proportional to χ_d^{-1}. If the hyperfine

coupling constant H_{hfs}^{d} does not depend on X, T_K may be estimated from the ratio of K_d for respective $X \neq 0$ alloys to that of X=0 alloy. These estimated values of T_K are also listed in Table Ⅳ. T_K increases with the increase of X.

(D). T_1 of ^{51}V and ^{59}Co in $(Mo_{0.7}Re_{0.3})_{96}V_3Co_1$ Alloy in Superconducting State.

T_1 supplies a useful information for the spectrum of excited state in superconductor. The effects of magnetic impurity against the excitation spectrum has been studied theoretically in two stand points. One is Müller-Hartmann Zittartz theory[31] based upon the s-d exchange model and the other is a theory by HF approximation of Anderson model with superconducting matrix by Shiba.[32] We will discuss the experimental results in terms of the magnetic state in normal phase described above refering the present theories.

In the experiment, as the magnetic field is applied, the imputity effect and the magnetic field effect to superconducting state may overlap. The presence of a magnetic field leads to a finite life time for Cooper pair between superconducting electrons, which makes the excitation spectrum spread. As a result, a field induced gapless superconducting state appears just below $T_C(H)$. Cyrot[33] calculated the nuclear spin-lattice relaxation rate in this gapless region in the dirty limit of a superconductor and indicated that a finite dip in the relaxation time appears in the case of $T_C(0) \geq T_C(H) \geq 0.6T_C(0)$ and

this dip becomes smaller and smaller when $T_c(H)$ approches to $0.6T_c(0)$, and in the case of $T_c(H) < 0.6T_c(0)$ the dip disappears. This magnetic field effect has been observed in many type II superconductors.[26]

T_1 of ^{51}V deviates apparently from the relation of $T_1T=$ const. at about $0.6T_c(0)$ which is consistent with the above magnetic field effect. However, in the region $T_c(0) \geq T \geq 0.6T_c(0)$, T_1 has not clear dip, and rather obeys the relation $T_1T=$const. This behavior may suggest that the life time of Cooper pairing would become shorter due to impurity-spin fluctuations. Apparent spin fluctuation effect in superconducting state has been reported in T_1 measurement of ^{27}Al in AlMn alloy,[34] where HF calculation of T_1 can not explain the observations with reasonable parameters of AlMn system.[35]

One may expect that the magnetic impurity effect may appear more directly in T_1 of imputity nucleus itself. As described in previous section, the different energy gap $2\Delta' = 1.8 k_B T_c(0)$ at Co sites from that of V sites may be attributed to this magnetic effect directly. The two theories described above have predicted a localized excited state in the superconducting energy gap. According to the HF theory which has not included the dynamical effect of impurity spin, a localized excited state is formed at very near the gap edge in HF nonmagnetic region. Then it will be not sufficient to explain the relaxation behavior of ^{59}Co in this frame work. On the other hand, MZ theory has predicted the existence of the localized excited state in terms of T_K and T_{CO} in the system as[36]

$$\omega = \pm \gamma \Delta \quad , \quad \gamma = \ln(T_K/T_{C0}) / \sqrt{(\ln(T_K/T_{C0}))^2 + \pi^2 S(S+1)}$$

where T_{C0} is the transition temperature in the sample with no impurities. For our system, T_{C0}=10 K , T_K=165 K and S=1 from the magnetic susceptibility measurement in MoCo alloy.[16] The value γ is estimated to be about 0.5, which means that the position of the localized excited state is fairly deep. MZ theory has also predicted the concentration dependence of $T_C(0)$ with a parameter, T_K/T_{C0}.[37] From this prediction, T_K are convertly estimated to be about 135 K and 1000 K for X=0.2 and 0.3 alloys, respectively. Using this T_K for X=0.3 alloy, γ is estimeted to be 0.7. It is considered that this localized excited state spread out in energetically when the impurity concentration increases. This deep excited state may be responsible for the observed energy gap at impurity Co site.

However, it has been considered that the MZ theory will not be appropriate in the case $T_{C0} \ll T_K$, since this theory is based upon Suhl-Nagaoka approximation. It is desirable to establish a theory for nuclear spin relaxation which includes the dynamical spin fluctuation correctly in any value of T_K.

Acknowledgements

I would like to express my sincere thanks to Professor J.Itoh for his valuable discussions. I would also like to express my sincere thanks to Professor K.Asayama for his guidances, valuable discussions and kind encouragements in the course of this work. I wish to express my hearty thanks to Professor A.Yoshimori for his stimulating discussions. I am gratefully indebted to Professor A.Tasaki and Mr. H.Akoh for their kind co-operation on the magnetic susceptibility measurement. Thanks are also due to Dr. T.Kohara and Dr. S.Wada for their discussions, and to Mr. Y.Ogawa for asistances in the experiments.

References

1) J.Friedel: Nuovo Cimento Suppl. 7(1958)287

2) P.W.Anderson: Phys. Rev. 124(1961)41

3) P.A.Wolff: Phys. Rev. 124(1961)1030

4) J.R.Schrieffer and P.A.Wolff: Phys. Rev. 149(1966)491

5) for example Magnetism vol.5 Part II(ed. by H.Suhl Academic, 1973)

6) K.Yosida and K.Yamada: Prog. Theor. Phys.Suppl.No46(1970)244
K.Yamada: Prog. Theor. Phys. 53(1975)970
K.Yosida and K.Yamada: Prog. Theor. Phys. 53(1975)1286
A.Yoshimori: Prog. Theor. Phys. 55(1976)116

7) T.Suzuki: J. Phys. Soc. Japan 21(1966)442
J.G.Booth: J. Phys. Chem. Solids 27(1966)1639

8) Y.Endoh,Y.Ishikawa and H.Ohno: J. Phys. soc. Japan 24(1968)263

9) T.Kohara and K.Asayama: J. Phys. Soc. Japan 39(1975)1263

10) S.Wada and K.Asayama: J. Phys. Soc. Japan 39(1975)352

11) H.Nagasawa and N.Sakai: J. Phys. Soc. Japan 27(1969)1150

12) L.J.Swartzendruber: Int. J. Magn. 2(1972)129

13) V.Jaccarino and L.R.Walker: Phys. Rev. Letters 15(1965)258

14) K.C.Brog and W.H.Jones: Phys. Rev. Letters 24(1970)58

15) A.Narath, K.C.Brog and W.H.Jones,Jr: Phys. Rev. B2(1970)58
A.Narath: Phys. Rev. B13(1976)3724

16) H. Claus: Phys. Rev. B5(1972)1134

17) T.Sugawara, M.Takano and S.Takayanagi: J. Phys. Soc. Japan 36(1974)451

18) J.K.Hulm and R.D.Blaugher: Phys. Rev. 5(1961)1569

19) R.E.Walstedt, J.H.Wernick, V.Jaccarino: Phys. Rev. 162(1967)301

20) Y.Hamaguchi, E.O.Wollan and W.C.Koehler: Phys. Rev. 138(1965)A737
W.C.Koehler, R.M.Moon, A.L.Trego and A.R.Mackintosh: Phys. Rev. 151(1966)405

21) A.Narath and A.C.Gossard: 183(1969)391

22) S.Wada and K.Asayama: J. Phys. Soc. Japan 30(1971)1337

23) B.Caroli: J. Phys. Chem. Solids 28(1967)1427

24) K.Kume and T.Fujita: J. Phys. Soc. Japan 19(1964)1245

25) R.E.Walstedt: Phys. Rev. Letters 19(1967)146, 19(1967)816

26) D.E.MacLaughlin: Solid State Phys. vol.31 (ed. by H.Ehrenreich, F.Seitz, and D.Turnbull Academic, 1976)

27) L.Dworin and A.Narath: Phys. Rev. Letters 25(1970)1287

28) H.Shiba: Prog. Theor. Phys. 54(1975)967

29) A.Narath and D.C.Barham: Phys. Rev. B7(1973)2195

30) V.Jaccarino: Proceedings Int. School Phys. (Enrico Fermi Course, ed. by W. Marshall Academic, 1967)

31) E.Müller-Hartmann: Magnetism vol.5 p.353 (ed. by H.Suhl Academic, 1973)

32) H.Shiba: Prog. Theor. Phys. 50(1973)50

33) M.Cyrot: J.Phys. (Paris) 27(1966)283

34) M.Daugherty, K.Parvin and D.E.MacLaughlin: Phys. Rev. Letters 31(1973)1485

35) K.Machida and A.Nakanishi: Prog. Theor. Phys. 55(1976)1

36) J.Zittartz and E.Müller-Hartmann: Z.Phys. 232(1970)11

37) E.Müller-Hartmann and J.Zittartz: Phys. Rev. Letters 26(1971)428

Figure Captions

Fig.1 Electronic specific heat coefficient γ in matrix CrV and MoRe alloys are represented. Open circle denotes the superconducting transition temperature. On the figure, magnetic state of Co impurity is indicated.

Fig.2 The temperature dependences of magnetic susceptibilities in $(Cr_{0.95}V_{0.05})_{99}Co_1$ and $Cr_{0.95}V_{0.05}$ alloys are indicated.

Fig.3 The temperature dependence of $\Delta\chi^{-1}$ for respective X alloys at $T \geq T_N$. $\Delta\chi^{-1}$ of X=0.05 alloy is placed between the results of X=0.03 and 0.1 alloys and omitted from this figure.

Fig.4 V concentration dependence of the observed effective moment(open circle). The closed circle denotes the estimated effective moment μ_0 (see the text).

Fig.5 NMR line shapes for respective X alloys in antiferromagnetic states. Solid and dotted curve represent the line shapes for Co 3 and 1 at% alloys, respectively.

Fig.6 X dependence of the Knight shift of ^{59}Co in $(Cr_{1-x}V_x)_{99}Co_1$ alloys measured at 10 MHz, T=1.2 K.

Fig.7 Co concentration dependence of the Knight shift measured at 10 MHz, T=1.2 K. ● $\underline{Cr_{0.8}V_{0.2}}Co$, ○ $\underline{Cr_{0.75}V_{0.25}}Co$

Fig.8 X dependence of the linewidth of ^{59}Co in $\underline{Cr_{1-x}V_x}Co$ alloys measured at 10 MHz, T=1.2 K.

○ Co 1 at%, ● Co 0.5 at%, ⊙ Co 0.3 at%.

Fig.9 X dependence of the integrated intensity of ^{59}Co resonance in $(Cr_{1-x}V_x)_{99}Co_1$ alloys measured at 10 MHz, T=1.2K.

Fig.10 Co concentration dependence of the integrated intensity of ^{59}Co resonance in $\underline{Cr_{0.8}V_{0.2}}Co$ alloys measured at 10 MHz, T=1.2 K.

Fig.11 Co concentration dependence of the integrated intensity of ^{59}Co resonance in $\underline{Cr_{0.75}V_{0.25}}Co$ alloys measured at 10 MHz, T=1.2 K.

Fig.12 X dependence of T_1T of ^{51}V(●) and ^{59}Co(○) in $(Cr_{1-x}V_x)_{99}Co_1$ alloys. T_1T of ^{51}V is measured at 77 K.

Fig.13 The temperature dependences of $(T_1T)^{-1}$ of ^{51}V in $Cr_{0.8}V_{0.2}$, $\underline{Cr_{0.8}V_{0.2}}Co$ and $\underline{Cr_{0.7}V_{0.3}}Co$ alloys measured at 10 MHz.

● $Cr_{0.8}V_{0.2}$, ⊗ $(Cr_{0.8}V_{0.2})_{99.9}Co_{0.1}$,
○ $(Cr_{0.8}V_{0.2})_{99}Co_1$ △ $(Cr_{0.7}V_{0.3})_{99}Co_1$

Fig.14 The temperature dependences of T_2^{-1} of ^{59}Co in $\underline{Cr_{0.8}V_{0.2}}Co$ alloy measured at 10 MHz.

● Co 0.5 at% ○ Co 1 at%

Fig.15 Co concentration dependence of $T_c(0)$ in MoRe(V)Co alloys.

⊗ $Mo_{0.7}Re_{0.3}$, ▲ $Mo_{0.8}Re_{0.2}$
● $(Mo_{0.7}Re_{0.3})V_3Co$ ⊙ $(Mo_{0.7}Re_{0.3})_{99}V_1$
△ $(Mo_{0.8}Re_{0.2})V_1Co$

Fig.16 X dependences of the Knight shift in $\underline{Mo_{1-x}Re_x}Co$ alloys and $(Mo_{1-x}Re_x)_{96}V_3Co_1$ alloys measured at 10 MHz, T=1.2K.

○ $(Mo_{1-x}Re_x)_{96}V_3Co_1$, ⊙ $\underline{Mo_{1-x}Re_x}Co$, ○ $\underline{Mo}Co$ from ref.15
The number indicates the Co concentration. In X=0.3 alloys, no concentration dependence on Co is observed within experimental errors.

Fig.17 Temperature dependences of T_2^{-1} of ^{59}Co in $(Mo_{0.8}Re_{0.2})_{96}V_3Co_1$ alloy, at 4.7 MHz ● and 10 MHz ○.

Fig.18 T_1 of ^{51}V and ^{59}Co estimated from T_2 in $(Mo_{0.8}Re_{0.2})_{96}V_3Co_1$ alloy are plotted against T^{-1}.
△ and ▲ are T_1 of ^{51}V at 3 MHz and 4.7 MHz, respectively.
○ and ● are T_1 of ^{59}Co at 10 MHz and 4.7 MHz, respectively.

Fig.19 X dependences of T_1T of ^{59}Co and ^{51}V in normal phase in $(Mo_{1-x}Re_x)_{96}V_3Co_1$ and $(Mo_{1-x}Re_x)_{99}Co_1$ alloys.
● ^{51}V in $(Mo_{1-x}Re_x)_{96}V_3Co_1$ alloys.
△ ^{59}Co by comb pulse method in $(Mo_{1-x}Re_x)_{96}V_3Co_1$ alloys.
○ ^{59}Co estimated from T_2 in $(Mo_{1-x}Re_x)_{96}V_3Co_1$ alloys.
◬ ^{59}Co by comb pulse method in $(Mo_{1-x}Re_x)_{99}Co_1$ alloys.
⊗ ^{59}Co from ref. 15

Fig.20 T_1 of ^{51}V in $(Mo_{0.7}Re_{0.3})_{96}V_3Co_1$ alloy is plotted against $T_c(0)/T$.
△ 3 MHz ● 4.7 MHz ○ 10 MHz
$T_c(H)$ in each resonance field is indicated by arrows.

Fig.21 The temperature dependences of T_2^{-1} of ^{59}Co in $(Mo_{0.7}Re_{0.3})_{96}V_3Co_1$ alloy at 4.7 MHz ● and 10 MHz ○ .

Fig.22 T_1 of ^{59}Co estimated from T_2 and obtained by comb pulse method in $(Mo_{0.7}Re_{0.3})_{96}V_3Co_1$ alloy are plotted against $T_c(0)/T$.
● 4.7MHz from T_2 ($T_2^{*-1}=1.05(msec)^{-1}$)
⊗ 4.7 MHz from T_2 ($T_2^{*-1}=1.10(msec)^{-1}$)
○ 10 MHz from T_2 ($T_2^{*-1}=0.90(msec)^{-1}$)
▲ 4.7 MHz by comb pulse △ 10 MHz by comb pulse
$T_c(H)$ in each resonance field is indicated by arrows.

Fig.23 X dependence of internal field of ^{59}Co and $\mu_{Co}=g\mu_B S$ in $\underline{Cr_{1-x}V_x}Co$ alloys normalized to $\underline{Cr}Co$ alloy.
● and ⊗ denote the normalized $H_{int.}$ for 1 and 3 at% Co alloys, respectively. ○ denotes the μ_{Co} which was estimated from $\mu_{eff}=g\mu_B\sqrt{S(S+1)}$ assuming g=2.

Fig.24 $(\mu_{eff}/\mu_0)^2$ is plotted against X. Solid lines represent $P_Z^z(X)$ on which z values are shown.
○ $(\mu_{eff}/\mu_0)^2$ for $\underline{Cr_{1-x}V_x}Co$ alloys
● N_{mag}/N from integrated intensity.
⊗ $(\mu_{eff}/\mu_0)^2$ for $\underline{Mo_{1-x}Nb_x}Fe$ alloys from ref. 11.

Table I

$(Cr_{1-x}V_x)_{99}Co_1$ Alloys

X	χ_o (10^{-6} emu/g)	θ (K)	μ_{eff} (μ_B)	T_N (K)
0	0.00(0.05)	0(5)	3.0(0.1)	300
0.03	0.16(0.02)	12(4)	2.7(0.1)	70
0.05	0.02(0.01)	25(5)	2.6(0.1)	25
0.10	0.00(0.01)	5(5)	2.4(0.1)	-----
0.15	0.22(0.05)	9(3)	2.0(0.1)	-----
0.20	0.04(0.01)	10(2)	1.6(0.1)	-----
0.25	0.29(0.08)	11(5)	0.8(0.2)	-----
0.30	----------	-----	0.0(+0.1)	-----

Table Ⅱ

$(Mo_{0.7}Re_{0.3})_{96}V_3Co_1$ Alloy

Nucleus	^{51}V			^{59}Co	
Frequency (MHz)	3	4.7	10	4.7	10
Resonance Field (KOe)	2.68	4.20	8.93	4.67	9.97
$T_C(H)$ (K)	5.1	4.9	3.4	4.8	2.8
$T_C(0)/T_C(H)$	1.08	1.12	1.62	1.15	1.96

Table III

$(Cr_{1-x}V_x)_{99}Co_1$ Alloys

X	K (%)	T_1T (secK)	$K^2T_1T/\mathcal{S}$	K_d (%)	K_{orb} (%)
1.0*	+1.57	1.10	57		
0.9	+1.74	1.02	65		
0.8	+1.69	1.12	68		
0.7	+1.63	1.14	64		
0.6	+1.60	1.28	69		
0.5	+1.56	1.40	72		
0.4	+1.30	1.06	38		
0.3	+0.99	0.34	7.1	-0.2	+1.2
0.25	+0.70	0.11	1.1	-0.9	+1.6
0.2	+0.25	0.06	0.08	-1.5	+1.8
0.2**	+0.11	0.05	0.01	-1.7	+1.8

* Ref. 10

** Co 0.5 at.% alloy

Table Ⅳ

$(Mo_{1-x}Re_x)_{96}V_3Co_1$ Alloys

X	K (%)	T_1T (msecK)	K^2T_1T/S	K_d (%)	K_{orb} (%)	T_K (K)
0*	-6.8	2.6	2.5	-9.5	+2.7	45
0.1	-2.3	15	1.7	-3.8	+1.5	110
0.2	-0.7	20.5	0.2	-3.0	+2.3	140
0.3	-0.2	25	0.02	-2.6	+2.4	165

* $Mo_{99.9}Co_{0.1}$ alloy by ref.15

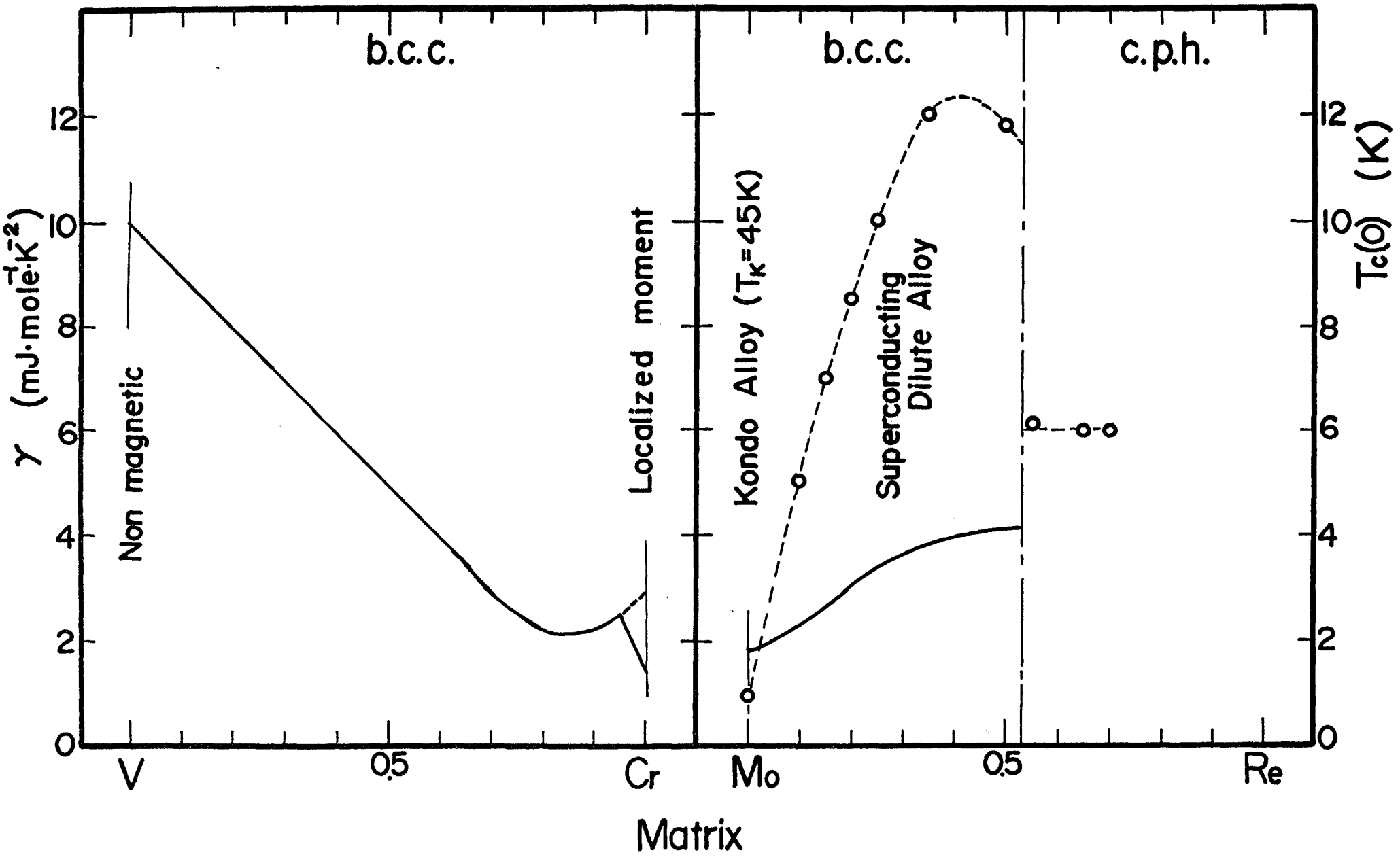
b.c.c.
b.c.c.
c.p.h.
γ (mJ·mole⁻¹·K⁻²)
Tc(0) (K)
Non magnetic
Localized moment
Kondo Alloy (Tk=45K)
Superconducting
Dilute Alloy
0
2
4
6
8
10
12
V
0.5
Cr
Mo
0.5
Re
Matrix

Fig. 1

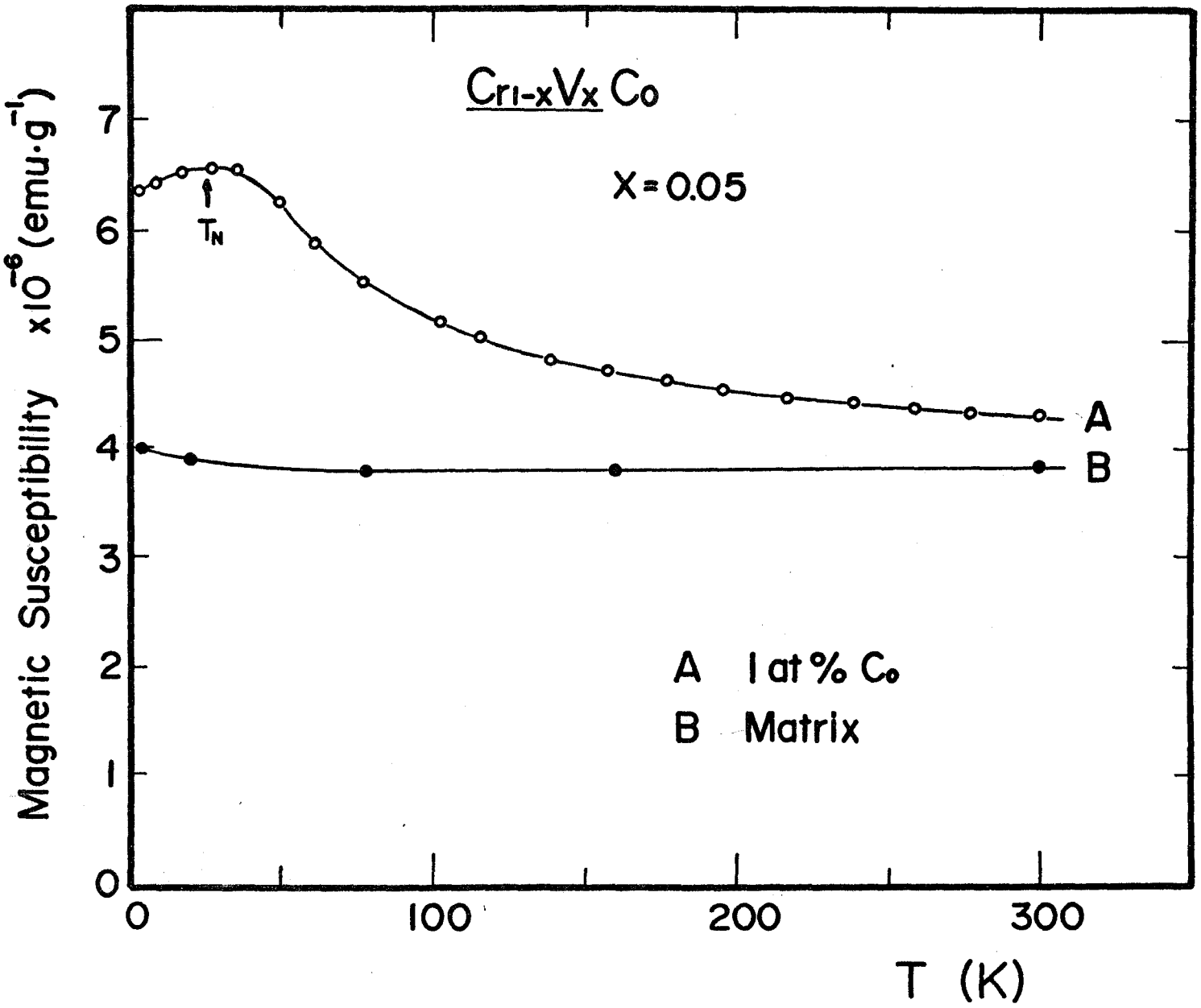
Cr1-xVx Co
X=0.05
TN
A
B
A 1 at % Co
B Matrix
Magnetic Susceptibility x10⁻⁶(emu·g⁻¹)
0
1
2
3
4
5
6
7
0
100
200
300
T (K)

Fig. 2

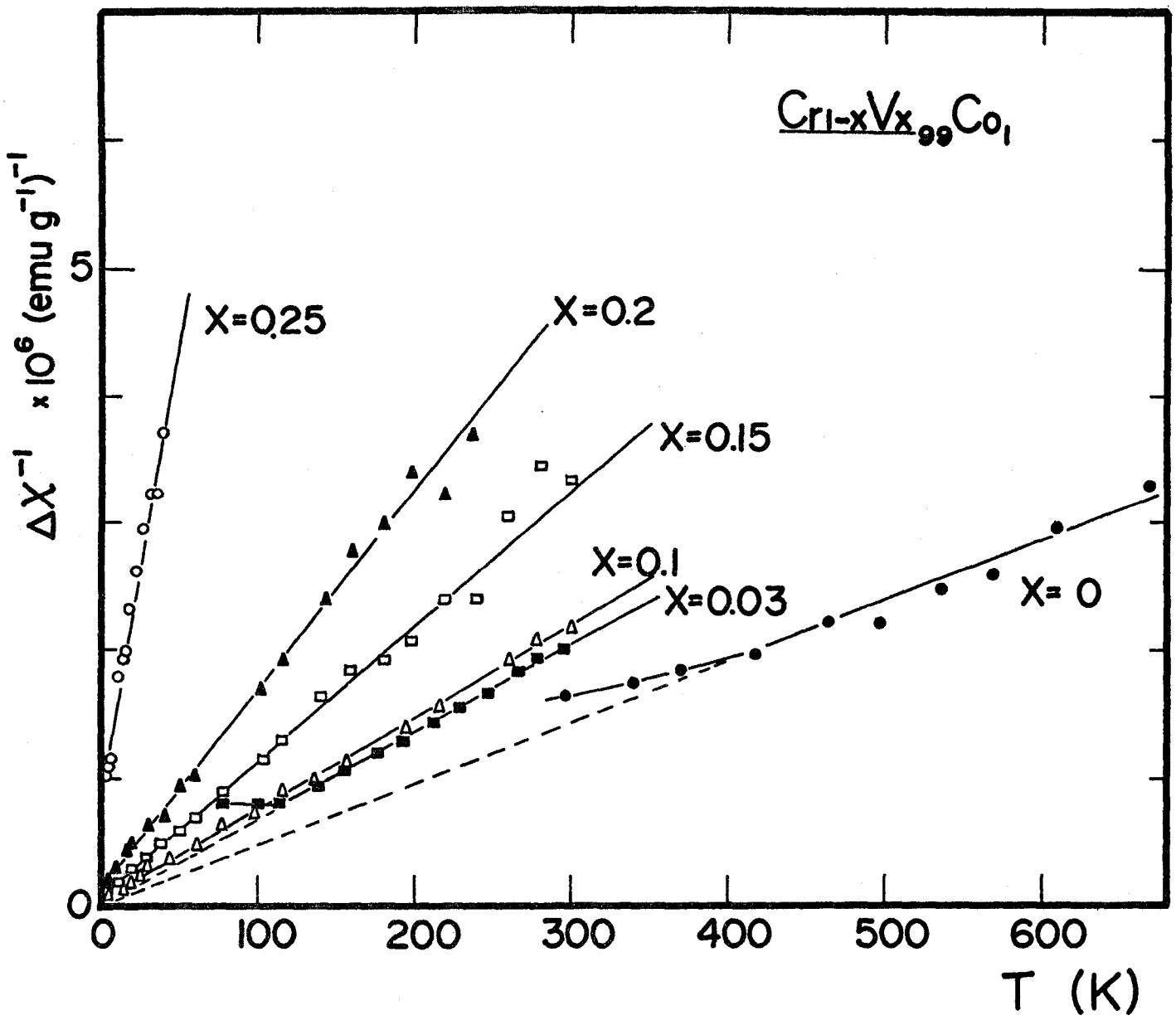
$Cr_{1-x}V_{x_{99}}Co_1$
$\Delta\chi^{-1}$ x 10^6 (emu g^{-1})$^{-1}$
X=0.25
X=0.2
X=0.15
X=0.1
X=0.03
X= 0
0
5
0
100
200
300
400
500
600
T (K)

Fig. 3

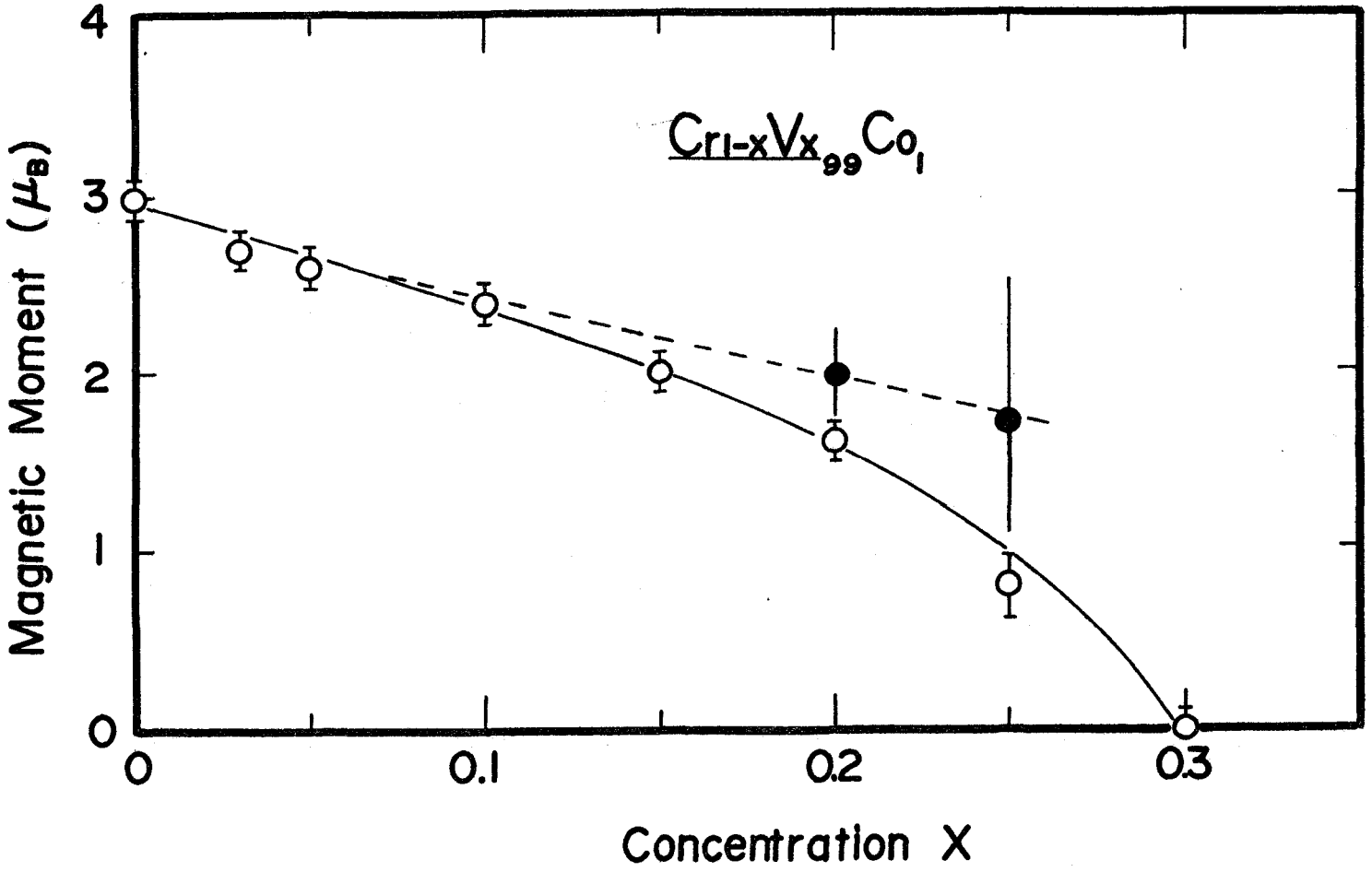
Cr1-xVx99Co1
Magnetic Moment (μB)
Concentration X
0
1
2
3
4
0
0.1
0.2
0.3

Fig.4

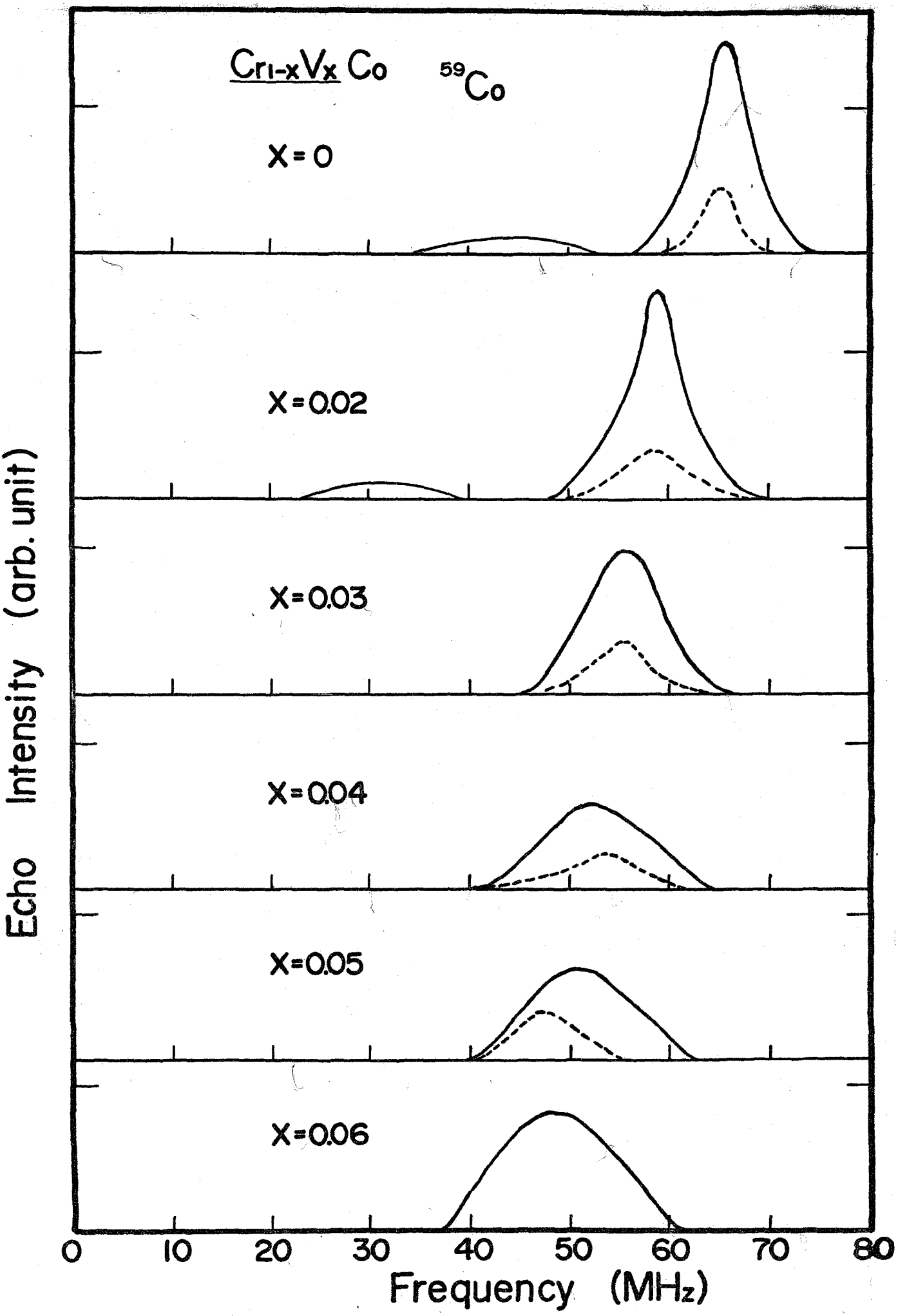
Cr1-xVx Co
59Co
X=0
X=0.02
X=0.03
X=0.04
X=0.05
X=0.06
Echo Intensity (arb. unit)
0
10
20
30
40
50
60
70
80
Frequency (MHz)

Fig. 5

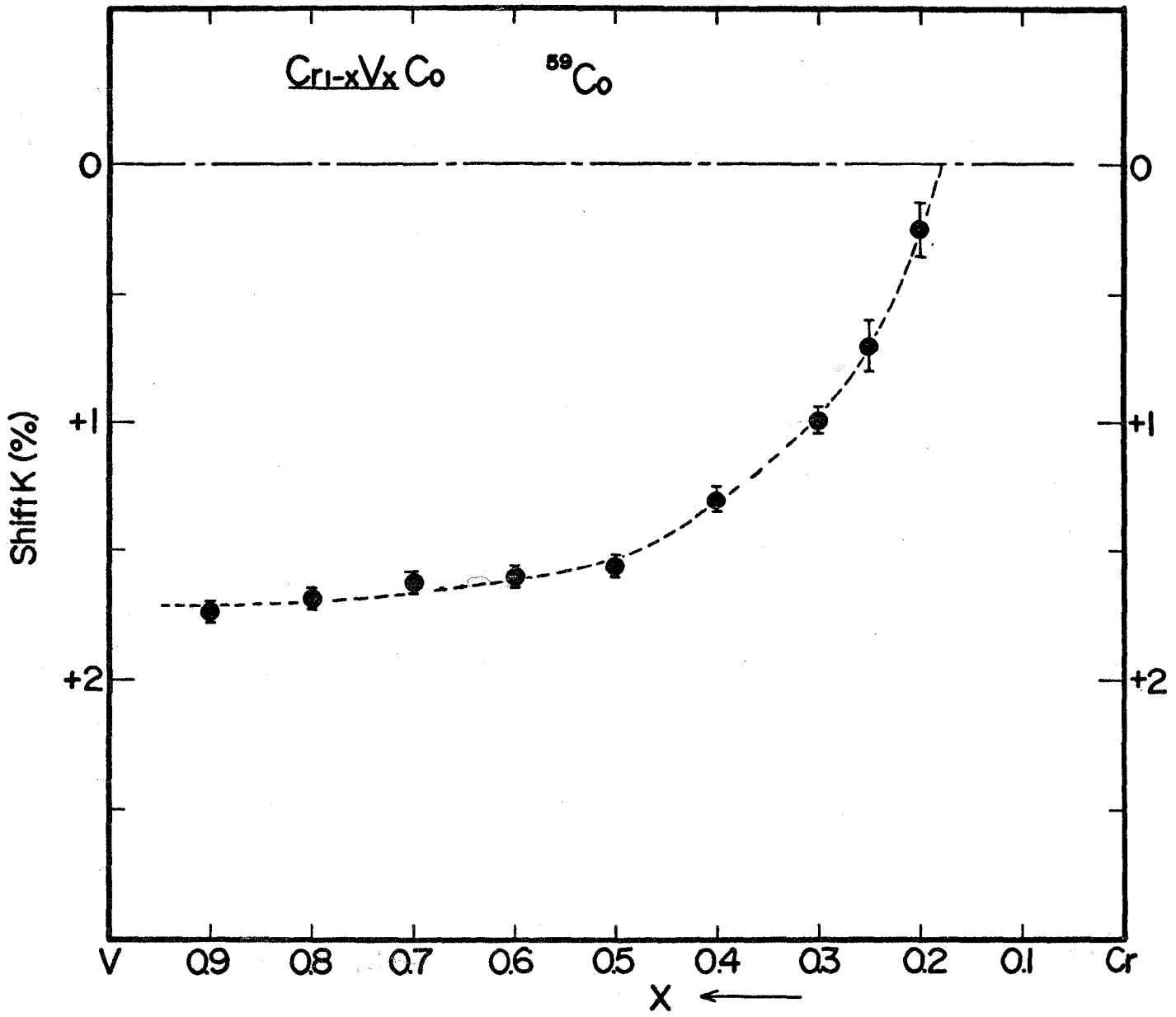

Fig. 6

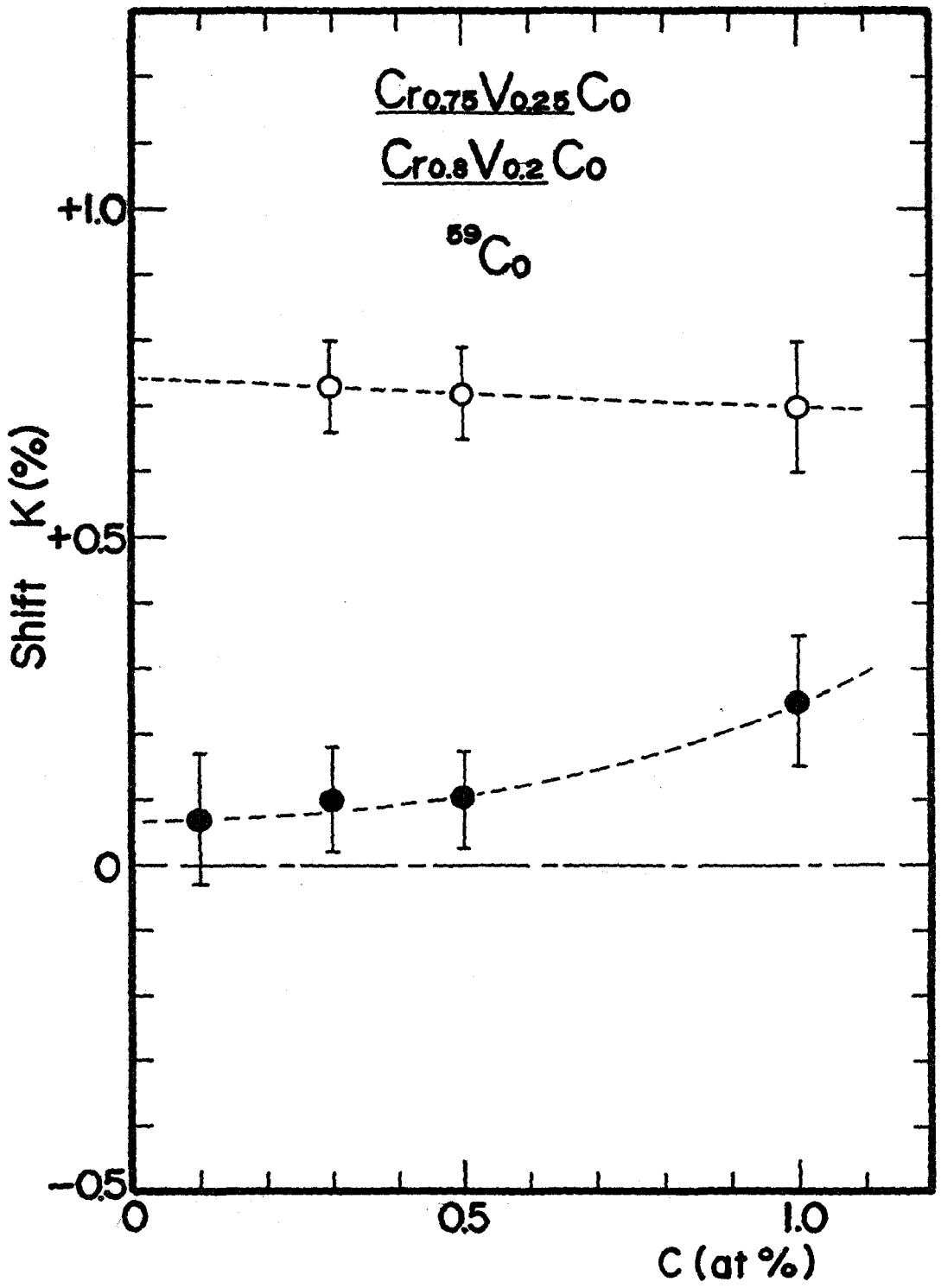

Fig. 7

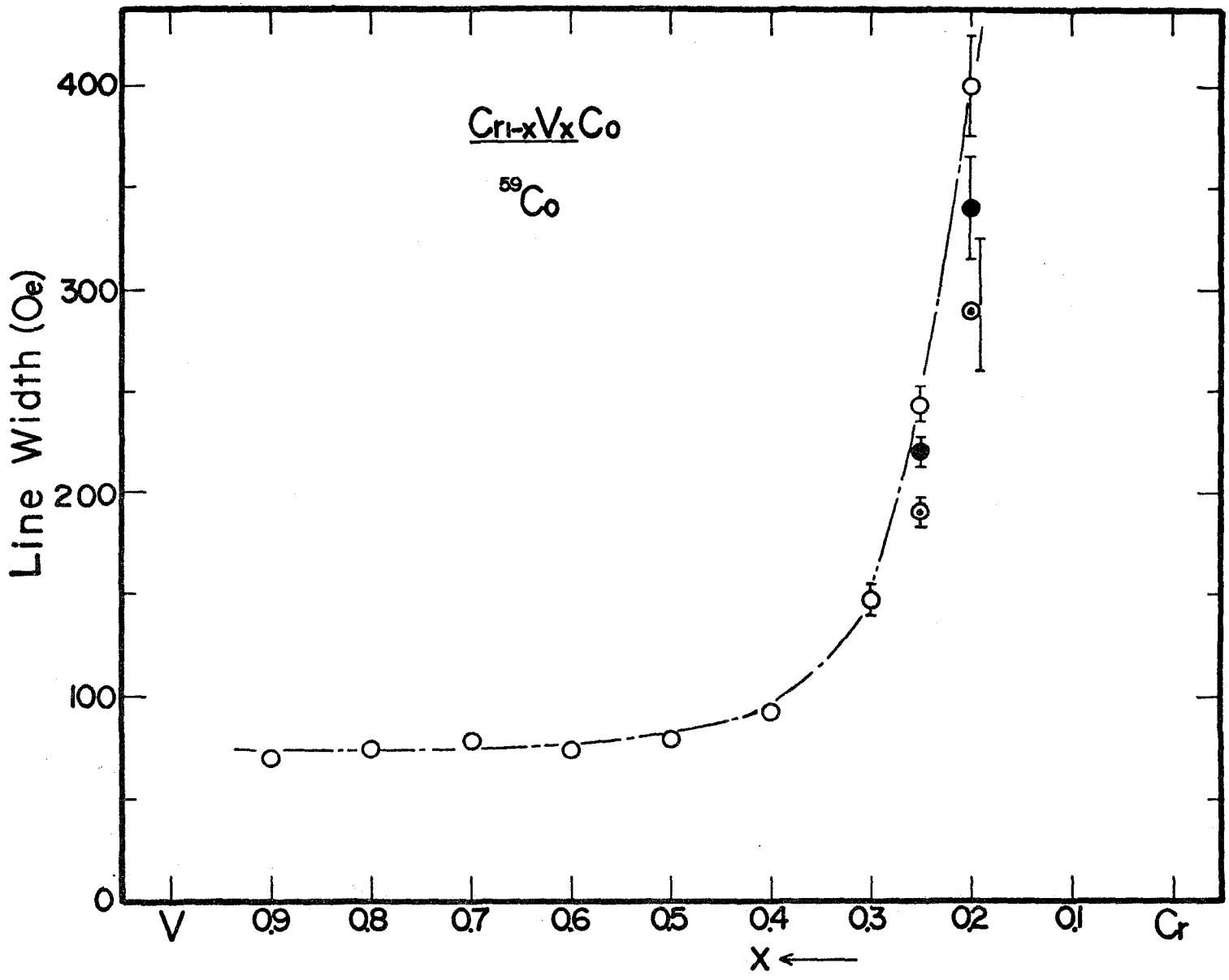
Cr1-xVxCo
59Co
Line Width (Oe)
400
300
200
100
0
V
0.9
0.8
0.7
0.6
0.5
0.4
0.3
0.2
0.1
Cr
X ←

Fig. 8

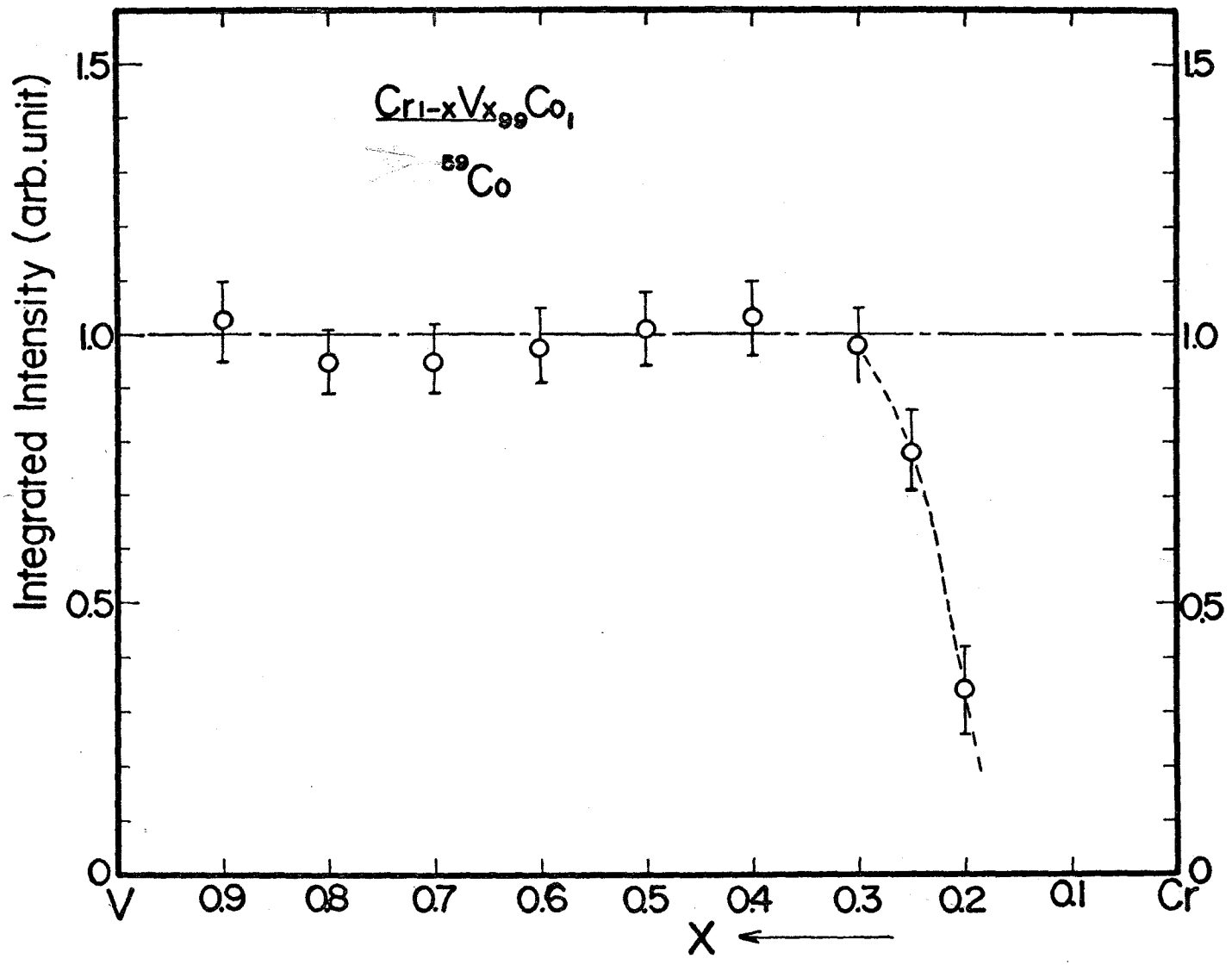
Integrated Intensity (arb.unit)
1.5
1.0
0.5
0
$Cr_{1-x}V_{x_{99}}Co_1$
^{59}Co
V
0.9
0.8
0.7
0.6
0.5
0.4
0.3
0.2
0.1
Cr
X

Fig. 9

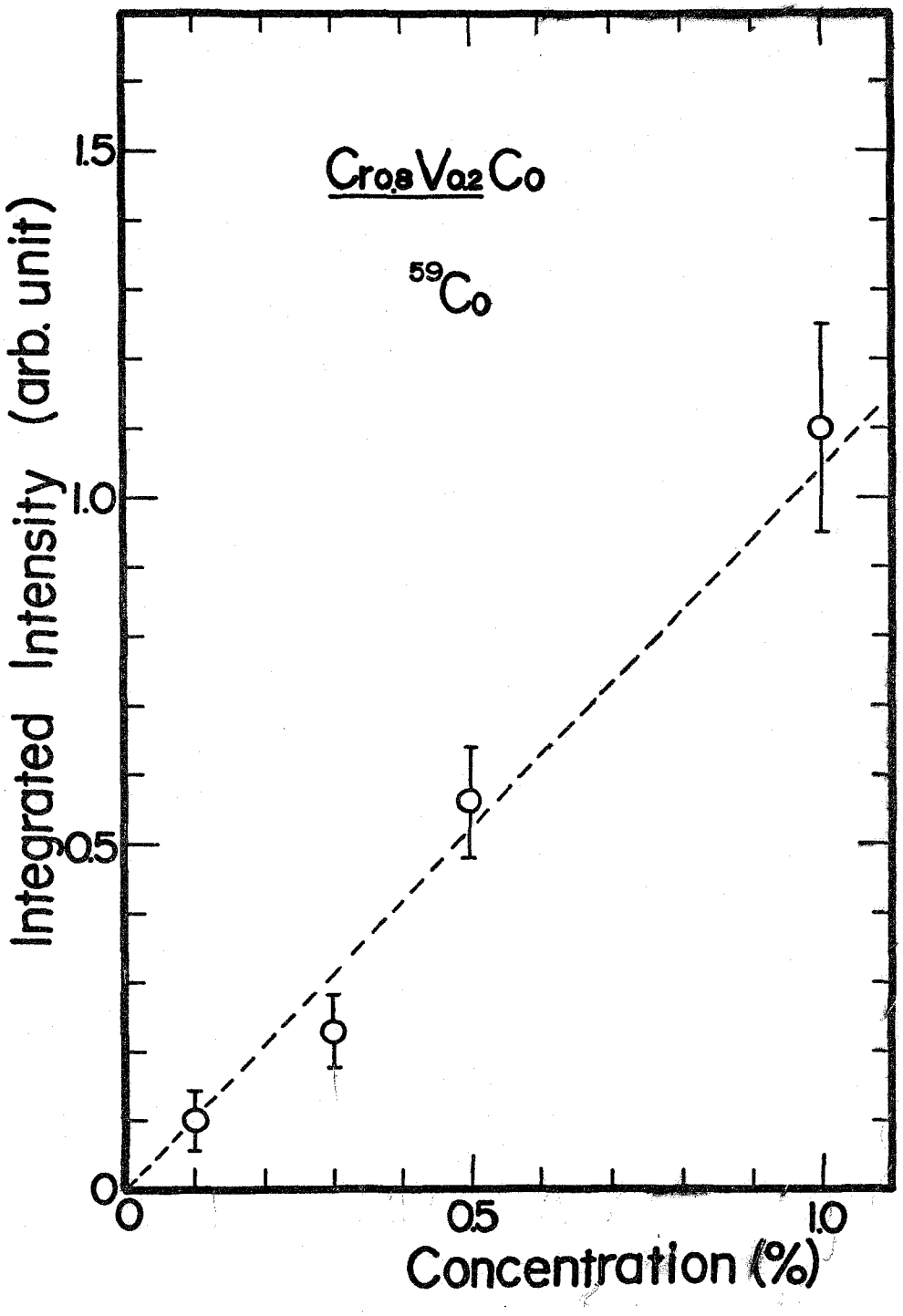
Cr0.8V0.2Co
59Co
Integrated Intensity (arb. unit)
1.5
1.0
0.5
0
0
0.5
1.0
Concentration (%)

Fig. 10

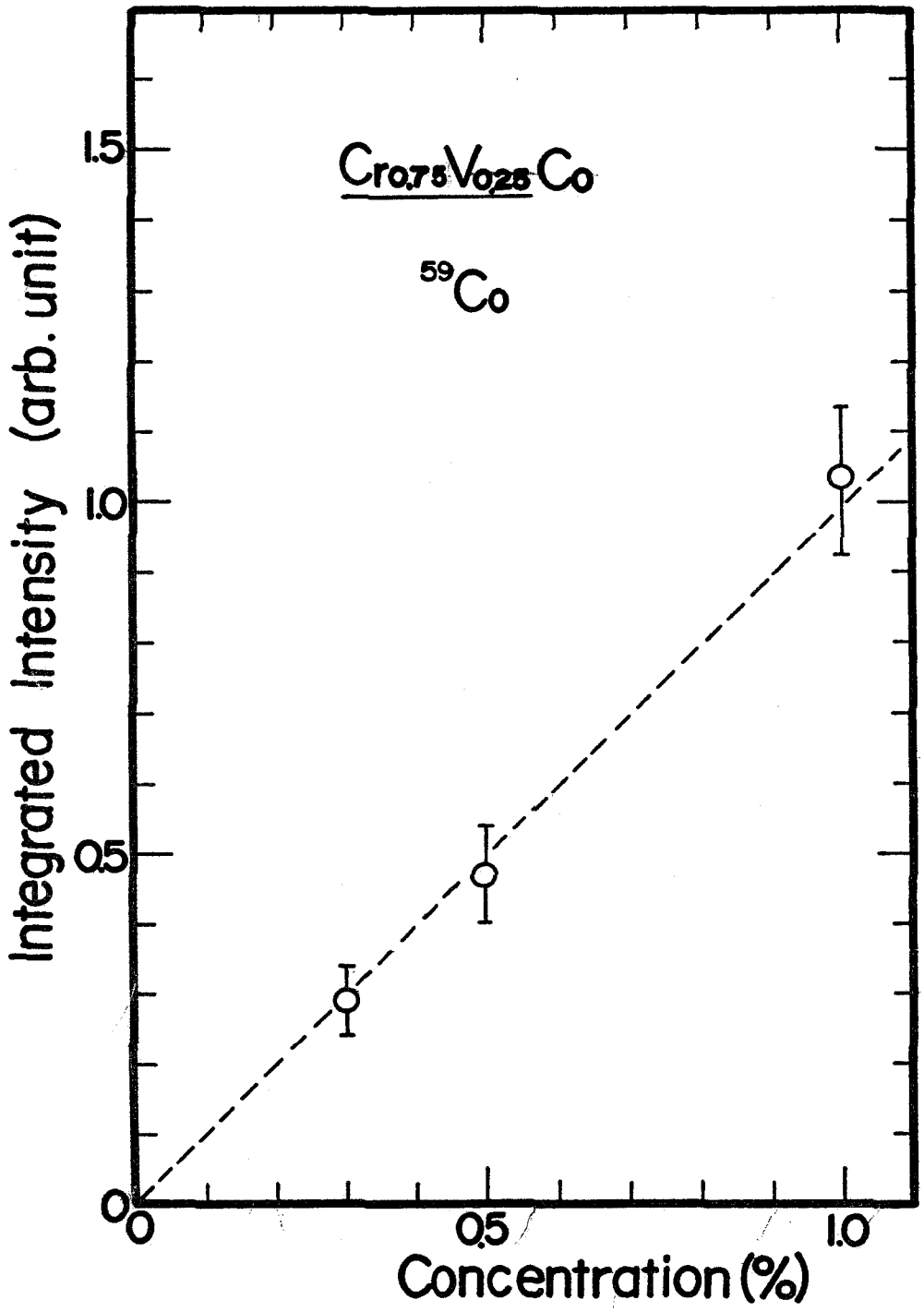
Cr0.75V0.25Co
59Co
Integrated Intensity (arb. unit)
1.5
1.0
0.5
0
0
0.5
1.0
Concentration (%)

Fig. 11

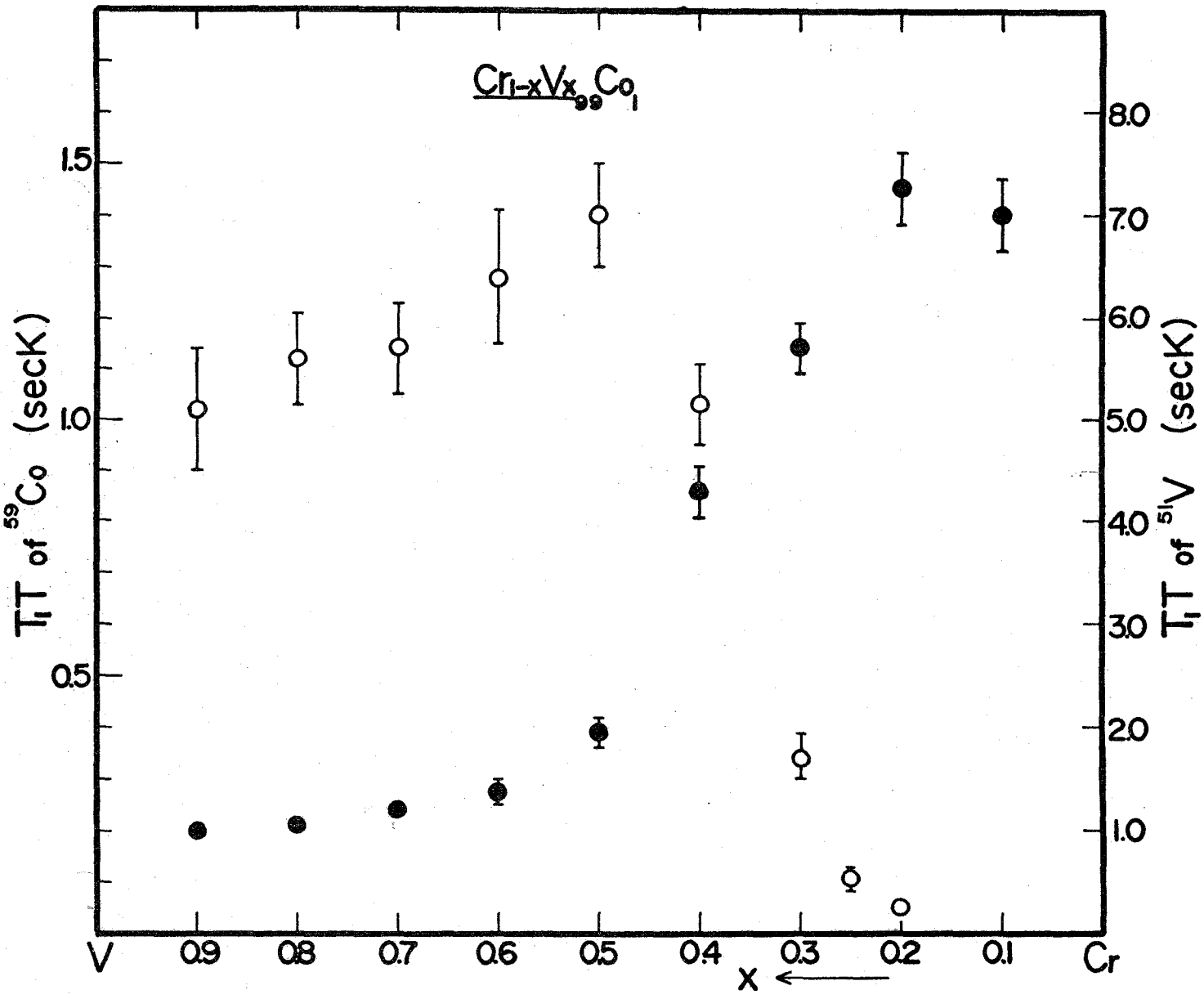
$Cr_{1-x}V_{x_{.99}}Co_{.01}$
T_1T of ^{59}Co (secK)
T_1T of ^{51}V (secK)
1.5
1.0
0.5
8.0
7.0
6.0
5.0
4.0
3.0
2.0
1.0
V
0.9
0.8
0.7
0.6
0.5
0.4
0.3
0.2
0.1
Cr
X

Fig. 12

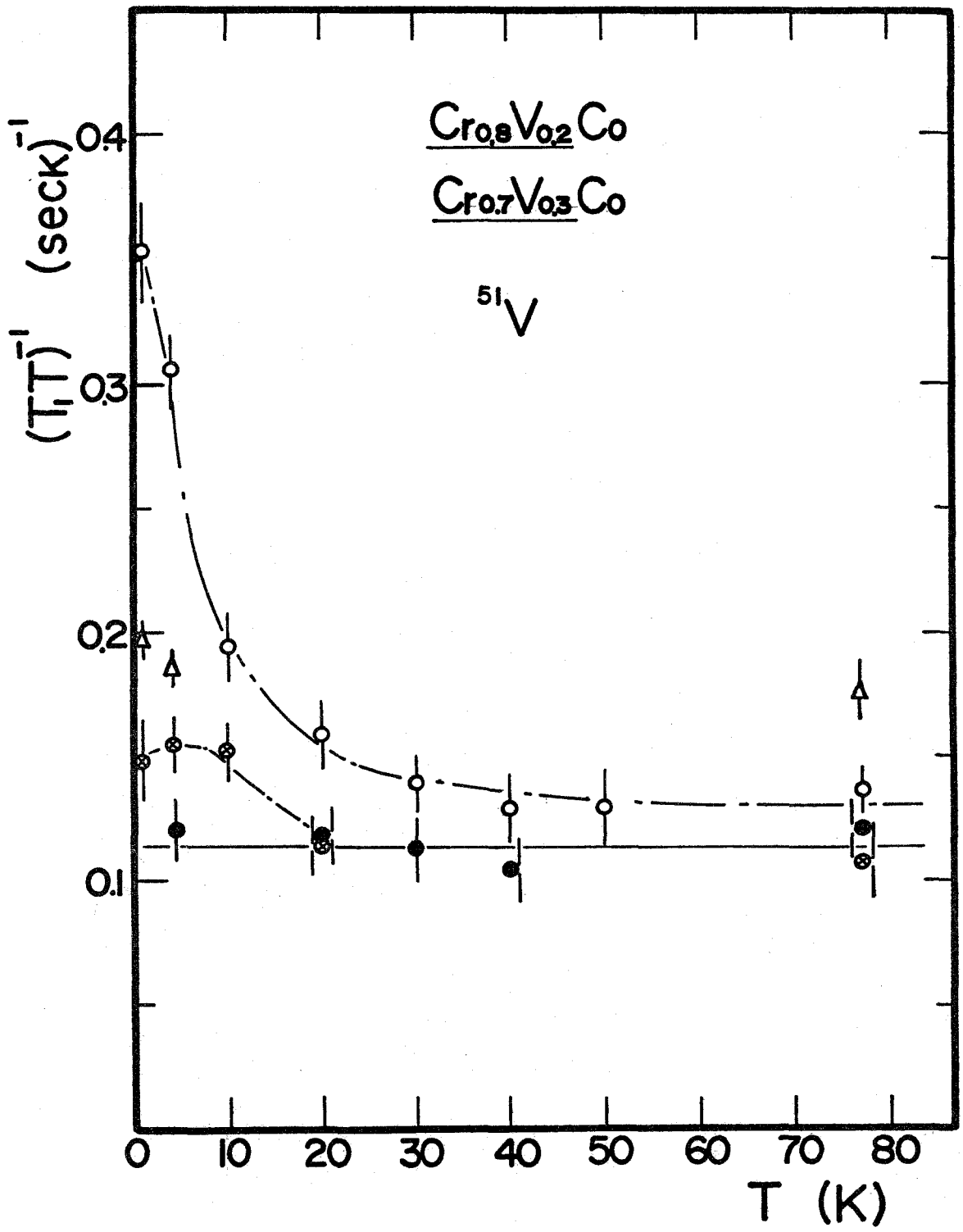
Cr0.8V0.2Co
Cr0.7V0.3Co
51V
(T1T)-1 (seck)-1
0.4
0.3
0.2
0.1
0
10
20
30
40
50
60
70
80
T (K)

Fig. 13

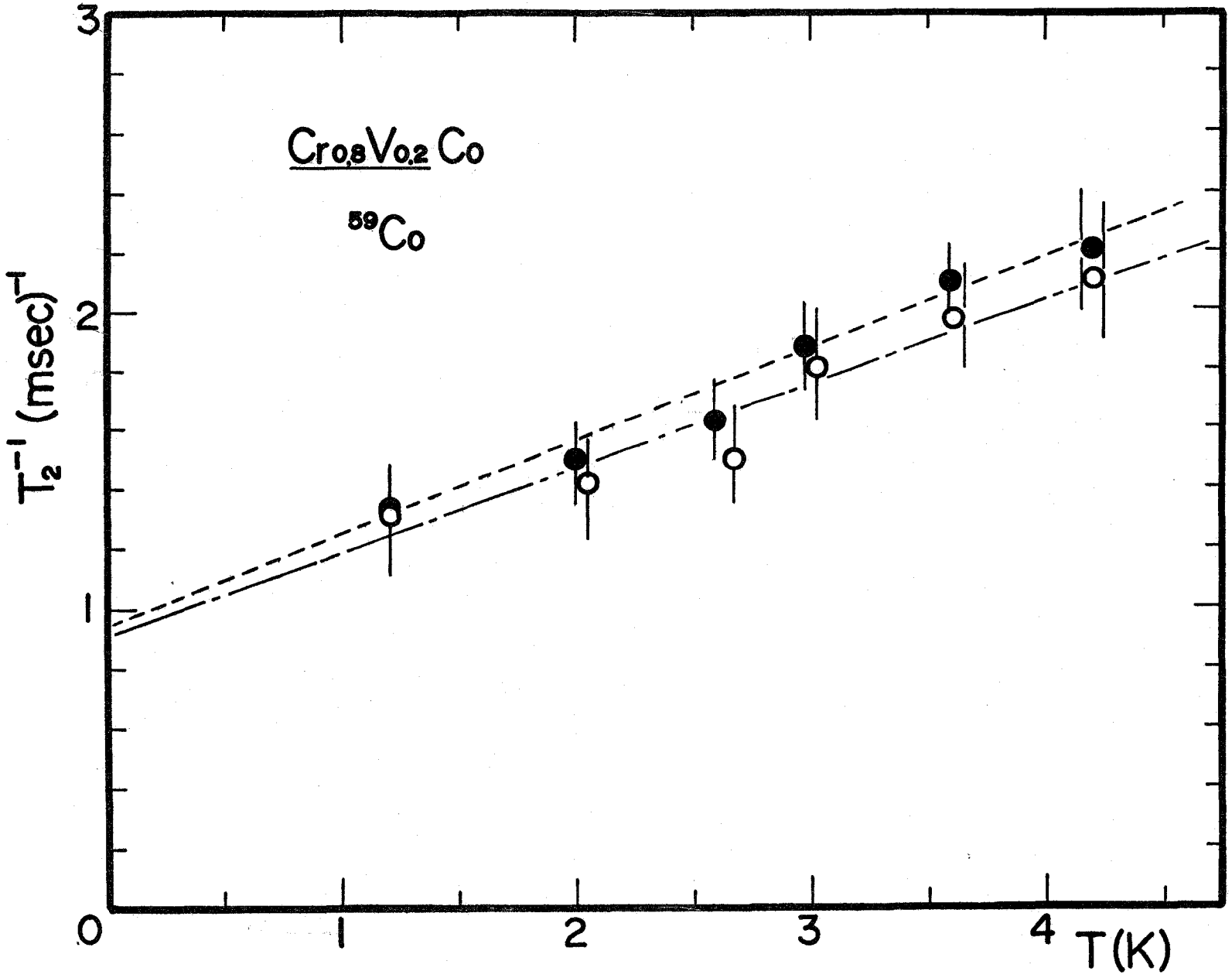

Fig. 14

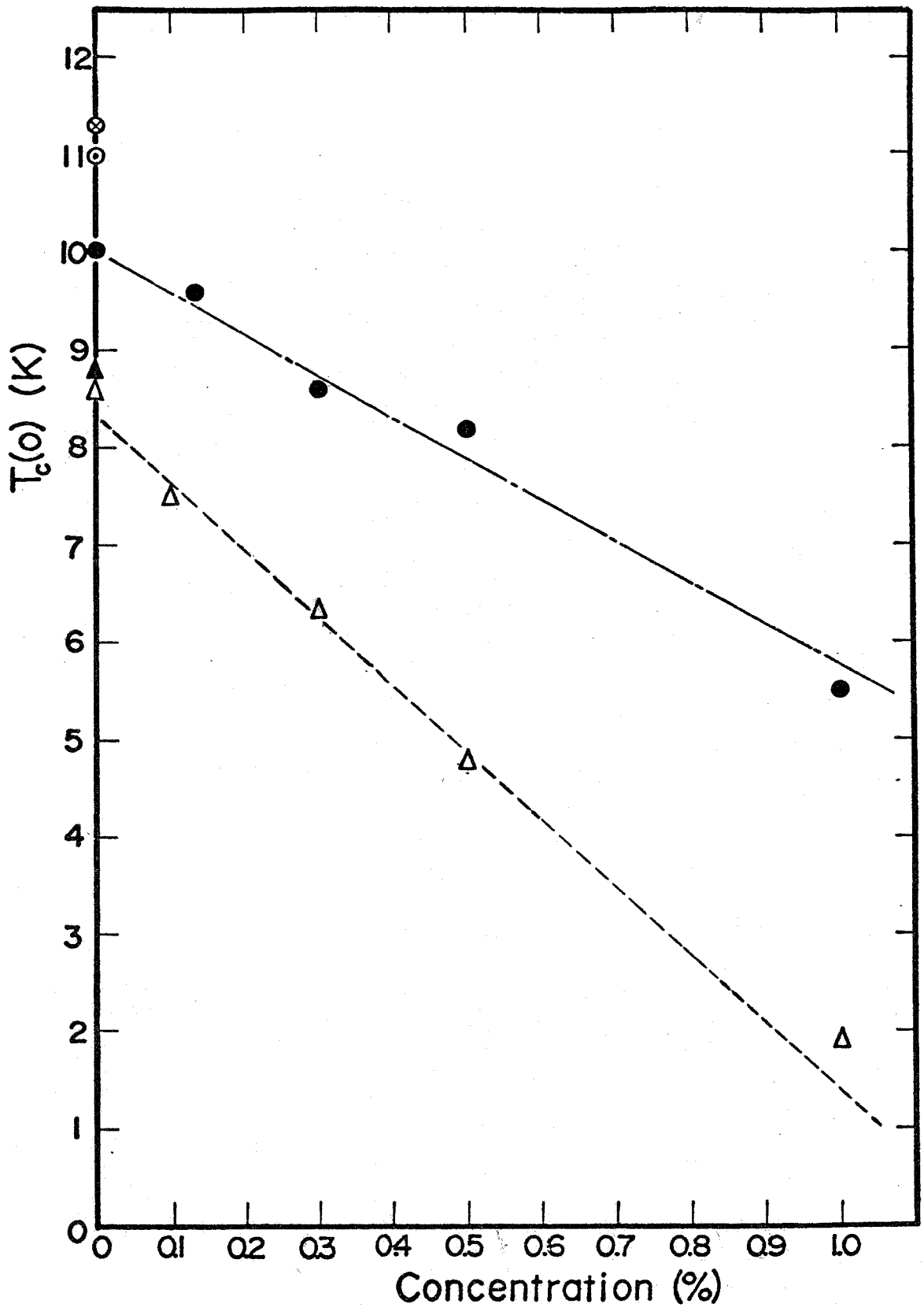
12
11
10
9
8
7
6
5
4
3
2
1
0
$T_c(0)$ (K)
0
0.1
0.2
0.3
0.4
0.5
0.6
0.7
0.8
0.9
1.0
Concentration (%)

Fig. 15

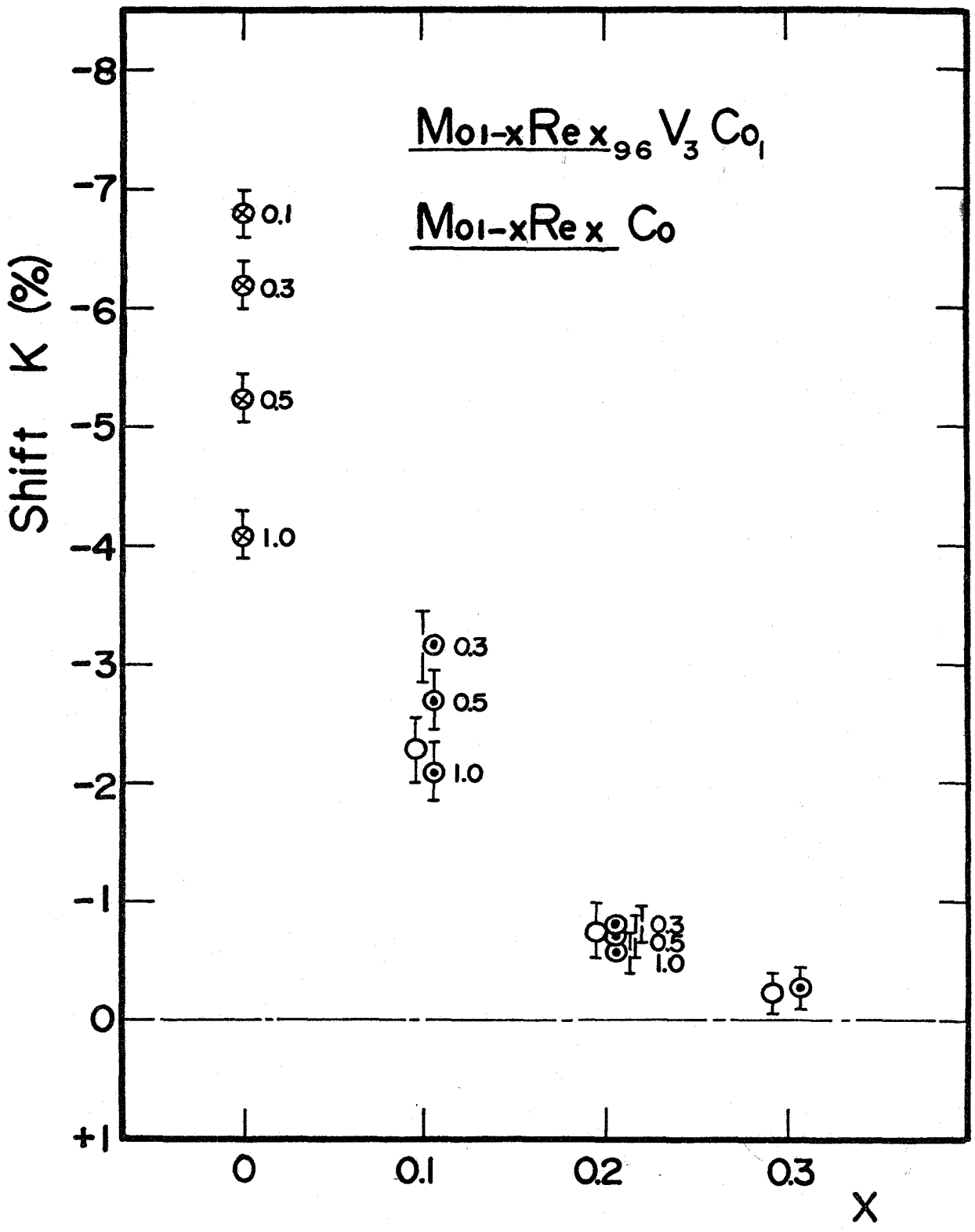
Mo1-xRex96 V3 Co1
Mo1-xRex Co
Shift K (%)
-8
-7
-6
-5
-4
-3
-2
-1
0
+1
0.1
0.3
0.5
1.0
0.3
0.5
1.0
0.3
0.5
1.0
0
0.1
0.2
0.3
X

Fig. 16

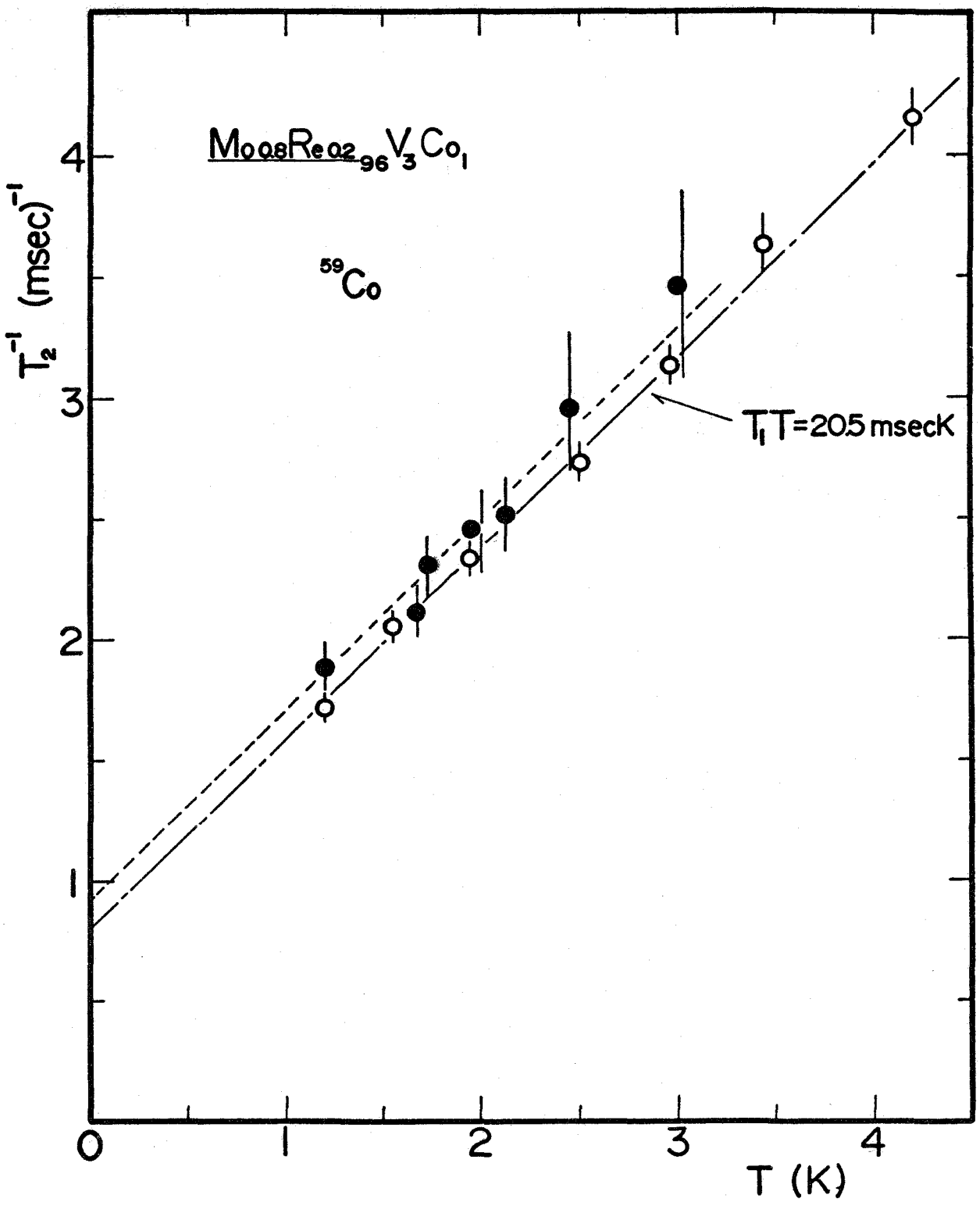

Fig. 17

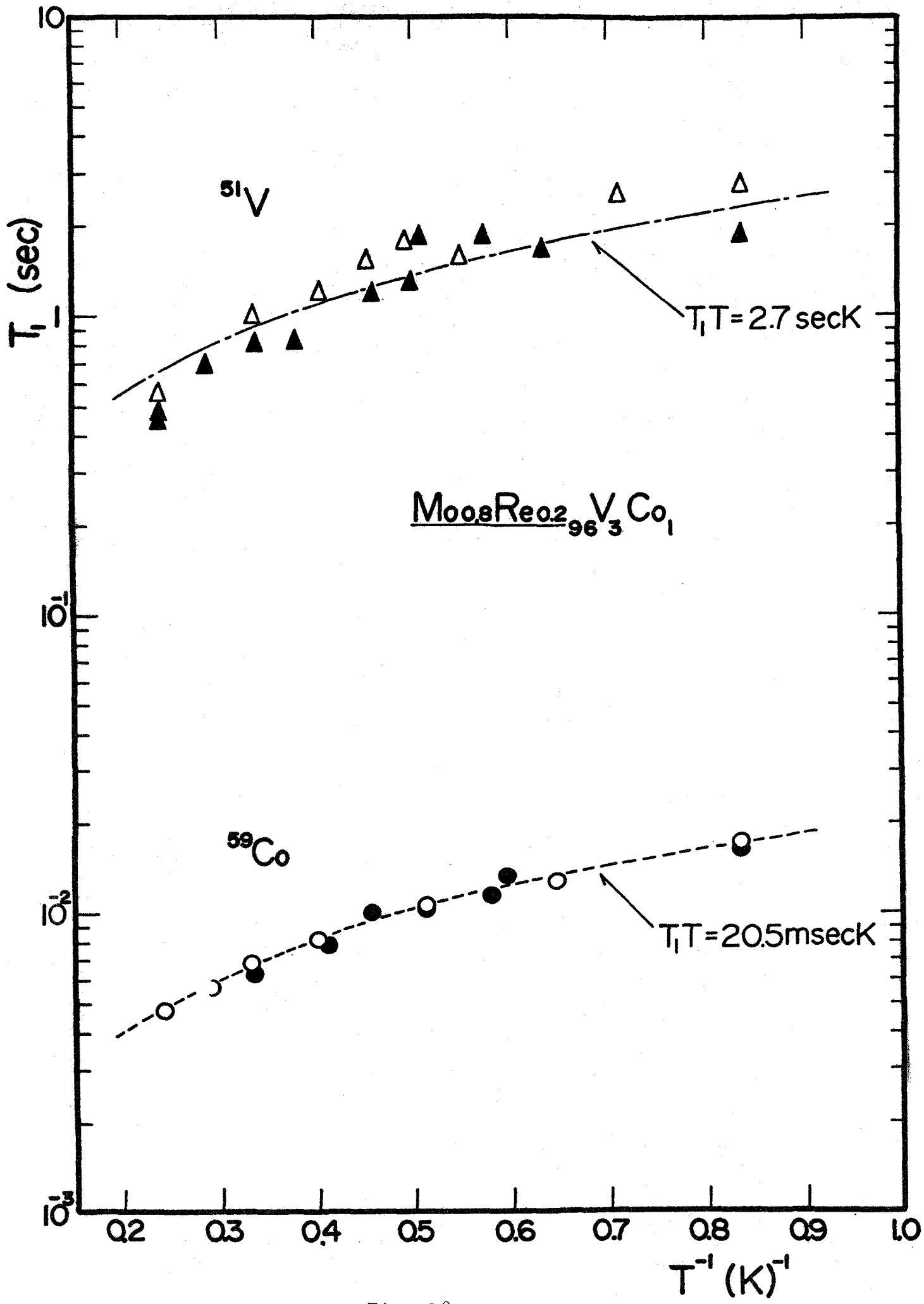
10
1
10^{-1}
10^{-2}
10^{-3}
T_1 (sec)
^{51}V
$T_1T = 2.7$ secK
$Mo_{0.8}Re_{0.2}{}_{96}V_3Co_1$
^{59}Co
$T_1T = 20.5$msecK
0.2
0.3
0.4
0.5
0.6
0.7
0.8
0.9
1.0
T^{-1} $(K)^{-1}$

Fig. 18

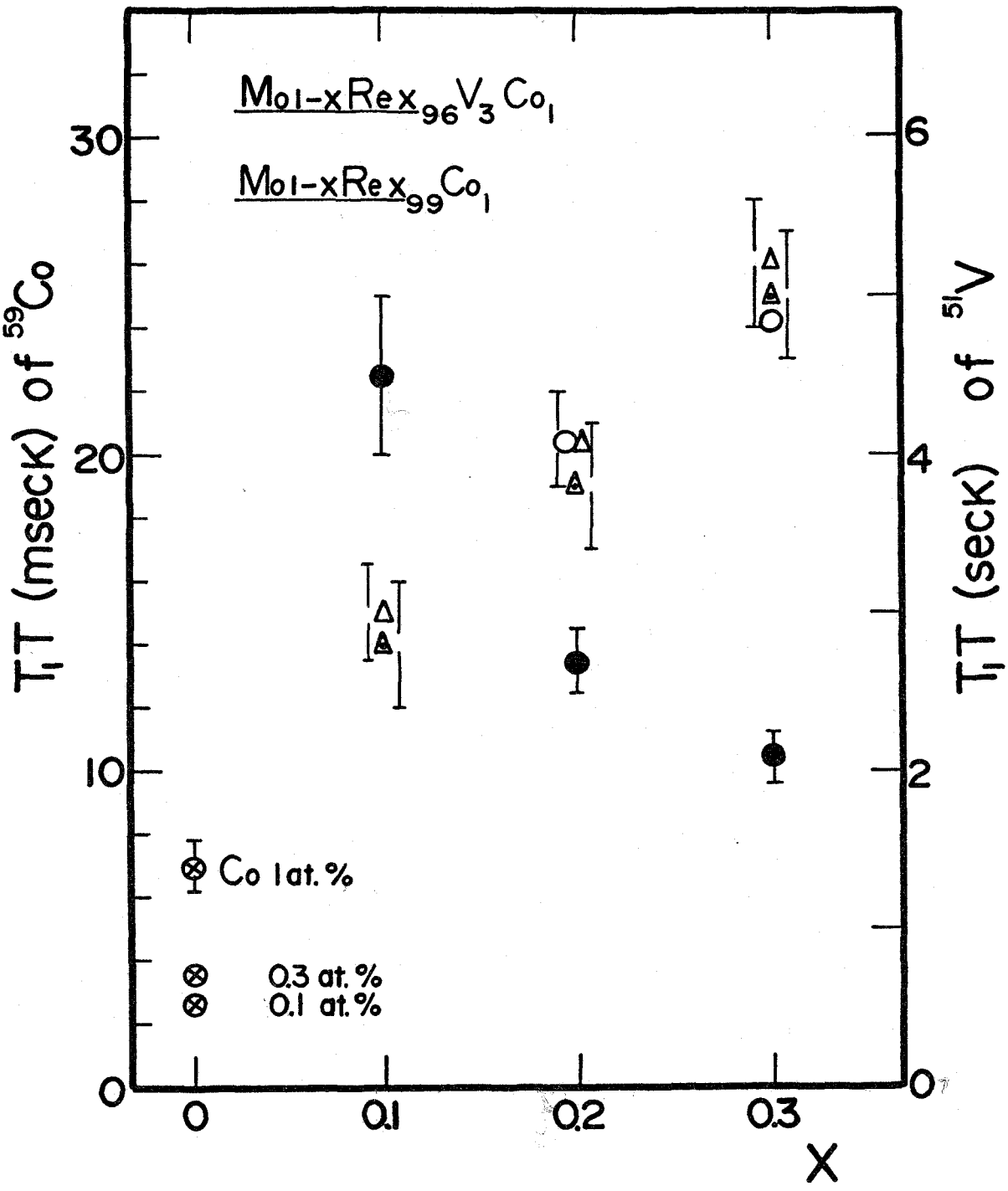
Mo1-xRex96V3Co1
Mo1-xRex99Co1
T1T (mseck) of 59Co
T1T (seck) of 51V
Co 1at.%
0.3 at.%
0.1 at.%
30
20
10
0
6
4
2
0
0
0.1
0.2
0.3
X

Fig. 19

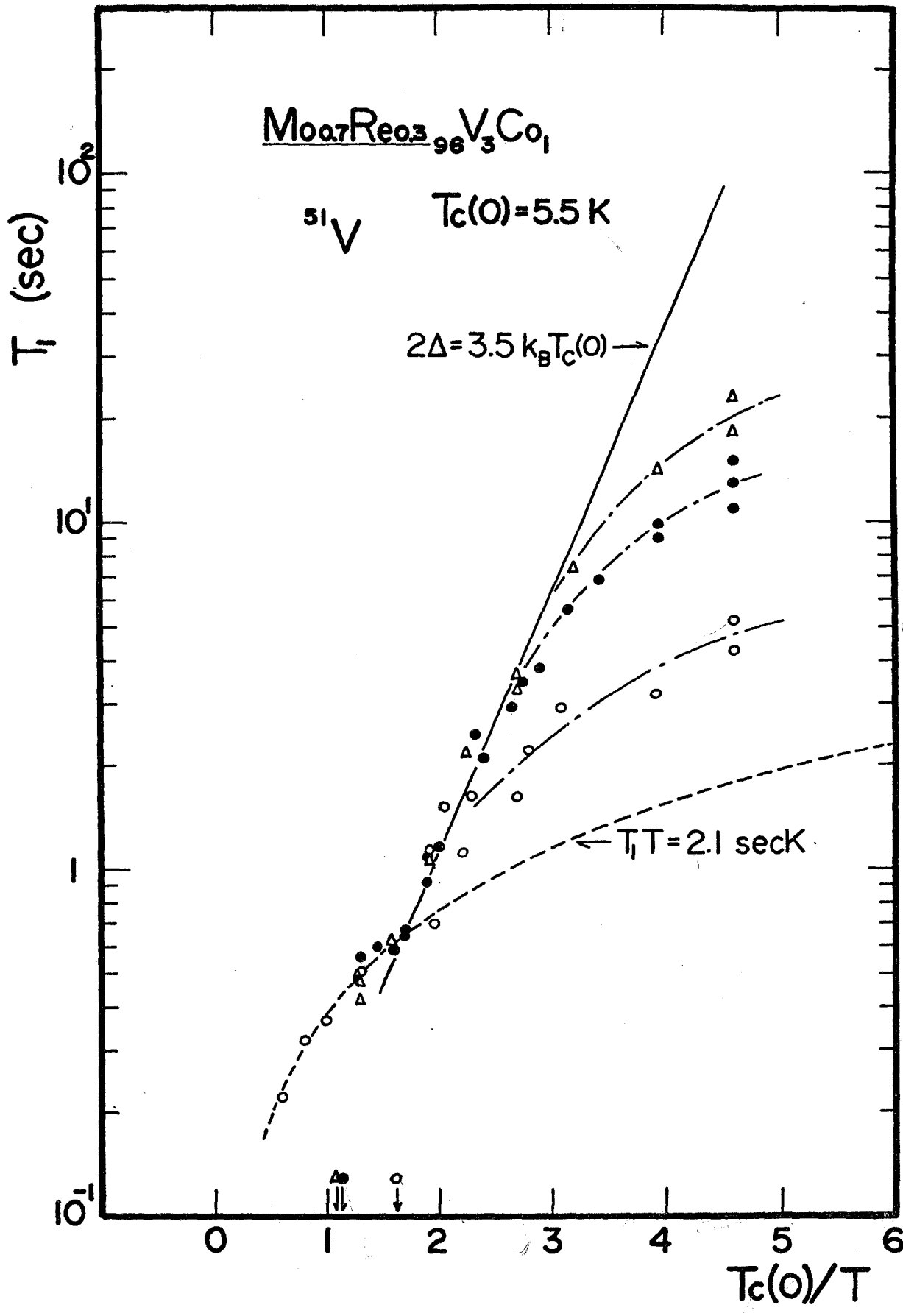
Mo0.7Re0.3 96 V3 Co1
51V
Tc(0)=5.5 K
2Δ=3.5 kB Tc(0)
T1 T = 2.1 secK
T1 (sec)
Tc(0)/T
10²
10¹
1
10⁻¹
0
1
2
3
4
5
6

Fig. 20

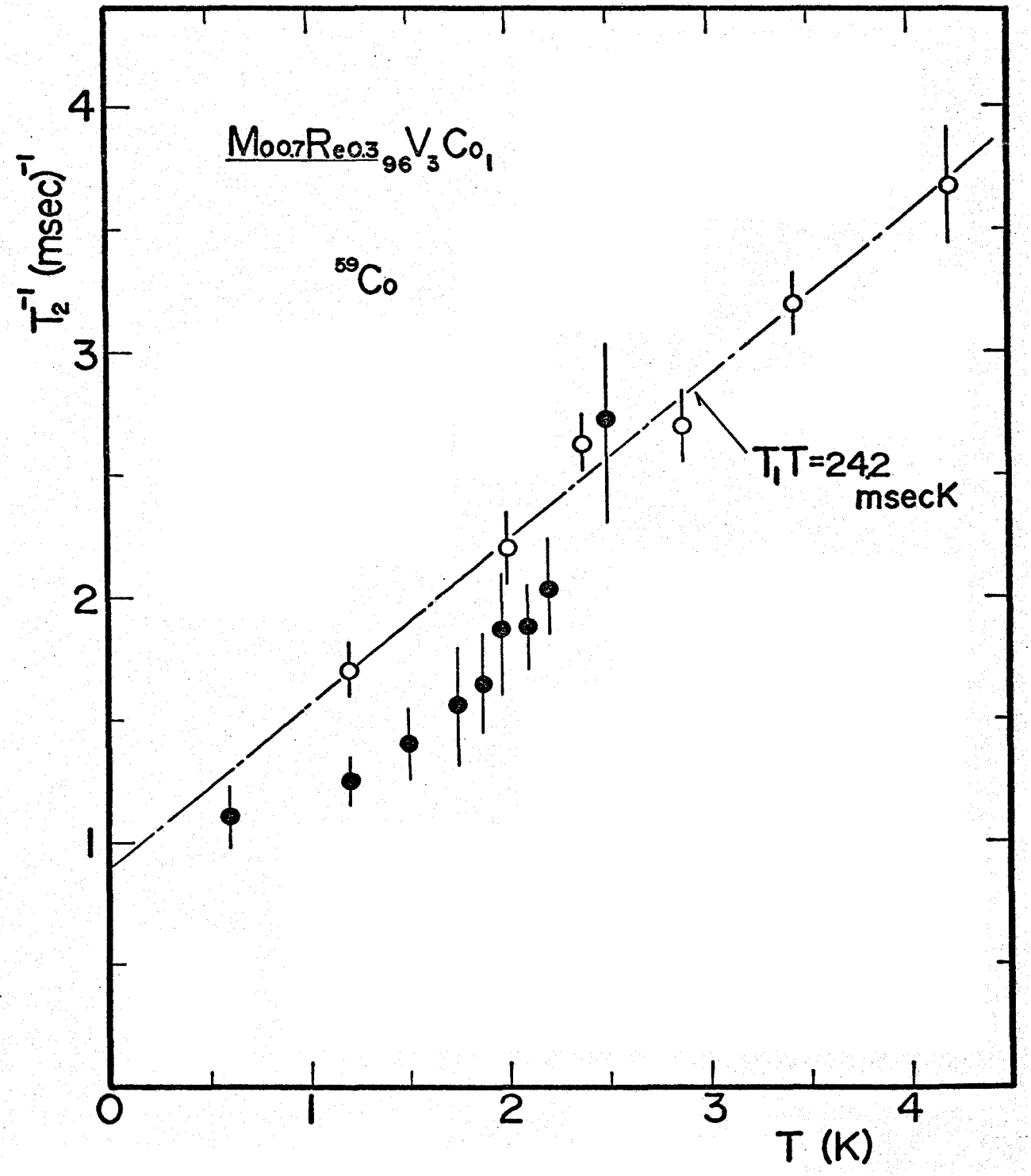
Mo0.7Re0.3 96 V3 Co1
59Co
T1T=242 mseck
T2-1 (msec)-1
T (K)
0
1
2
3
4

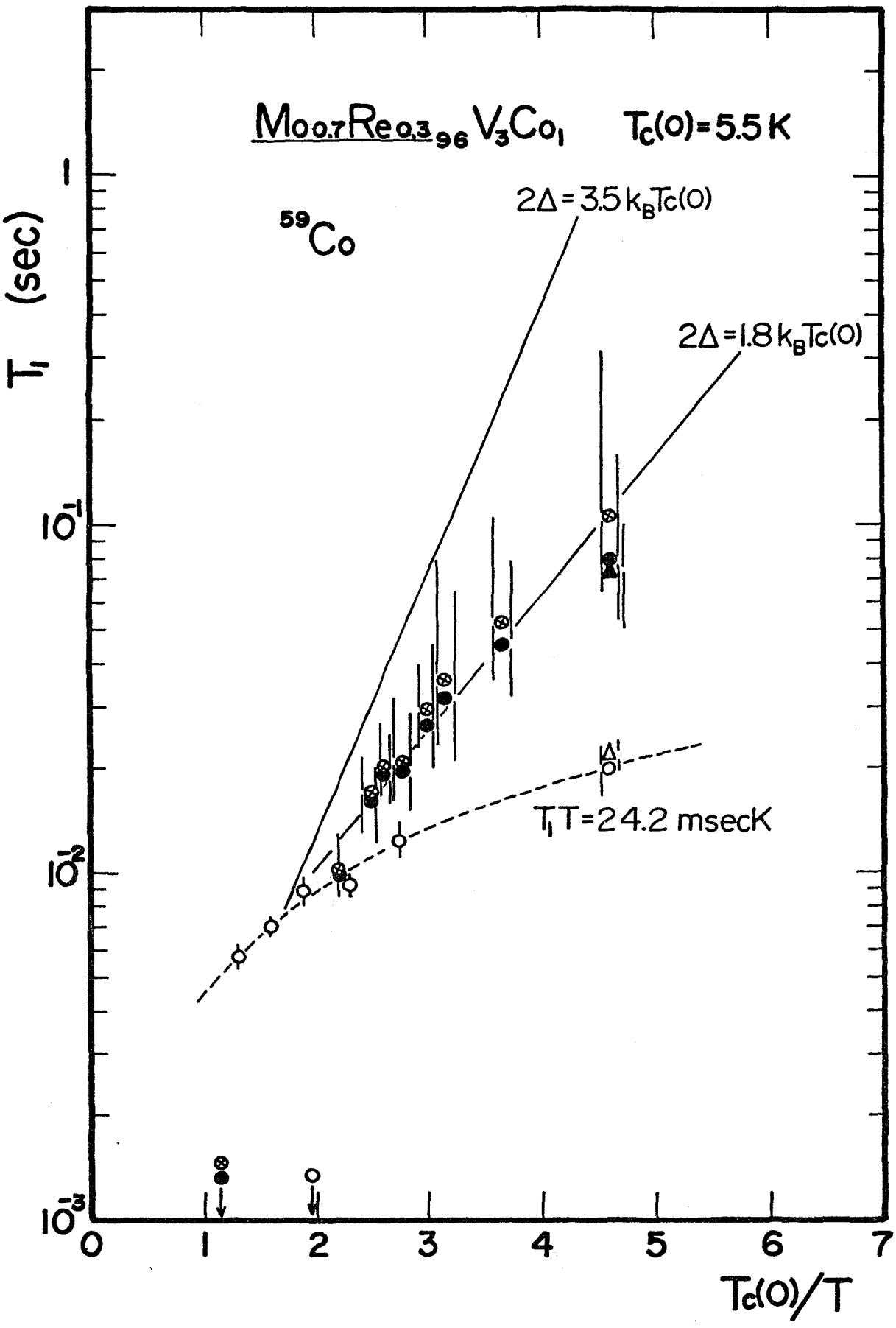
Mo0.7Re0.3 96 V3Co1 Tc(0)=5.5 K
59Co
2Δ=3.5 kBTc(0)
2Δ=1.8 kBTc(0)
T1T=24.2 msecK
T1 (sec)
Tc(0)/T
1
10-1
10-2
10-3
0
1
2
3
4
5
6
7

Fig. 22

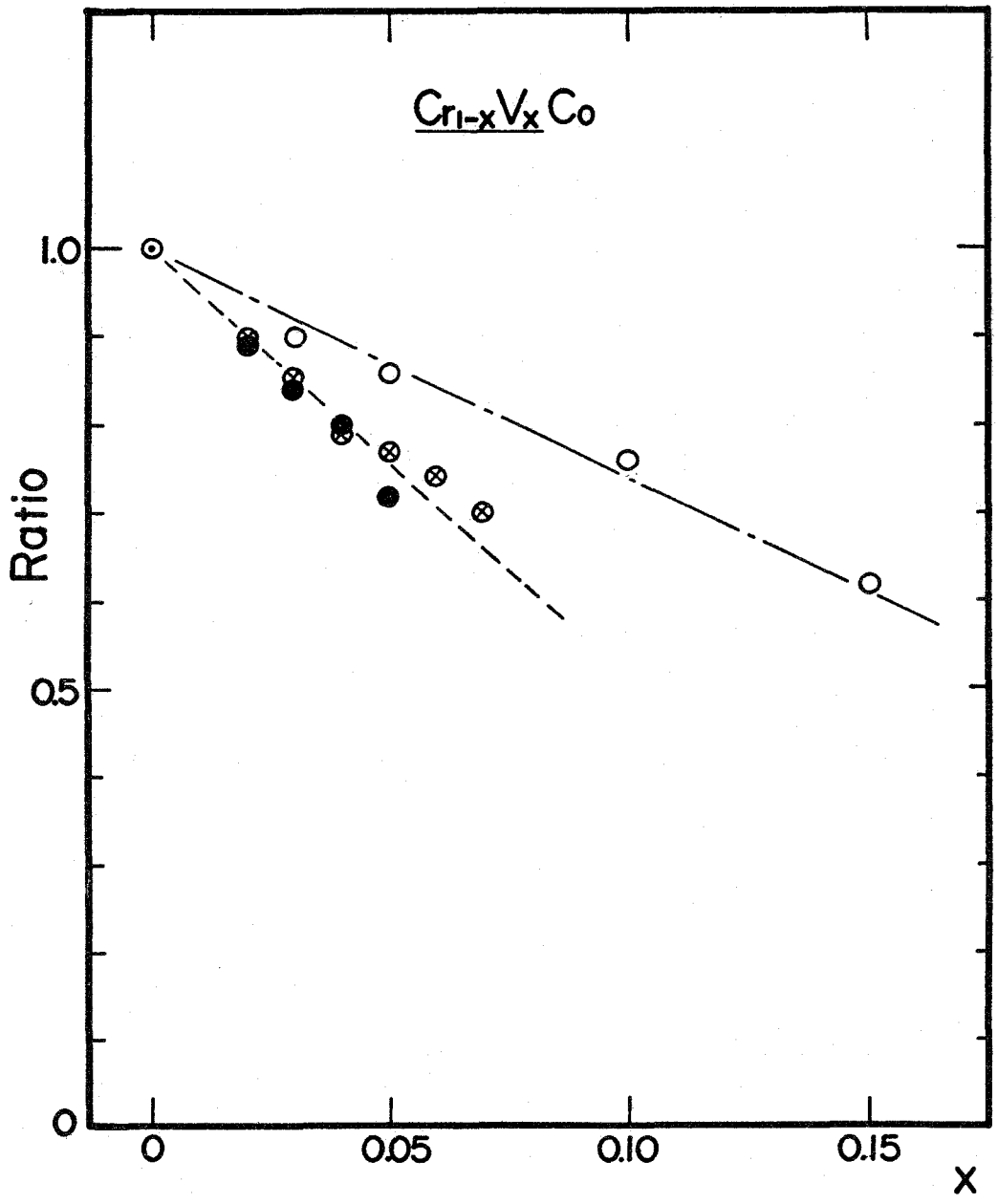

Fig. 23

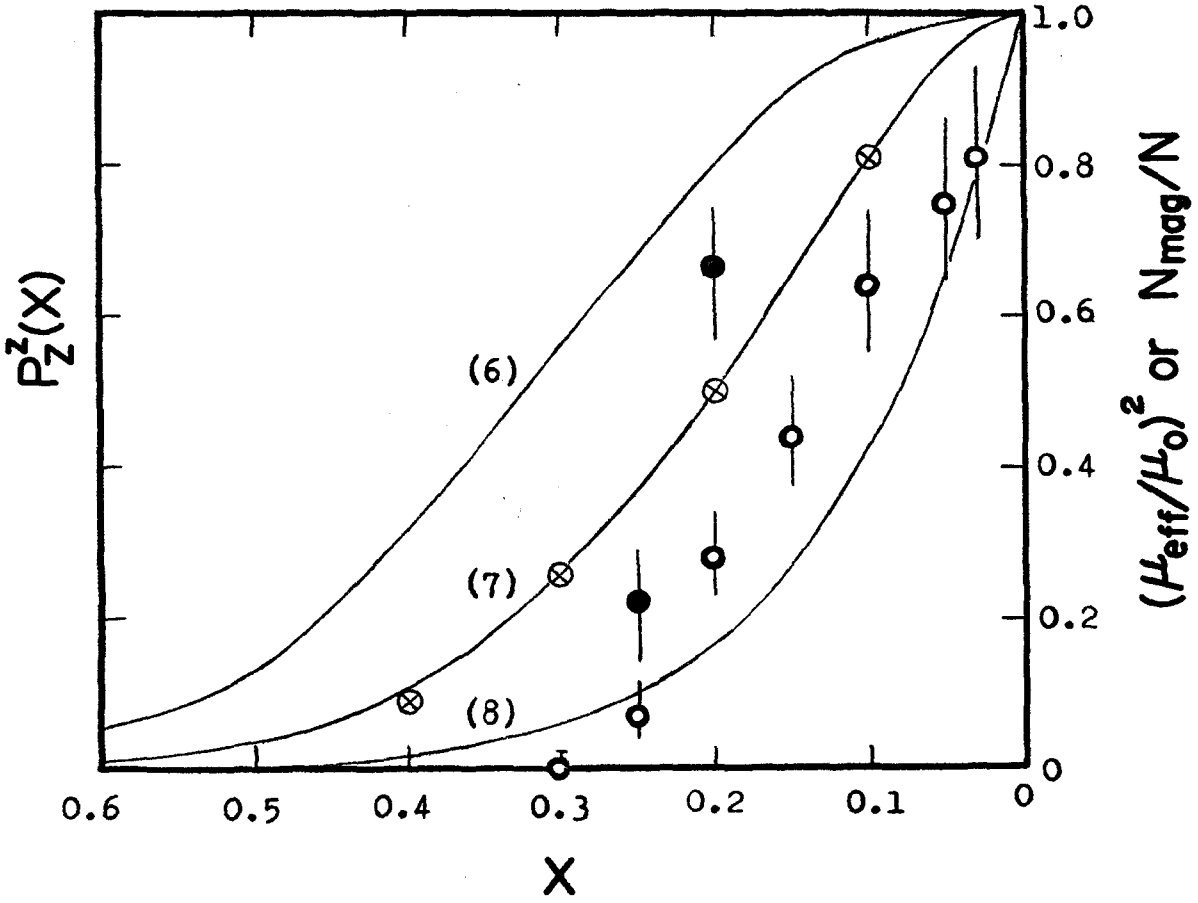

Fig. 24

PART II

NUCLEAR MAGNETIC RELAXATION IN ANTIFERROMAGNETIC CrVCo AND CrMoCo ALLOYS

Contents

Abstract

The nuclear magnetic relaxation of ^{59}Co in dilute $\underline{Cr_{1-x}V_x}Co$ ($X \lesssim 0.5$) and $\underline{Cr_{1-x}Mo_x}Co$ ($X \lesssim 0.25$) alloys in the ordered state was investigated. T_1 was proportional to $1/T$ in a region of $T \ll T_N$. T_1T decreases rapidly with the decrease of the ordering temperature associated with the increase of X. This decrease of T_1T with the decrease of the ordering temperature is generally observed in randomly ordered system in metals irrespective of the ferro and antiferromagnet. An approximate model calculation is carried out in terms of the Weger mechanism, where the nuclear energy relaxes to the kinetic energy of the conduction electrons via the virtual excitation of the spin waves. The same calculations are applied to T_1 of ^{57}Fe and ^{59}Co in ferromagnetic PdFe and PdCo alloys.

§1. Introduction

In dilute CrCo alloys Co atom has a localized magnetic moment of about 2.9 μ_B.[1,2] This Co moment is strongly coupled with the matrix spin density wave. In the alloys with Co more than about 1 at% the sinusoidal spin density wave state transforms into a simple antiferromagnetic state.[3]

An addition of V or Mo metal to Cr reduces the ordering temperature.[4] The spin density wave state persists to the alloy of V 4 % and Mo 25 % at liquid helium temperatures. The alloys of CrVCo and CrMoCo are considered to be the systems where the localized Co moments are randomly distributed in the band electron antiferromagnet.

As similar systems to these alloys, where the randomly distributed localized moments are ordered through the conduction electron spin polarizations, there are antiferromagnetic CuMn and ferromagnetic PdCo, PdFe, $(Ce_{1-x}Gd_x)Ru_2$ and so on. In these systems the nuclear spin-lattice relaxation time, T_1, of the nuclei associated with the localized moments shows a rapid decrease with the decrease of the transition temperature, T_C or T_N, keeping T_1T=const. in the temperature region sufficiently lower than the ordering temperature.[5,6,7] It would be considered that these decreases of T_1 arise from a same mechanism.

In order to investigate this relaxation mechanism, T_1 of ^{59}Co was measured in CrVCo and CrMoCo alloys and the relaxation

mechanism was discussed. On this mechanism an approximate calculation was carried out. The same calculation was also applied to the ferromagnetic PdFe and PdCo alloys.

§ 2. Experimental.

Starting metals Cr, V, Mo and Co used in this work were of 99.99, 99.99, 99.98 and 99.9 % purity, respectively. The concentration of Co were 1 and 3 at%. The samples were prepared by arc melting the components in an argon atmosphere. The ingots were remelted repeatedly for the homogeneization and crushed into powder for the NMR experiment. X ray diffraction study showed that all the specimens were of bcc phase and the lattice constant increases monotonically with V or Mo concentration. The measurements were carried out by frequency variable spin echo technique at liquid helium temperatures in zero external field. T_1 was measured from the temperature dependence of the spin echo decay time, T_2. T_2 measurements were made at the peak position of ^{59}Co resonance line in each sample. The signal averager was used in order to improve the signal to noise ratio.

§ 3. Experimental Results.

The variation of the internal field at ^{59}Co was shown in Fig.1. The internal field of ^{59}Co in CrCo alloy was reported to be 66 kOe.[8] It decreases with increasing V or Mo concentration. Fig.2(a) and 2(b) show the temperature dependences of T_2 of ^{59}Co in CrVCo and CrMoCo alloys.

The observed T_2 may be expressed as

$$(T_2)^{-1} = (T_2^*)^{-1} + (T_\perp)^{-1} + (T_{/\!/})^{-1}$$

where $(T_\perp)^{-1}$ and $(T_{/\!/})^{-1}$ denote the relaxation rate due to a transverse and longitudinal local field fluctuations, respectively. $(T_2^*)^{-1}$ is a contribution from the nuclear spin-spin interaction. If the observed signal corresponds to the transition $-1/2 \leftrightarrow 1/2$ of the nuclear spin state, the transverse relaxation part is enhanced as $(T_\perp)^{-1} \rightarrow 1/2(4I(I+1)-1)(T_\perp)^{-1}$. [9,10] T_1 relates to $T_\perp$ as $2(T_\perp)^{-1} = (T_1)^{-1}$. In a condition $T \ll T_N$ the longitudinal part is considered to be negligibly small compared with the transverse relaxation part. The enhancement factor for ^{59}Co amounts to 31/2.

To confirm the relation between T_1 and T_2 described above, direct measurements of T_1 at x=0 and x=0.02 in $(Cr_{1-x}V_x)_{97}Co_3$ alloys were performed by a saturating comb pulse method. T_1T measured directly were 89 msecK and 9 msecK for x=0 and 0.02, respectively, while those obtained from T_2 were 65 msecK and 7 msecK for x=0 and 0.02, respectively. The agreement is satisfactory.

As is seen in the figures the temperature dependence of T_2 shows T_1T=const. This suggests that the nuclear Zeeman energy relaxes to the kinetic energy of the conduction electrons. The concentration dependence of $(T_1T)^{-1}$ is shown in Fig.3(a) and 3(b).

§ 4. Discussions.

Let us discuss the relaxation mechanism of Co nuclei. When the nuclear spin energy relaxes to the kinetic energy of the conduction electrons, $(T_1T)^{-1}$ should be proportional to $\rho(E_F)^2$, where $\rho(E_F)$ is the density of state of the conduction electrons at the Fermi surface. In the case of the direct relaxation to the kinetic energy of the conduction electrons the x dependence of $(T_1T)^{-1}$ will follow the variation of $\rho(E_F)^2$ with x. However as is shown in Fig.3(a) and (b), the experimental $(T_1T)^{-1}$ varies more drastically with x than that expected from γ^2, where γ is the specific heat coefficient of the conduction electrons.[11] The rapid change of T_1T correlates with the change of the transition temperature with the change of x. Therefore the indirect mechanism including the fluctuation of the localized electron spins is considered to contribute mainly to the nuclear relaxation. In these alloys the localized moments are distributed randomly and interact with each other through the conduction electron spin polarizations. The hyperfine interaction between the localized electron spin and nuclear spin excites the spin wave in this randomly distributed electron spin system. So the relaxation process in this system may be attributed to the energy flow of the nuclear Zeemen energy to the conduction electron energy via the excitation of the spin waves and the decrease of T_1T may be attributed to the decreases of the effective exchange inter-

action between the localized electrons with the increase of V or Mo concentration.

The interaction between the nuclear spin and conduction electron spin via the spin wave was first proposed by Weger in the ferromagnetic regular lattice systems, Fe, Co and Ni.[12] Sano et al applied this to the ferromagnetic Dy metal and obtained a good agreement between the theoretical and experimental values.[13] Referring to these calculations we first discuss T_1 in ferromagnetic PdFe and PdCo alloys and then in antiferromagnetic CrVCo and CrMoCo which are rather complex for the calculation.

Sablik et al [14] have measured the concentration dependence of T_1 of ^{57}Fe in PdFe. They observed first a decrease and then an increase in T_1 with decreasing Fe concentration. This behavior was explained by changes of intra atomic exchange of 4d-4d and 3d-4d electrons. However the decrease of T_1 with lowering the ordering temperature is quite generally observed as mentioned previously. So we try to explain the decrease of T_1 in PdFe with decreasing Fe concentration by Weger mechanism.

In order to obtain a rough estimation of T_1 in these systems we replace the random system by a regular one.

(A) Ferromagnetic Case.

The Hamiltonian responsible for the nuclear spin relaxation due to the hyperfine interaction between the nuclear spin and the localized electron spin, and due to the s-d exchange interaction between the localized electron spin and conduction electron spin are expressed, respectively, as

$$\mathcal{H}'_{hf} = A\sqrt{\frac{S}{2N_i}}\sum_{\ell}\sum_{q}\left(e^{-i\vec{q}\vec{R}_\ell}\, c_q I_\ell^- + e^{i\vec{q}\vec{R}_\ell} c_q^* I_\ell^+ \right) \tag{1}$$

$$\mathcal{H}'_{sd} = -\frac{J_{sd}}{N}\sqrt{\frac{2S}{N_i}}\sum_{\ell}\sum_{q}\sum_{k}\sum_{k'} e^{i(\vec{k}-\vec{k}')\vec{R}_\ell}\left(a_{k'\uparrow}^+ a_{k\downarrow}\, e^{i\vec{q}\vec{R}_\ell} c_q^* + a_{k'\downarrow}^+ a_{k\uparrow}\, e^{-i\vec{q}\vec{R}_\ell} c_q \right) \tag{2}$$

where N and N_i are the numbers of atoms and the localized electron spins, respectively. J_{sd} and A are the s-d exchange and the hyperfine coupling constants, respectively. The suffix ℓ denotes the lattice site of the localized spins. c_q and c_q^* are the Fourier transform of the Holstein-Primakoff operators defined as

$$S_\ell^z = S - c_\ell^* c_\ell\,, \quad S_\ell^+ = \sqrt{2S}\, f_\ell(S) c_\ell \approx \sqrt{2S} c_\ell\,, \quad S_\ell^- = \sqrt{2S} c_\ell^* f_\ell(S) \approx \sqrt{2S} c_\ell^* \tag{3}$$

$$c_\ell = \sqrt{\frac{1}{N_i}}\sum_{q} e^{-i\vec{q}\vec{R}_\ell} c_q \qquad c_\ell^* = \sqrt{\frac{1}{N_i}}\sum_{q} e^{i\vec{q}\vec{R}_\ell} c_q^* \tag{4}$$

where $f_\ell = \sqrt{1-\frac{c_\ell^* c_\ell}{2S}} \approx 1$ is assumed for $T \ll T_C$.

The matrix element corresponding to the process where the ℓth nuclear state changes from m to m+1 and , at the same time, a spin wave $\vec{q}$ is virtually excited through the hyperfine interaction is

$$\left(m+1,q \left| \mathcal{H}'_{hf} \right| m,0 \right) = A\sqrt{\frac{S}{2N_i}}\sqrt{(I-m)(I+m+1)}\; e^{i\vec{q}\vec{R}_\ell} \tag{5}$$

The matrix element for an absorption of the excited spin wave by the scattering of a conduction electron from $\vec{k}_{\uparrow}$ to $\vec{k}'_{\downarrow}$ through the s-d exchange interaction is

$$(k'_{\downarrow}, 0 \mid \mathcal{H}'_{sd} \mid k_{\uparrow}, q) = - \frac{J_{sd}}{N}\sqrt{\frac{2S}{N_i}} \sum_{\ell} e^{i(\vec{k}-\vec{k}'-\vec{q})\vec{R}_{\ell}} \tag{6}$$

Then the resultant second order perturbation matrix element is

$$(k'_{\downarrow}, m+1 \mid \mathcal{H}' \mid k_{\uparrow}, m) = -\frac{AJ_{sd}S}{NN_i} \sqrt{(I-m)(I+m+1)} \sum_{q} \sum_{\ell'} \frac{e^{i(\vec{k}-\vec{k}'-\vec{q})\vec{R}_{\ell'}} e^{i\vec{q}\vec{R}_{\ell}}}{\varepsilon(\vec{q}) + \varepsilon_{m+1} - \varepsilon_m} \tag{7}$$

Here $\varepsilon(\vec{q})$ represents the excitation energy of the spin wave. ε_m is the nuclear Zeeman energy and $\varepsilon(\vec{q}) \gg \varepsilon_{m+1} - \varepsilon_m$.
Then the transition probability from the nuclear Zeeman state m to m+1 is

$$W_{m\ m+1} = \frac{2\pi}{\hbar} \left(\frac{J_{sd}AS}{N}\right)^2 (I-m)(I+m+1) \frac{V^2}{(2\pi)^6} k_B T$$

$$\times \int\int_{\text{Fermi surface}} d\sigma_{k_{\uparrow}}\, d\sigma_{k'_{\downarrow}} \frac{1}{|\vec{\nabla}_k E|_{F_{\uparrow}}} \frac{1}{|\vec{\nabla}_{k'} E|_{F_{\downarrow}}} \left\{\frac{1}{\varepsilon(\vec{k}_{F_{\uparrow}} - \vec{k}_{F_{\downarrow}})}\right\}^2 \tag{8}$$

For simplicity we have neglected the "Umklapp process". Here V and E are the volume of the crystal and the kinetic energy of a conduction electron, respectively.

We consider that the localized spin system constructs a regular fcc ferromagnetic lattice approximately, and that long wave excitations only contribute to the relaxation rate. Then

$$\varepsilon(\vec{q}) = 2JS\, a^2 q^2 + g\mu_B H_a \tag{9}$$

Here the effective exchange interaction J between nearest neighbour localized spins and an axial anisotropy in the localized spin direction are assumed. H_a is the anisotropy field. a is the lattice constant of the assumed regular lattice. Strictly in a small concentration of localized spins it may occur that an upper limit of the spin wave excitations, q_{max}, becomes smaller than $|\vec{k}_{F\uparrow} - \vec{k}'_{F\downarrow}|$. This means that one must not extend the integration in eq.(8) to cover all the Fermi surface. However, the transition rate is dominated by the process via the spin wave excitations for $q \approx 0$. So it will be available for a rough estimation to assume that the formula (9) persists to $|\vec{k}_{F\uparrow} - \vec{k}'_{F\downarrow}|_{max} = k_{F\uparrow} + k'_{F\downarrow}$ and the integration covers all the Fermi surface except for the case of a extremely low concentration of localized spins. Then assuming that the Fermi surface is spherical and $|\vec{\nabla}_k E|_{F\uparrow} \approx |\vec{\nabla}_{k'} E|_{F\downarrow}$, $W_{m\ m+1}$ is obtained as

$$W_{m\ m+1} = \frac{2\pi}{\hbar}(J_{sd}AS)^2(I-m)(I+m+1)\frac{a_0^6}{(2\pi)^6}k_B T \sum \left(\frac{1}{|\vec{\nabla}_k E|_F}\right)^2 \frac{\pi}{(2JSa)^2}\frac{k_{F\downarrow}}{k_{F\uparrow}}$$

$$\times \left[\frac{1}{a^2(k_{F\uparrow}-k_{F\downarrow})^2 + \frac{g\mu_B H a}{2JS}} - \frac{1}{a^2(k_{F\uparrow}+k_{F\downarrow})^2 + \frac{g\mu_B H a}{2JS}}\right] \qquad (10)$$

Here $\sum$ indicates the area of the Fermi surface. We can neglect the second term since $(k_{F\uparrow}-k_{F\downarrow})^2 \ll (k_{F\uparrow}+k_{F\downarrow})^2$. As pointed out by Weger, a polarization of the spin density of the conduction electrons by the s-d exchange interaction induces the differences between $k_{F\uparrow}$ and $k_{F\downarrow}$. Then the spin wave excitations with the wave vector $|\vec{q}| < |\vec{k}_{F\uparrow}-\vec{k}_{F\downarrow}|$ do not contribute to the relaxation. This difference, $k_{F\uparrow}-k_{F\downarrow}$, plays an important role in ferromagnetic Fe,Co and Ni. Weger neglected the anisotropy term. However, we keep this term because $k_{F\uparrow}-k_{F\downarrow}$ can become small when the concentration of the localized spin is reduced. The average difference of the Zeeman energy between "up" and "down" spins of the conduction electrons is

$$\Delta E = 2J_{sd}Sc \qquad (11)$$

Here c is the concentration of the localized spins. In Pd metal it is well known that the exchange interaction of the conduction electrons is large and this enhances the spin polarization of the conduction electrons.[15] Then it will be reasonable in this system to take

$$\Delta E = 2J_{sd}Sc/(1-\alpha) \qquad (12)$$

instead of $2J_{sd}Sc$. α is the exchange enhancement factor.

The effective exchange coupling constant J is estimated from the ordering temperature T_C following the molecular field theory.

$$k_B T_C = \frac{2}{3} z J S(S+1) \qquad (13)$$

Here z is the number of the nearest neighbour atoms.

Using $a=c^{-\frac{1}{3}}\sqrt{2}a_o$ $\quad |\vec{\nabla}_k E|_F = \dfrac{\Delta E}{|k_{F\uparrow} - k_{F\downarrow}|}$, $\quad \dfrac{a_o^3}{(2\pi)^3}\dfrac{\Sigma}{|\vec{\nabla}_k E|_F} = \rho(E_F)$

the final result is as follows:

$$T_1T = A_W T_C^2 c^{\frac{2}{3}} + A_a T_C c^{-\frac{2}{3}} \tag{14}$$

$$A_W = \frac{4\hbar \pi^3 k_B}{(S+1)^2 A^2} \frac{1}{a_o^2 k_F^2 (1-\alpha)^2} \tag{15}$$

$$A_a = \frac{\hbar}{2\pi} \frac{1}{S^2(S+1)} \frac{a_o^2 k_F^2}{(J_{sd} A \rho(E_F))^2} g\mu_B H_a \tag{16}$$

In a limit of $H_a=0$, $c=1, \sqrt{2}a_o \rightarrow a_o$ and $\alpha=0$, eq.(14) is reduced to Weger's result.

In PdCo A is 70 kOe/μ_B from $H_{int}\sim$200 kOe and $g\mu_B S\sim 3\mu_B$. In PdFe A is -75 kOe/μ_B from $H_{int}\sim$300 kOe and $g\mu_B S\sim 4\mu_B$. The exchange enhancement factor is estimated $\alpha\sim$0.83 in Pd metal from the specific heat and susceptibility measurements.[15] On the other hand a spatial extension of about 10 Å of the giant moments in dilute PdFe alloy indicates $\alpha\sim$0.95.[15] We adopt α=0.85 as a tentative value. The other unknown parameters are listed in Table Ⅰ. The calculated values are shown in Table Ⅱ.

As is seen in Table Ⅱ the relaxation time is mostly determined by A_W term which involves less unknown parameters, A, k_F, S and α. The difference in the anisotropy field in PdFe and PdCo does not affect the relaxation times in the above calculation. This is consistent with the experimental feature that T_1T depends only on the difference of gyromagnetic ratios γ_N of ^{57}Fe and ^{59}Co.[6]

The agreement between the experimental and calculated values is satisfactory in spite of the rough approximations.[6,14]

(B) Antiferromagnetic Case.

In antiferromagnetic CrVCo and CrMoCo alloys, similar calculations can be easily performed applying the treatment in ferromagnet to antiferromagnet. The Hamiltonian responsible for the nuclear relaxation corresponding to (1) and (2) in the ferromagnetic case are expressed in terms of the antiferromagnetic sublattice.

$$\mathcal{H}'_{hf} = A\sqrt{\frac{S}{N_i}}\left\{\sum_{\ell}\sum_{q}(e^{-i\vec{q}\vec{R}_\ell}c_q I_\ell^- + e^{i\vec{q}\vec{R}_\ell}c_q^* I_\ell^+) + \sum_{m}\sum_{q}(e^{-i\vec{q}\vec{R}_m}b_q^* I_m^- + e^{i\vec{q}\vec{R}_m}b_q I_m^+)\right\} \quad (17)$$

$$\mathcal{H}'_{sd} = -\frac{2J_{sd}}{N}\sqrt{\frac{S}{N_i}}\left\{\sum_{\ell}\sum_{q}\sum_{k}\sum_{k'}e^{i(\vec{k}-\vec{k}')\vec{R}_\ell}(a_{k'\uparrow}^+ a_{k\downarrow}c_q^* e^{i\vec{q}\vec{R}_\ell} + a_{k'\downarrow}^+ a_{k\uparrow}c_q e^{-i\vec{q}\vec{R}_\ell})\right.$$
$$\left. + \sum_{m}\sum_{q}\sum_{k}\sum_{k'}e^{i(\vec{k}-\vec{k}')\vec{R}_m}(a_{k'\uparrow}^+ a_{k\downarrow}b_q e^{i\vec{q}\vec{R}_m} + a_{k'\downarrow}^+ a_{k\uparrow}b_q^* e^{-i\vec{q}\vec{R}_m})\right\} \quad (18)$$

The suffix ℓ and m denote the sublattice of the antiferromagnet. q must be taken in the first Brillouin zone constructed by this sublattice. c_q and b_q are the Fourier transform of the Holstein-Primakoff operators. The Hamiltonian of the localized electron spin system is taken as

$$\mathcal{H}_{ss} = \sum_{\ell}\sum_{m} 2|J|\vec{S}_\ell\cdot\vec{S}_m - D\left[\sum_{\ell}(S_\ell^z)^2 + \sum_{m}(S_m^z)^2\right] \quad (19)$$

D is the anisotropy energy of axial symmetry and $|J|$ is the effective exchange interaction between nearest neighbours. Then one makes further transformations to diagonalize $\mathcal{H}_{ss}$

$$c_q = \alpha_q\cosh\theta_q - \beta_q^*\sinh\theta_q \qquad c_q^* = \alpha_q^*\cosh\theta_q - \beta_q\sinh\theta_q$$
$$b_q = -\alpha_q^*\sinh\theta_q + \beta_q\cosh\theta_q \qquad b_q^* = -\alpha_q\sinh\theta_q + \beta_q^*\cosh\theta_q \quad (20)$$

Here $\tanh 2\theta_q = \frac{\gamma_q}{1+d}$, $d = \frac{D(2S-1)}{2z|J|S}$ and $\gamma_q = \frac{1}{z}\sum_{\vec{\rho}} e^{i\vec{q}\vec{\rho}}$

$\vec{\rho}$ is the vector to the nearest neighbour.

Using the operators α_q, α_q^*, β_q and β_q^*, $\mathcal{H}'_{hf}$ $\mathcal{H}'_{sd}$ are rewritten as

$$\mathcal{H}'_{hf} = A\sqrt{\frac{S}{N_i}}\sum_{\ell}\sum_{q}\left\{e^{-i\vec{q}\vec{R}_\ell} I_\ell^-(\alpha_q\cosh\theta_q - \beta_q^*\sinh\theta_q) + e^{i\vec{q}\vec{R}_\ell} I_\ell^+(\alpha_q^*\cosh\theta_q - \beta_q\sinh\theta_q)\right\}$$

$$+A\sqrt{\frac{S}{N_i}}\sum_{m}\sum_{q}\left\{e^{-i\vec{q}\vec{R}_m} I_m^-(-\alpha_q\sinh\theta_q + \beta_q^*\cosh\theta_q) + e^{i\vec{q}\vec{R}_m} I_m^+(-\alpha_q^*\sinh\theta_q + \beta_q\cosh\theta_q)\right\} \qquad (21)$$

$$\mathcal{H}'_{sd} = -\frac{2J_{sd}}{N}\sqrt{\frac{S}{N_i}}\sum_{\ell}\sum_{K}\sum_{K'}\sum_{q}\left\{e^{i(\vec{k}-\vec{k}'+\vec{q})\vec{R}_\ell} a^+_{K'\uparrow}a_{K\downarrow}(\alpha_q^*\cosh\theta_q - \beta_q\sinh\theta_q)\right.$$
$$\left. + e^{i(\vec{k}-\vec{k}'-\vec{q})\vec{R}_\ell} a^+_{K'\downarrow}a_{K\uparrow}(\alpha_q\cosh\theta_q - \beta_q^*\sinh\theta_q)\right\}$$

$$-\frac{2J_{sd}}{N}\sqrt{\frac{S}{N_i}}\sum_{m}\sum_{K}\sum_{K'}\sum_{q}\left\{e^{i(\vec{k}-\vec{k}'+\vec{q})\vec{R}_m} a^+_{K'\uparrow}a_{K\downarrow}(-\alpha_q^*\sinh\theta_q + \beta_q\cosh\theta_q)\right.$$
$$\left. + e^{i(\vec{k}-\vec{k}'-\vec{q})\vec{R}_m} a^+_{K'\downarrow}a_{K\uparrow}(-\alpha_q\sinh\theta_q + \beta_q^*\cosh\theta_q)\right\} \qquad (22)$$

The matrix element corresponding to the process where the ℓ th nuclear state transfers from m to m+1 and, at the same time, a spin wave $\vec{q}$ is virtually excited through $\mathcal{H}'_{hf}$ is

$$(m+1, q|\mathcal{H}'_{hf}|m, 0) = A\sqrt{\frac{S}{N_i}}\sqrt{(I-m)(I+m+1)}\; e^{i\vec{q}\vec{R}_\ell}\cosh\theta_q \qquad (23)$$

One would expect two ways to absorb the excited spin wave $\vec{q}$ by scattering a conduction electron.

(a) A spin wave $\vec{q}$ scatters a conduction electron from $\vec{k}_\uparrow$ to $\vec{k}'_\downarrow$.

The matrix element for this process is

$$(k'_\downarrow, 0|\mathcal{H}'_{sd}|k_\uparrow, q) = -2\frac{J_{sd}}{N}\sqrt{\frac{S}{N_i}}\left\{\sum_{\ell} e^{i(\vec{k}-\vec{k}'-\vec{q})\vec{R}_\ell}\cosh\theta_q\right.$$
$$\left. - \sum_{m} e^{i(\vec{k}-\vec{k}'-\vec{q})\vec{R}_m}\sinh\theta_q\right\} \qquad (24)$$

(b) A spin wave $\vec{q}$ scatters a conduction electron from $\vec{k}_\downarrow$ to $\vec{k}'_\uparrow$.

The matrix element for this process is

$$\left(k'_\uparrow, 0 \left| \mathcal{H}'_{sd} \right| k_\downarrow, q\right) = -\frac{2J_{sd}}{N}\sqrt{\frac{S}{N_i}}\left\{\sum_\ell e^{i(\vec{k}-\vec{k}'+\vec{q})\vec{R}_\ell}\cosh\theta_q - \sum_m e^{i(\vec{k}-\vec{k}'+\vec{q})\vec{R}_m}\sinh\theta_q\right\} \tag{25}$$

The resultant second order matrix elements are obtained as

(a) $$\left(k'_\downarrow, m+1 \left| \mathcal{H}' \right| k_\uparrow, m\right)$$

$$= -\frac{J_{sd}}{N} AS\sqrt{(I-m)(I+m+1)}\,\frac{e^{i(\vec{k}-\vec{k}')\vec{R}_\ell}\left(\cosh^2\theta_{kk'} - \sinh\theta_{kk'}\cosh\theta_{kk'}\right)}{\mathcal{E}(\vec{k}_\uparrow - \vec{k}'_\downarrow)} \tag{26}$$

(b) $$\left(k'_\uparrow, m+1 \left| \mathcal{H}' \right| k_\downarrow, m\right)$$

$$= -\frac{J_{sd}}{N} AS\sqrt{(I-m)(I+m+1)}\,\frac{e^{i(\vec{k}'-\vec{k})\vec{R}_\ell}\left(\cosh^2\theta_{k'k} - \sinh\theta_{k'k}\cosh\theta_{k'k}\right)}{\mathcal{E}(\vec{k}_\downarrow - \vec{k}'_\uparrow)} \tag{27}$$

where $\theta_{kk'} = \theta_{\vec{k}-\vec{k}'}$

Then the transition probability is obtained as

$$W_{m\,m+1} = \frac{2\pi}{\hbar}\left(\frac{J_{sd}AS}{N}\right)^2 (I-m)(I+m+1)$$

$$\times\left\{\sum_{k_\uparrow}\sum_{k'_\downarrow} f(E_{k\uparrow})(1-f(E_{k'\downarrow}))\,\delta(E_{k\uparrow}-E_{k'\downarrow})\,\frac{\left(\cosh^2\theta_{kk'} - \sinh\theta_{kk'}\cosh\theta_{kk'}\right)^2}{\left(\mathcal{E}(\vec{k}_\uparrow - \vec{k}'_\downarrow)\right)^2}\right.$$

$$\left. + \sum_{k_\downarrow}\sum_{k'_\uparrow} f(E_{k\downarrow})(1-f(E_{k'\uparrow}))\,\delta(E_{k\downarrow}-E_{k'\uparrow})\,\frac{\left(\cosh^2\theta_{k'k} - \sinh\theta_{k'k}\cosh\theta_{k'k}\right)^2}{\left(\mathcal{E}(\vec{k}'_\uparrow - \vec{k}_\downarrow)\right)^2}\right\} \tag{28}$$

here $\theta_{kk'} = \theta_{k'k}$, $\mathcal{E}(\vec{k}-\vec{k}') = \mathcal{E}(\vec{k}'-\vec{k})$

$$\cosh^2\theta_q - \cosh\theta_q\sinh\theta_q = \frac{1}{2}\left(1 + \sqrt{1-\left(\frac{\gamma_q}{1+d}\right)^2}\right) . \tag{29}$$

The spin wave excitation energy is

$$\mathcal{E}(\vec{q}) = 2z|J|S\sqrt{(1+d)^2 - \gamma_q^2} . \tag{30}$$

Using these relations and $\gamma_{kk'} = \gamma_{\vec{k}-\vec{k}'}$, $W_{m\,m+1}$ is expressed as

$$W_{m\,m+1}=\frac{2\pi}{\hbar}\left(\frac{J_{sd}AS}{N}\right)^2(I-m)(I+m+1)\frac{V^2}{(2\pi)^6}\frac{k_BT}{(2z|J|S)^2}$$

$$\times\frac{1}{2}\iint_{\text{Fermi surface}}d\sigma_{k\uparrow}\,d\sigma_{k'\downarrow}\frac{1}{|\vec{\nabla}E_k|_{F\uparrow}}\frac{1}{|\vec{\nabla}E_{k'}|_{F\downarrow}}\left\{\frac{1}{1+d+\gamma_{kk'}}+\frac{1}{\sqrt{(1+d)^2-\gamma_{kk'}^2}}\right\}^2 \qquad (31)$$

We approximately consider that the localized spin system constructs a regular bcc antiferromagnetic lattice. Then $0\leq\gamma_q\leq 1$. In long wave excitations ($\gamma_q\approx 1$) which contribute mainly to the relaxation rate, $\dfrac{1}{1+d+\gamma_{kk'}}\ll\dfrac{1}{\sqrt{(1+d)^2-\gamma_{kk'}^2}}$ for $d\ll 1$.

So we can neglect the first term in bracket for a crude estimation. Using long wave excitation formula, $\gamma_q\approx 1-\frac{1}{4}a^2q^2$ and making the same approximations as in the ferromagnetic case on the integration range at the Fermi surface and so on, we have

$$W_{m\,m+1}=\frac{2\pi}{\hbar}\left(\frac{J_{sd}AS}{N}\right)^2(I-m)(I+m+1)\frac{V^2}{(2\pi)^6}\frac{k_BT}{(2z|J|S)^2}\frac{1}{2}\left(\frac{1}{|\vec{\nabla}_kE|_F}\right)^2$$

$$\times 4\pi\sum\frac{k_{F\downarrow}}{k_{F\uparrow}}\frac{1}{a^2}\ln\left\{\frac{d(d+2)+\frac{1}{4}a^2(k_{F\uparrow}+k_{F\downarrow})^2}{d(d+2)+\frac{1}{4}a^2(k_{F\uparrow}-k_{F\downarrow})^2}\right\} \qquad (32)$$

In antiferromagnetic case, it is expected generally that energy gaps appear in some directions of $\vec{k}$-space on the Fermi surface when the magnetic order of the localized spins takes place by the indirect interaction via the conduction electrons. We have ignored this effect for the crude estimation of the relaxation time. Then taking $k_{F\uparrow}=k_{F\downarrow}$, the simple calculation gives

$$W_{m\,m+1} = \frac{\pi}{256\hbar}\left(J_{sd} A \rho(E_F)\right)^2 (I-m)(I+m+1)\, k_B T \frac{1}{J^2}\frac{1}{a^2 k_F^2} \ln\left(\frac{a^2 k_F^2}{d(d+2)}\right) \qquad (33)$$

where $1 \ll \frac{a^2 k_F^2}{d(d+2)}$ is considered.

Following the molecular field theory, $k_B T_N = \frac{2}{3} z|J| S(S+1)$

Using $a = c^{-\frac{1}{3}} a_o$ and expressing $D = k_B T_D$, the final result is

$$(T_1 T)^{-1} = \frac{2\pi}{9}\frac{k_B}{\hbar}\left(\frac{S(S+1)}{a_o k_F}\right)^2 \left(J_{sd}\rho(E_F)\right)^2 \left(\frac{A}{k_B T_N}\right)^2 c^{\frac{2}{3}} \ln\left(\frac{3 a_o^2 k_F^2\, T_N}{2(2S-1)(S+1)\, T_D}\, c^{-\frac{2}{3}}\right) \qquad (34)$$

T_N in this relation means the ordering temperature due to the interaction between the localized spins. For the alloys of larger x the spin polarization of the matrix is negligebly small and the localized electron spin system may be ordered via the RKKY interaction. In this case it will be reasonable to assume that T_N in the above relation is equal to the ordering temperatur of the total system. For the alloys of small x the spin density polarization in the matrix is not so small and the estimation becomes complicated. Anyway the rapid decrease of the relaxation rate with increasing x is attributed to the decrease of the effective exchange interaction. For a crude estimation in a region of $x \geq 0.3$, where our model calculation is considered to be appropriate, we adopt the parameters shown in Table Ⅲ . A is estimated to be 30 kOe using the internal field of Co 47kOe and the effective moment 2.6 μ_B.[22] No information exists on the anisotropy factor T_D.

However the transition probability does not depend on the factor T_D, because T_D appear only in the natural logarithm term. We assume T_D= 0.1 K. The other parameters are shown tentatively in Table Ⅲ . The calculated values are shown in Table Ⅳ . As seen in Table Ⅳ , the agreement between the experimental and the calculated values is satisfactory in spite of the crude approximations.

Althourh at random condition, long range interactions between localized spins and so on must be taken into account for precise quantitative discussions, it may be concluded that the nuclear spin lattice relaxation time at $T \ll T_C$ (T_N) in the randomly ordered system in metals can be generally interpreted in terms of the Weger mechanism.

Acknowledgements

I would like to express my sincere thanks to Professor J. Itoh for his valuable discussions. I would also like to express my sincere thanks to Professor K. Asayama for his continued guidance, valuable discussions and kind encouragement. I would also like to thank Professor T. Moriya of Tokyo University for his discussions and valuable comments. Thanks are also due to Dr. N. Sano , Dr. K. Kumagai and Mr. M. Katayama for their advices and discussions.

References

1) T.Suzuki: J.Phys.Soc.Japan. 21(1966)442.

2) J.G.Booth: J.Phys.Chem.Solids 27(1966)1639.

3) Y.Endoh,Y.Ishikawa and H.Ohno: J.Phys.Soc.Japan 24(1968)263.

4) Y.Hamaguchi, E.O.Wollan and W.C.Koehler: Phys.Rev.138(1965)A737.
W.C.Koehler, R.M.Moon, A.L.Trego and A.R.Mackintosh:
Phys.Rev.151(1966)405.

5) H.Takenaka and K.Asayama: J.Phys.Soc.Japan 35(1973)734.

6) M.Katayama, K.Kumagai, T.Kohara, K.Asayama, I.A.Campbell,
N.Sano, S.Kobayashi and J.Itoh: J.Phys.Soc.Japan 40(1976)429.

7) K.Kumagai: private communications.

8) T.Kohara and K.Asayama: J.Phys.Soc.Japan 39(1975)1263.

9) R.E.Walstedt: Phys.Rev.Letters 19(1967)146,19(1967)816.

10) A.Narath: Phys.Rev. B13(1976)3724.

11)F.Heiniger, E.Bucher and J.Muller: Phys.Kondens.Materie 5(1966)243

12) M.Weger:Phys.Rev.128(1962)1505.

13) N.Sano,S.Kobayashi and J.Itoh: Prog.Theor.Phys.Suppl.46(1970)84.

14) M.Sablik, S.Skalski and J.I.Budnik: Phys.Rev.88(1973)2222.

15) T.Moriya: Prog.Theor.Phys.34(1965)329.

16) O.M.S.Baggneley and J.A.Robertson: J.Phys.F4(1974)2282.

17) For example, Superconductivity, ed. R.D.Parks (Marcel Dekker
Inc. New York, 1969) vol.2,P.678.

18) J.Crangle and W.R.Scott: J.Appl.Phys. 36(1965)921.

19) J.A.Mydosh, J.I.Budnick, M.P.Kawatra and S.Skalski:
Phys.Rev.Letters. 21(1968)1346.

20) M.P.Kawatra, J.I.Budnick and J.A.Mydosh: Phys.Rev.B2(1970)1587.

21) R.M.Bozorth, P.A.Wolff, D.O.Davis and V.B.Compton:
Phys.Rev.122(1961)1157.

22) H.Akoh, M.Matsumura, K.Asayama and A.Tasaki: in preparation.

Figure Captions

Fig.1 x dependence of the internal field at ^{59}Co in $\underline{Cr_{1-x}V_x}Co$ and $\underline{Cr_{1-x}Mo_x}Co$ alloys at 1.4 K.

○ $(Cr_{1-x}V_x)_{99}Co_1$ ● $(Cr_{1-x}V_x)_{97}Co_3$ ⊙ $\underline{Cr}Co$ [8)]

△ $(Cr_{1-x}Mo_x)_{99}Co_1$ ▲ $(Cr_{1-x}Mo_x)_{97}Co_3$

Fig.2(a) The temperature dependence of T_2^{-1} in $(Cr_{1-x}V_x)_{97}Co_3$.

Fig.2(b) The temperature dependence of T_2^{-1} in $(Cr_{1-x}Mo_x)_{97}Co_3$.

Fig.3(a) x dependence of $(T_1T)^{-1}$ estimated from the temperature dependence of T_2^{-1} in $\underline{Cr_{1-x}V_x}Co$ alloys.
The dotted line represents the variation of the square of the electronic specific heat coefficient normalized to the value of $(T_1T)^{-1}$ at x=0.

Fig.3(b) x dependence of $(T_1T)^{-1}$ estimated from the temperature dependence of T_2^{-1} in $\underline{Cr_{1-x}Mo_x}Co$ alloys.
The dotted line represents the variation of the square of the electronic specific heat coefficient normalized to the value of $(T_1T)^{-1}$ at x=0.

Table I

Parameters for the calculations of T_1T in PdFe and PdCo.

	PdFe	PdCo
J_{sd}(eV)	1	1
A (kOe/μ_B)	-75	+70 *
$k_F(cm^{-1})$	1×10^8	1×10^8
S	2	3/2
α	0.85	0.85 **
a_o (cm)	2.8×10^{-8}	2.8×10^{-8}
$\rho(E_F)(eVatom)^{-1}$	1.4	1.4 ***
H_a (Oe)	50	1000 ****

* ref 6.

** ref 15.

*** ref 17.

**** ref 16.

Table Ⅱ

T_1T in secK calculated and observed in PdFe and PdCo alloys

^{57}Fe in PdFe alloys

c(%)	$T_C(K)^*$	$A_W T_C^2 c^{2/3}$	$A_a T_C c^{-2/3}$	$(T_1T)_{cal}$	$(T_1T)_{exp}^{**}$
0.5	20	7.2×10^{-3}	1.9×10^{-6}	7.2×10^{-3}	1.6×10^{-3}
1	35	3.4×10^{-2}	2.0×10^{-6}	3.4×10^{-2}	3.8×10^{-3}
2.5	70	2.5×10^{-1}	2.2×10^{-6}	2.5×10^{-1}	1.6×10^{-2}
3	90	4.8×10^{-1}	2.6×10^{-6}	4.8×10^{-1}	3.3×10^{-2}
4	110	8.4×10^{-1}	2.6×10^{-6}	8.4×10^{-1}	--------
5	130	1.4	2.6×10^{-6}	1.4	--------
6	160	2.4	2.8×10^{-6}	2.4	8.6×10^{-2}
7	180	3.3	3.0×10^{-6}	3.3	8.8×10^{-2}

^{59}Co in PdCo alloys

c(%)	$T_C(K)^{***}$	$A_W T_C^2 c^{2/3}$	$A_a T_C c^{-2/3}$	$(T_1T)_{cal}$	$(T_1T)_{exp}^{****}$
o.5	25	3.4×10^{-4}	2.2×10^{-6}	3.4×10^{-4}	4.8×10^{-5}
1	45	1.8×10^{-3}	2.4×10^{-6}	1.8×10^{-3}	2.0×10^{-4}
2	70	6.8×10^{-3}	2.4×10^{-6}	6.8×10^{-3}	6.1×10^{-4}
5	180	8.4×10^{-2}	3.4×10^{-6}	8.4×10^{-2}	1.2×10^{-3}
8	250	2.2×10^{-1}	3.4×10^{-6}	2.2×10^{-1}	2.1×10^{-3}

* ref 18, 19, 20.

** ref 14.

*** ref 21.

**** ref 6.

Table III

Parameters for the calculations of T_1T in CrVCo alloys.

J_{sd}(eV)	1
A (kOe/μ_B)	30 *
a_o(cm)	2.9×10^{-8}
$\rho(E_F)$ (eVatom)$^{-1}$	0.35 **
k_F (cm^{-1})	1×10^{-8}
S	1 ***
T_D (K)	0.1

* ref 22.

** for x=0 ref 17.

*** ref 22.

Table Ⅳ

$(T_1T)^{-1}$ of Co calculated and observed in $Cr_{1-x}V_x$Co in msecK.

Alloy	T_N(K)	$(T_1T)^{-1}_{cal}$	$(T_1T)^{-1}_{exp}$
x=0			
Co1%	300 *		0.017
Co3%	300		0.015
x=0.02			
Co1%	150		0.13
Co3%	150		0.14
x=0.03			
Co1%	70**	0.01	0.16
Co3%	80	0.02	0.27
x=0.04			
Co1%	40	0.03	0.33
Co3%	50	0.04	0.43
x=0.05			
Co1%	25**	0.1	1.0
Co3%	30	0.1	0.68
x=0.06			
Co3%	25	0.2	1.0

* ref 1,2 and 3.

** ref 22.

The other values for T_N are assumed by interpolation tentatively. In the calculation the x dependence of $\rho(E_F)$ estimated from the x dependence of γ [11] is adopted.

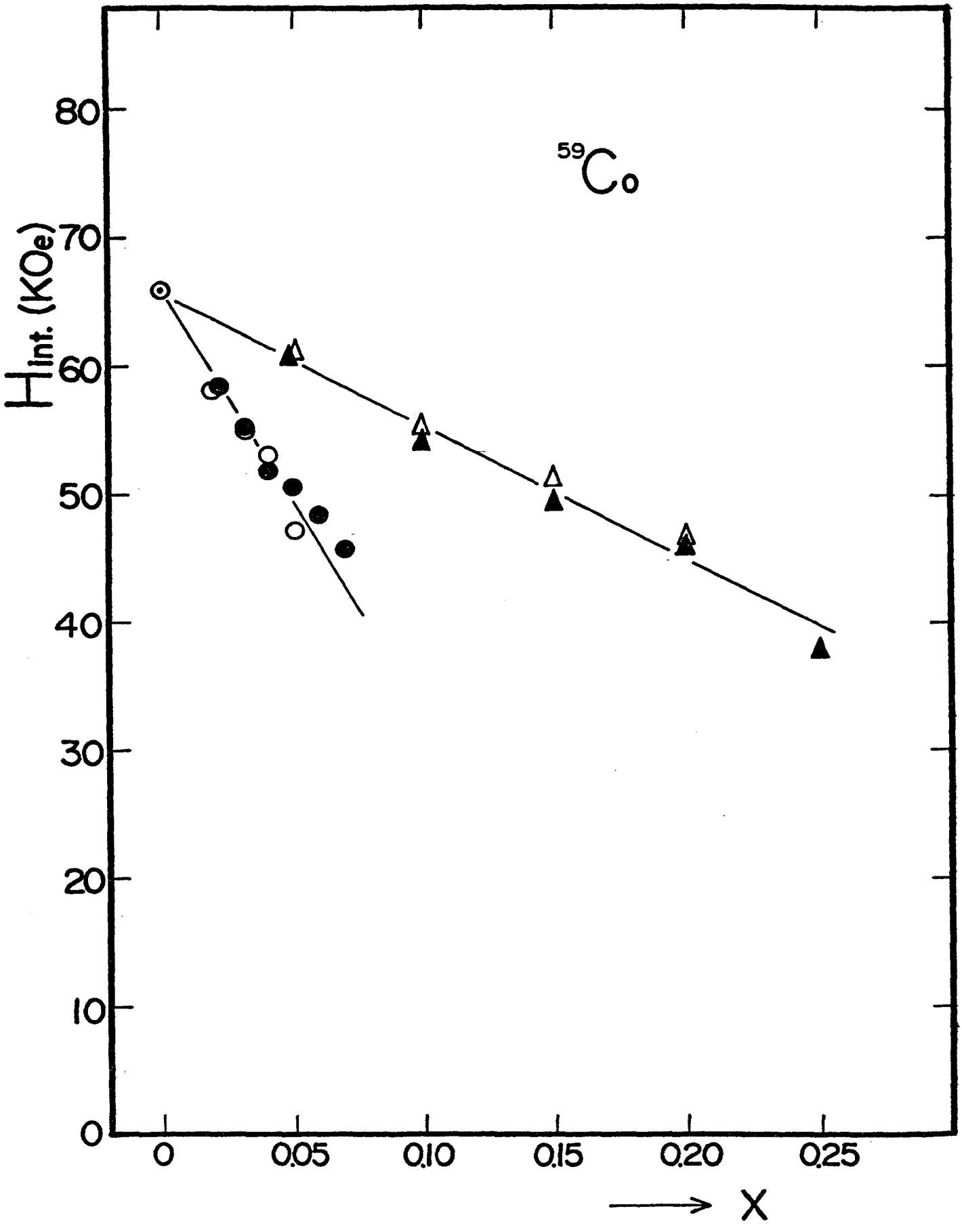

Fig.1

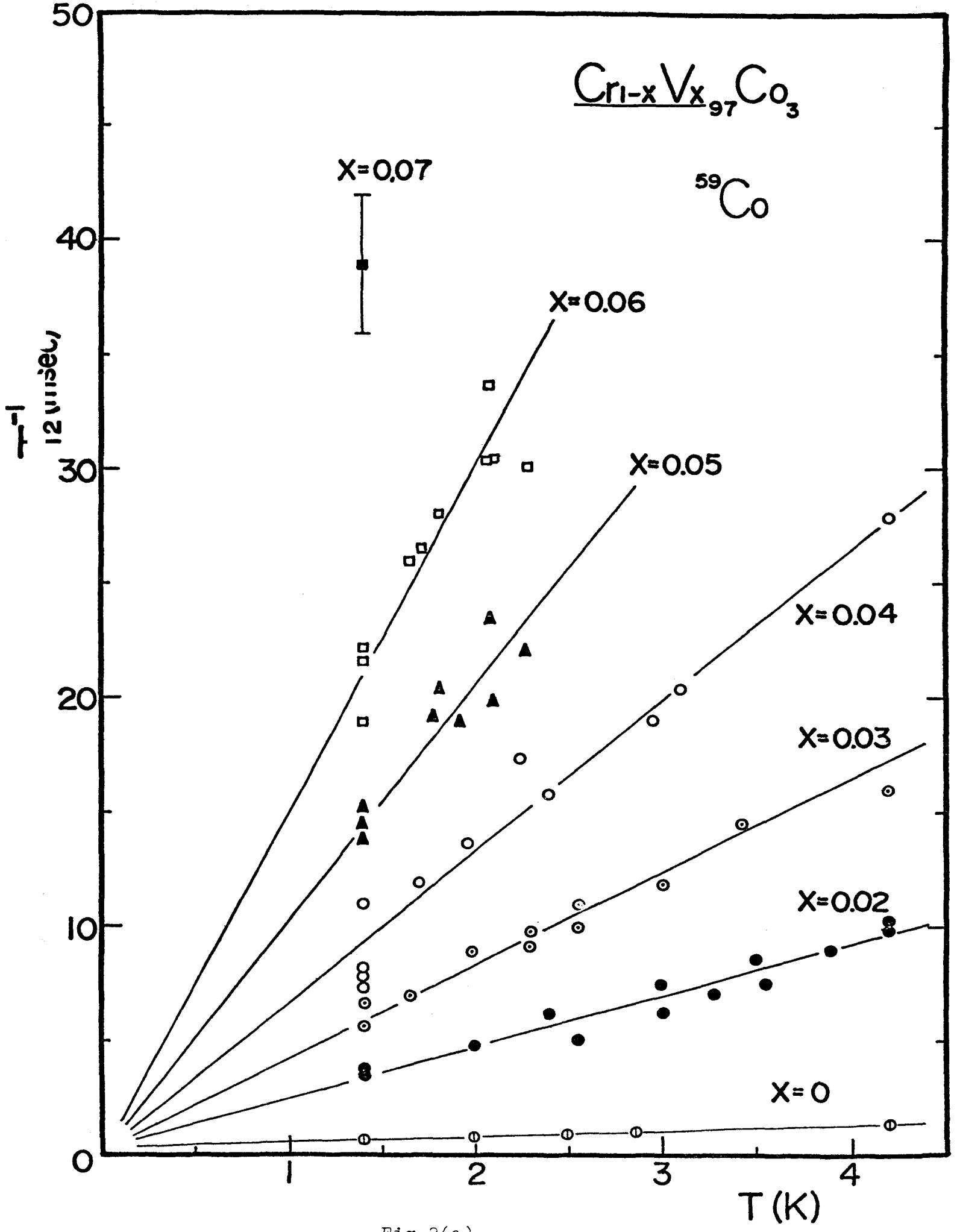
$Cr_{1-x}V_{x\,97}Co_3$
^{59}Co
X=0.07
X=0.06
X=0.05
X=0.04
X=0.03
X=0.02
X=0
T_1^{-1} (arbitrary)
T (K)
0
10
20
30
40
50
1
2
3
4

Fig.2(a)

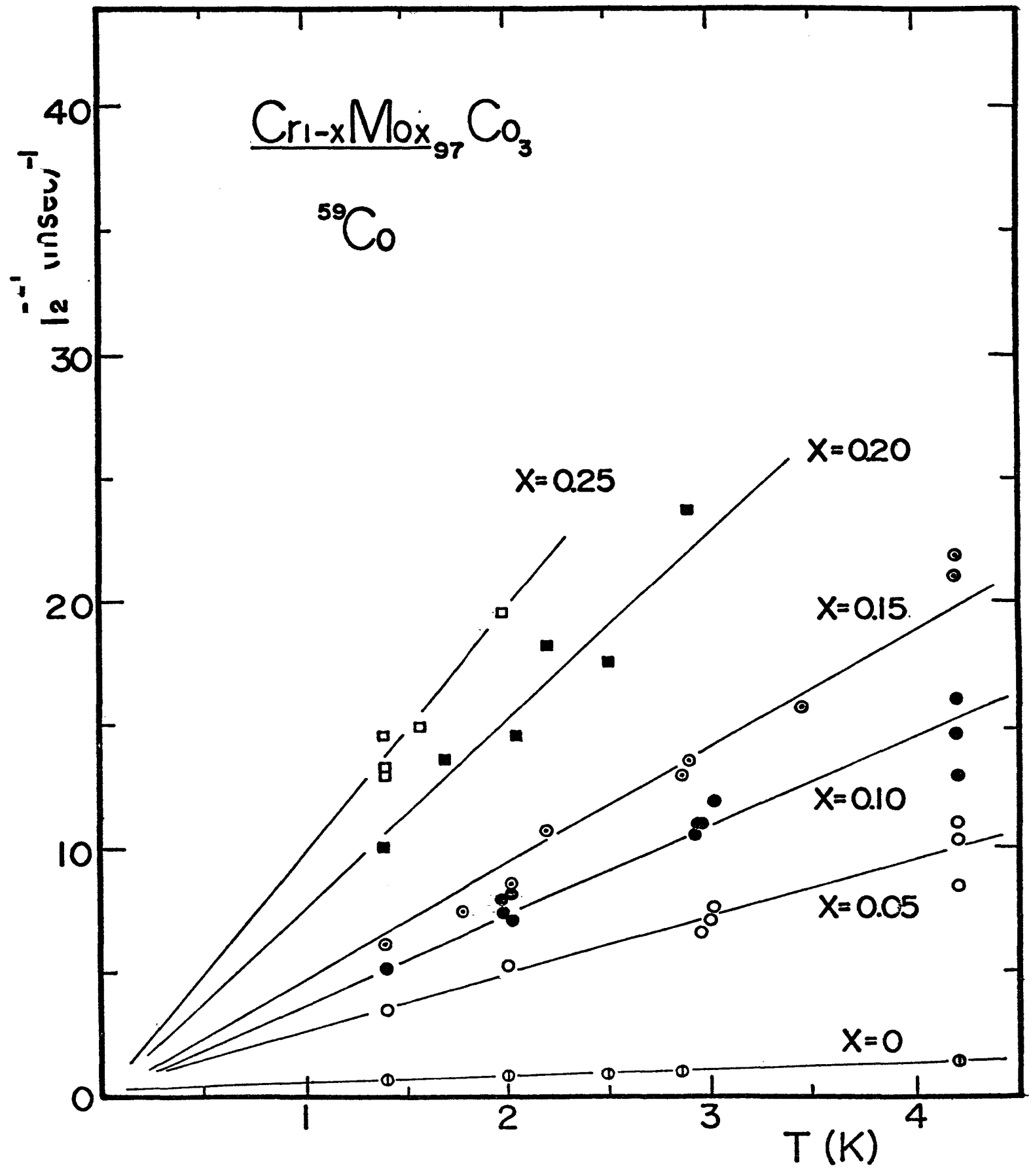

Fig.2(b)

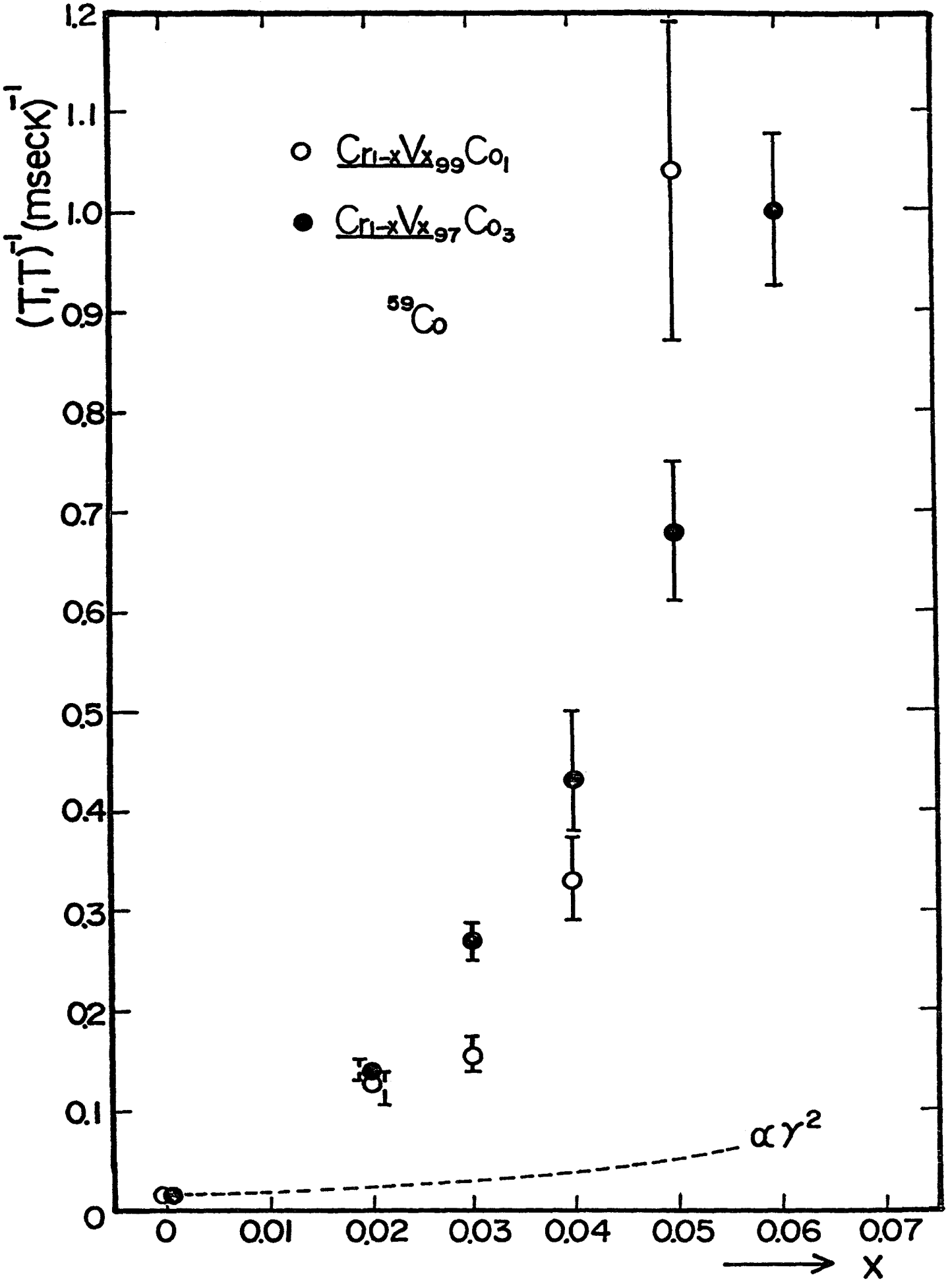
1.2
1.1
1.0
0.9
0.8
0.7
0.6
0.5
0.4
0.3
0.2
0.1
0
$(T_1T)^{-1}$ (mseck)$^{-1}$
$Cr_{1-x}V_{x\,99}Co_1$
$Cr_{1-x}V_{x\,97}Co_3$
^{59}Co
$\alpha\gamma^2$
0
0.01
0.02
0.03
0.04
0.05
0.06
0.07
X

Fig.3(a)

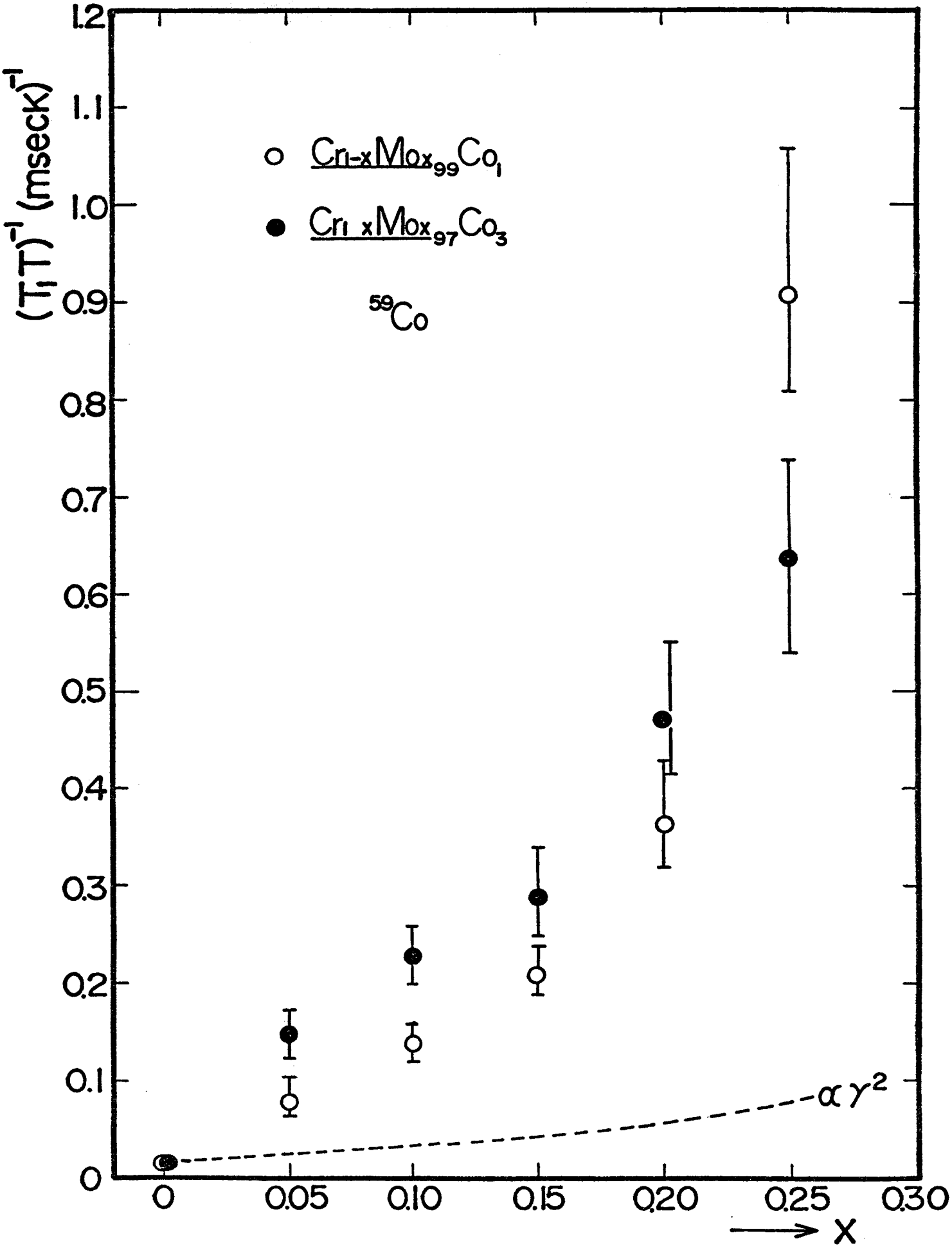
$(T_1T)^{-1}$ (mseck)$^{-1}$
1.2
1.1
1.0
0.9
0.8
0.7
0.6
0.5
0.4
0.3
0.2
0.1
0
$Cr_{1-x}Mo_{x_{99}}Co_1$
$Cr_{1-x}Mo_{x_{97}}Co_3$
^{59}Co
$\alpha\gamma^2$
0
0.05
0.10
0.15
0.20
0.25
0.30
X

Fig.3(b)